ACTA
UNIVERSITATIS PALACKIANAE
OLOMUCENSIS

FACULTAS RERUM NATURALIUM
CHEMICA 44
2005

ACTA
UNIVERSITATIS PALACKIANAE
OLOMUCENSIS

FACULTAS RERUM NATURALIUM
2005

CHEMICA 44

COLLECTED REPORTS
OF THE NATURAL SCIENCE FACULTY,
PALACKÝ UNIVERSITY OLOMOUC,
CZECH REPUBLIC

PALACKÝ UNIVERSITY OLOMOUC
OLOMOUC 2005

This volume has been accepted to be printed on October 17, 2005.

The authors are responsible for the content and for the translation of the papers.

© Jiří Kameníček, Juraj Ševčík, 2005

ISBN 80-244-1171-7

ISSN 0232-0061

ACTA UNIVERSITATIS PALACKIANAE OLOMOUCENSIS
FACULTAS RERUM NATURALIUM (2004) CHEMICA 44

CONTENTS

ACTA UNIVERSITATIS PALACKIANAE OLOMOUCENSIS
FACULTAS RERUM NATURALIUM (2005) CHEMICA 44

MICELLAR SYSTEMS – FACTORS INFLUENCING CRITICAL MICELLE CONCENTRATION AND MEASURING METHODS

Hana Strnadová* and Libor Kvítek

Department of Physical Chemistry, Palacký University, Tř. Svobody 8, 771 47 Olomouc, Czech Republic, E-mail: hana.strnadova@atlas.cz

Received May 19, 2005
Accepted August 30, 2005

Abstract

The use of surface-active agents (surfactants) in industry and also in research is widely extended. One of their main application fields is connected with their ability to create organized aggregates - micelles.

The aim of this review is to collect the common knowledge in the micellar aqueous solutions measurements and to evaluate the influence of different factors on these systems. At least some of the examples of using micelles in analytical separation methods are also mentioned in this review.

Keywords: *Critical micelle concentration (CMC); Surfactants; Micelles*

Introduction

Surface-active agents (surfactants) are amphiphilic compounds adsorbing themselves at interfaces of the phases and decreasing the solvent surface tension, in accordance with the Gibbs adsorption equation. Surfactant molecules associate above certain critical micelle concentration (CMC) to aggregates of colloid size, called micelles. The driving power of this process is the hydrophobic effect, which causes such geometrical arrangement, wherein hydrophobic parts form a liquid core and hydrophilic parts rearrange towards water surroundings.[1]

Whilst, people use soaps for centuries because of their advantageous properties arising from micelles formation, it wasn't until 19th century that their systematic study began. The initial period research was directed to solubilization ability of soaps. In 20th century, theories of aggregation as the process responsible for solubility properties of soaps were derived. In 1913, McBain introduced the term "micelle" for small colloid

* Author for correspondence

particles forming detergents and soaps.[2] Other important milestone in micellar research is 1930, when Bury and Davies[3] suggested the critical micelle concentration (CMC) concept for already denominated micelles as concentration, when micelles in the monomer solution begin to form. They also affirmed, this concentration is a function of the surfactants hydrocarbon chain length. Six years later, G. S. Hartley[4] explained micelles formation in connection with the hydrophobic effect and proposed the first model of micelle of the spherical shape. Development of optical spectroscopy, light scattering, NMR, ESR etc. enabled extending of micellar study possibilities up to molecular level. Later, during sixties and seventies, thanks to use of new experimental techniques and theoretical studies applied to micelle systems, has started a massive extend of information.[5,6]

The value of CMC is an important parameter in a wide field of industrial applications[7], including adsorption of surfactant molecules at interfaces, suspensions, surface coatings, foaming, wetting, emulsification, solubilization, and detergency.[8,9] Drummond publicated review[10] focused on publications operating with micelles as new drugs delivery. Recent research uses surfactants also in nanostructure materials synthesis.[11,12,13]

The main purpose of this review is the description of experimental methods used in CMCs measurements, the influence of environment upon the value of the CMC and some applications of micellar solutions in analytical separation methods.

1. Fundamentals of micellar systems creation

The critical micelle concentration is a parameter describing better the range than one-dimension value for micelles rise as can be seen from mass-action law applicated on micellar systems.[14] Critical parameters as size and its distribution, shape, structure, charge, and aggregation number of micelles characterize solutions containing aggregates of surfactants molecules. All properties of micellar systems depend upon components of the system, temperature and pressure.

Temperature effect – the rise of micelles is possible only above Krafft temperature (T_K). This temperature is an important point in the phase diagram of solubility versus temperature. Below T_K, the solubility is so small that micelles cannot form.
In the case of *ionic* surfactants the CMC decreases as the temperature increases because of the lowered hydration of the hydrophilic parts. Then the value of the CMC reaches its minimum and further increase in temperature is followed by increasing of the CMC due to disruption of the structured water surroundings hydrocarbon chains. The tendency of the CMC behaviour in a particular temperature region is influenced by the balance between effects promoting and opposing micellization.[8,15,16,17] The CMC values of *nonionic* surfactants decrease with the increasing temperature.[18,19,20] Chen[21] presented the temperature dependence of nonionic surfactants of the PEO type and describes reaching the minimum of the CMC for not charged surfactants, as well. This minimum point was estimated at high temperature, around 50ºC. Above this temperature the CMC increases again.

Increasing temperature promotes growing of large aggregates up to a certain temperature, called “cloud point”. The phase separation is realised due to the lowering of

number of hydrogen bonds between hydrophilic groups and water molecules.[8] The "cloud point" phenomenon is of a great interest of scientests.[22-31]

Pressure effect – change in the pressure acting on the surfactant system gives a rise to the change of the CMC. There is a common knowledge that the CMC increases with pressure increase till maximum (generally 150 MPa, newest, there is a monotonous increasing in the CMC until 550 MPa[15]). Above this maximum the CMC decreases with the increasing pressure again.[8]

Micellization is a process of spontaneous aggregation of surfactant monomers into the micellar form and the *micellization constant* is an equilibrium constant of this process. The aggregation number declares the average number of monomers in one micelle. For ionic surfactants, a *degree of ionisation* can be determined. It is a number of dissociated hydrophilic parts at the micelle surface. A zero value of this quantity indicates that all hydrophilic groups are bound to *counter-ions*. These ions originate in surfactant solution itself or from both, surfactant solution and the added solution of salt containing these ions.

Because of the fact that micelles are dynamic aggregates; it is complicated to assume an exact *shape* of micelles. Theoretical background operates with the *average micellar shape*. It is typical to suppose spherical shape for small micelles.

For example, ionic surfactant solutions without added electrolyte near the CMC region form micelles of this kind. But the majority of basic surfactants with simple hydrocarbon chain cannot, from the geometrical point of view, form aggregates of accurately spherical shape. In the core of the micelle cannot exist holes and the radius of the aggregate is limited by maximum hydrocarbon chain length. Tanford[32] supposes that the simplest way of joining the highest number of monomers into the micelle causes the distortion of the micellar shape to an ellipsoid.

The surfactant concentration increase causes the shape change of the micelles from spherical geometry up to liquid crystals. It is necessary to mention that micellar shape is influenced not only by the surfactant concentration but also by temperature, surfactant molecular structure and additives in the system.[15]

2. Thermodynamic models of micellization

For the theoretical treatment of micellization, the mass-action model or the phase separation model can be used. It is important to evaluate the reasons for more suitable model choice.[33-35]

Mass-action model

According to this model, micelles can be considered as large molecules and the micellar solution as the homogenous one-phase system. This approach describes the aggregation process as a reversible reaction[8]; which can be written in this form

$$nS \leftrightarrow M_n \qquad\qquad K = \frac{M_n}{S^n},$$

where *nS* is the number of surfactant monomers and M_n is the micelle, index *n* indicates number of monomers in the aggregate. *K* denotes the equilibrium constant of the reaction. Rusanov[36] presented the lifetime of surfactant molecule in the micelle in order 10^{-7} s and halftime of the micelle life from 10^{-3} s to 1 s. The aggregation number of micelles is very important from this point of view. The smaller the value of *n*, the more suitable is the mass-action model than the phase-separation model.

Phase-separation model

In this case, the micellar solution is a heterogeneous two-phase system, wherein micelles represent the pseudophase and the CMC is the concentration of saturation of solution by monomers. The addition of the surfactant above the CMC influences only concentration of the aggregates.

Only monomers are presented in solution below the CMC. The average value of the quantity Q is the same as $Q_{aq.}$

$$\langle Q \rangle = Q_{aq}$$

Above the CMC

$$\langle Q \rangle = p_{mic} Q_{mic} + p_{aq} Q_{aq} = \frac{1 - CMC}{c_{total}} Q_{mic} + \frac{CMC}{c_{total}} Q_{aq},$$

where *c* and *p* denote, respectively, the concentration and the phase fraction. For the concentration sufficiently above the CMC, $\langle Q \rangle$ comes up Q_{mic}.

This model is simple for the experimental measurements interpretation. More suitable is this approximation for micelles with high aggregation numbers.[8]

3. Common factors influencing CMC

Surfactant structure

Hydrophobic part

The nature of the hydrophobic part of charged surfactants leads to lowering of the CMC as the number of carbon atoms in the hydrocarbon chain increases. Higher number of carbon atoms increases the surfactant water repellence and due to this process, the CMC shifts to lower value. This effect has not been proved for chains longer than sixteen carbon atoms. The analogous effect can be achieved by benzene ring introducing to the surfactant structure. On the other hand, modification of the hydrocarbon chain by introducing another hydrocarbon branch, double bond or a polar functional group into the structure of surfactant, as well as substitution of hydrogen atoms by ionic groups, lead to the increasing CMC. The interfacial tension and the CMC are caused by the nature of hydrophobic terminal groups (CF_3 or H-CF_2) .[37,38] From the point of view of the geometrical isomerism, *cis*-isomers have higher values of the CMC than *trans*-isomers.[8,15]

Hydrophilic part

Considerably lower CMC values for *nonionic* surfactants comparing to the ionics is resulted in the fact that discharged surfactants do not need to carry out an electric work attached to the micelles formation. For nonionic surfactants of the polyoxyethylene type, the CMC increases with the molecule polyoxyethylene chain prolongation.

Most *ionic* surfactants with the certain chain length show very similar values of the CMC values.[8,15] With higher number of ionized groups included in the surfactant molecule, the value of the CMC increases, due to the increase in the electric work required to the micelle formation.[15] The location of the ionic group in the micelle of surfactant itself affects its micellar properties.

4. Effect of additives in solution on CMC

Electrolyte addition

The electrolyte effect is mostly pronounced for ionic and less for nonionic and amphoteric surfactants. As the ionic power of solutions rises up, the CMC decreases and the transition from spherical to cylindrical shape along with the increase of the micelle aggregation number occurs. The decrease of the CMC value is ascribed to the releasing of counter-ions from hydrophilic parts of surfactants (these ions form the surface cover of the micelle) and also from the added electrolyte. The counter-ions give rise to the Coulombic shielding of the electrostatic repulsions among charged hydrophilic parts of ionic molecules on the micelle surface. The electrolytes dehydration activity is an important effect, which also lowers the CMC of ionic surfactants. Solutions of electrolytes remove the lyosphere of surfactants and, as a consequence, ions become strongly hydrated. In addition, the effect depends on the type of counter-ion.
In the older literature[7], an opinion that the addition of electrolyte has no effect on nonionic surfactants can be found; nowadays it is proved this opinion was a mistake.

The main reason for the CMC lowering of the CMC of nonionic and amphoteric surfactants is the so-called salting-out effect. The work required for the surfactants association in water changes in an electrolyte solution due to water–ion interactions. If this work increases in the presence of an electrolyte, surfactant monomers are salted-out and the micellization is preferred. Electrolyte effects depend upon the radius of the hydrated ion. The smaller the radius is, the greater is the salting-out effect.[8]

Already Klevens[39] in 1948 was engaged not only in the CMC value measuring, but also with the electrolyte effect on the CMC of soaps. He concluded that CMC decreases with the addition of an electrolyte to solution.

As the other authors have also found, the value of the CMC decreases in the presence of an electrolyte in a micellar solution, and this CMC reduction depends on the nature and concentration of cations.[19,40,41] Srinivasan and Blankschtein[42,43] developed the molecular-thermodynamic theory of micellization for ionic surfactants in the solution with added electrolyte. By means of this theory, micellar properties of ionic surfactants in an electrolyte solution can be predicted.

Effect of a counter-ion nature

In connection with the electrolyte effect on the CMC, the effect of the counter-ion nature is strongly associated. The increasing degree of counter-ion binding to a micelle due to their increasing polarity, counter-ion valence or decreasing hydrated radius[8,15], a decrease of the CMC and increase of the aggregation number occurs. [7,44]

Alargova[45-47] compares effect of polyvalence counter-ions Al^{3+}, Ca^{2+} and Na^{+} on the micellar environment, on the growing of micelles, and on the transition between spherical and cylindrical shape of micelles. According to Esposito[41], the aggregation behaviour of anionic detergents is less sensitive to the nature of counter-ion than in the case of cationic surfactants. Bales[22] discusses the counter-ion size effect in the connection with the "cloud point" effect of the anionic surfactant tetrabutylammonium dodecylsulfate. Cloud point is a function of the counter-ion concentration (tetrabutylammonium ion) in aqueous phase. Kumar[23-27] studied also cloud points of ionic surfactants. It can be briefly noted that the cloud point is mentioned in the literature mainly in a context with nonionic surfactants. This effect is exploited for example in analytical separation methods. With ionic surfactants, the cloud point is seldom observed, since electrostatic interactions protect the phase separation.

Organic compound addition

In term of polarity, organic compounds can be divided into *structure forming* of low polarity (the CMC tends to decrease – urea, formamide) and *structure destroying* of high polarity (increases the CMC – xylose, fructosa, dioxan). There are compounds belonging to both of the above-mentioned groups as alcohols with short chain, methanol and ethanol increase the CMC but butanol and pentanol decrease the CMC value. In the case of pentanol, there is a dependence on the concentration of alcohol. The added pentanol of low concentration causes decrease of the CMC, but above 1 mol/l concentration of this alcohol the CMC increases.[7,15]

Polymer compounds addition

When a surfactant interacts with a polymer, mixed micelles of surfactant-micelle type arise.[48] The attractive interactions between the polymer and the surfactant depend upon both of the types of molecules. Two limiting cases of these interactions exist and the real state of this type mixtures is somewhere between these two limit cases. 1) The strong cooperative interactions evoke the surfactant binding onto the polymer that is more suitable for polymers with a hydrophobic chain; 2) The micellization of the surfactant onto or by the polymer is suitable for hydrophilic homopolymers. With the polymer or another added surfactant into the surfactant solution, the arising micelles have a lower value of the CMC. This lower associating concentration is generally not influenced by the added polymer concentration and is called the critical aggregation concentration (CAC). See *Figure 1*.[6,8] The size of growing aggregates is usually smaller then for simple micelles, also after the addition of the salt, whereas in simple micelles the addition of the salt causes the increase of the size.[6]

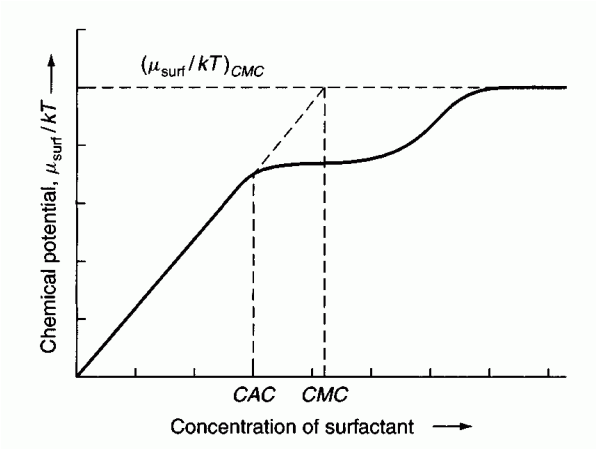

Figure 1. The lowering of the critical concentration in the presence of polymer compound in micellar solution.[8] Taken from D. F. Evans and H. Wennerstrom, *The Colloidal Domain: Where Physics, Chemistry, Biology and Technology Meet,* VCH, New York, (1994)

Other surfactant addition

Mixtures of surfactants are used in many practical applications. These systems often allow more advantageous properties than solutions of simple surfactants they are assembled from. In the mixture of two different surfactants, two kinds of micelles are presented, i.e. micelles of the pure surfactant and mixed micelles formed by both surfactants. Mixed systems of nonionic surfactants allow an ideal behaviour, whereas combinations of other types of surfactants behave not exactly in an ideal way. This no ideal behaviour results from synergistic (attractive) and antagonistic (repulsive) interactions between amphiphiles of different kinds. Factors that follow interactions can be of a different origin. By ionic surfactants, the forming of mixed micelles causes structural changes and changes of the aggregation number. A lot of the authors deal with the elaboration of the molecular theory of mixed micelles formation[49,50], their properties and experimental methods of measuring description[51-61].

5. Experimental methods of CMC measuring

Available literature of the micellar systems research supplies a long list of methods suitable for the obtaining CMC. *Table 1* shows a transparent list of experimental techniques used in the cited literature.

Sensitivity of individual methods corresponds to the value of concentration, which is evaluated as the critical micelle concentration.[8] It is supposed, absolutely

agreement among values of the CMC determined by various experimental techniques could not be achieved.[15] Mukerjee[62] composed the compendium of the CMC values measured by different techniques in different conditions. Van Os[63] updated this compendium in 1993.

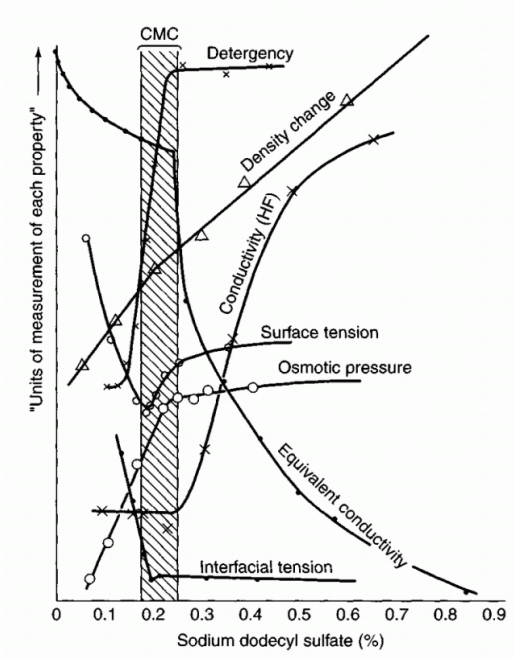

Figure 2. Changes in some physicochemical properties of sodium dodecylsulfate aqueous solution near the CMC.[8] Taken from Preston W.C., *J. Phys. Chem.* **52**, 84 (1948)

The value of the CMC is often obtained from the plot of the experimentally measured property of surfactants versus concentration.[64] The experimental values can be also modificated by certain function to linearise the curve. The most often graph is then composed of two lines, one in the low- and the second in the high-concentration area. Their intersection denotes the value of the CMC after reaching this concentration system containing monomers and micellar aggregates in the solution.[15]

Table 1. Experimental methods used in the CMC measuring.

Measuring method or measured property	***Number of reference***
Surface tension	18, 21, 65 – 68
Light scattering	69 - 71
Conductivity	14, 15, 19, 40, 64, 72 - 80
Capillary electrophoresis	81, 82
Chromatography	83
Refractometry	39
Microcalorimetry	84 - 86
Density	3, 77, 87 - 89
Sound velocity	90
Viscosity	87, 91
Solubilization	92
Magnetic resonance methods	93
Potentiometry	19
Voltammetry	94 - 97
Polarography	98, 99
Fluorescence	41, 100 - 110
Spectral methods	79, 111 – 116
Adsorption effect of optical fibres	117, 118
Heat capacity	119
Equilibrium dialysis	120
Kinetics	121

Detailed description of the important methods

A. The **surface tension** measurement is one of the most common methods used for the CMC determining. Measuring methods of this important property are of different types. Force methods are based on a detaching of the subjects of various shapes from the micellar solution-air interface.

The used subject can be the *Wilhelmy platinum plate*[18,21, 65] or *du Noűy ring*[66-68]. Surface tension measurements destined for the CMC evaluation come in particular from the force methods.[15]

Furthermore, profile methods evaluating the shape of the solution drop, drop weighing and maximum bubble pressure method or the evaluation of effects inside the capillary can be used for determination of surface tension of surfactant solution. The values obtained from these measurements of surfactant solutions are in most cases used for evaluating others physico-chemical properties than CMC.[122-124]

In the most cases, the influence of the surface tension on concentration is obtained from the plot of surface tension values against the logarithm of surfactant concentration. By the gradual increase of the surfactant concentration, the rapid decrease of the solvent surface tension occurs, until the CMC is achieved. Above this concentration the value of the surface tension remains almost constant. It is necessary to mention that the surface tension is strongly influenced by temperature changes and

impurities in the solution. These methods measure the surface concentration of all surface-active compounds included in the solution, not the presence of micelles in the bulk. Already small traces of impurities in the solution can deeply affect the time change of the surface tension. Mysels[125] assumed that time change of the surface tension or the dynamic surface tension can be used as the effective criterion of the surface purity.

B. **Light scattering methods**. There is a great importance of the solution purity again.[8] Debye and Anacker[126] measured the light scattering of surfactant solutions and found out that micelles were relatively small in solutions of small ionic power, however in the presence of salt in the solution, micelles grew up so, they were able to scatter the light beam dissymetrically. Size and shape of aggregates thus depends on the nature and concentration of other species in the solution. The concrete measurements of static and dynamic light scattering are mentioned for example in the publication[127].

C. **Conductometry** is a very simple method, which allows enough precise values of the CMCs for ionic surfactants. Necessary conditions for obtaining the most accurate values are the constant temperature maintenance through the whole measuring process and elimination of impurities influencing the movement of charged species in the solution. The Onsager dependence is valid for very diluted electrolyte solutions, and therefore can be applied to aqueous systems of charged surfactants, whose CMCs have been found in the 10^{-3} mol.dm^{-3} concentration region.[15,40,64] The value of CMC is simply obtained as the intersection point of two line parts of the curve.

The recently publicated experimental studies are focused on the precise evaluation of the CMC from measured data. Some surfactants have no sharp break point on the conductivity curve, but the section of curve between two linear parts is curved. This curvature can be evaluated statistically or by modification of the magnitude yielded up in the plot as the one point denoting the CMC.[72,73] The conductometry method can be also used for the evaluation of the CMC data for mixed micelles systems and for the surfactants with a small aggregation number. Described procedures are almost of a statistical or a numerical character.[14,74-76] The conductivity data are also used for evaluating of the micellization constant, aggregation number, number of counter-ions on a micelle, degree of micelle ionization and a lot of thermodynamic data determining for simple and mixed micelles.[128-130]

The best way in which the CMC values from **viscosity** data can be obtained is to yield the specific or the intrinsic viscosity on the y-axis of the concentration plot. The CMC is denoted by the change in the line slope. The viscometry technique used for this purpose needs a very sensitive measuring. Good results were gained using the Ostwald viscometer. The method is more suitable for nonionics because of the fact that no electroviscous effect is proposed.[8] The majority of scientists use the viscometric method more often for the explanation of electrolyte effects on the viscoelastic behaviour of micellar solutions.[131-134]

E. **Dye solubilization** works with dyes soluble in oils. These dyes can be solubilized in the aqueous solution containing micelles. Dye solubility is constant until the CMC is reached. Above the CMC, solubility rises quickly and almost linearly. This method is

suitable for aqueous and also for nonaqueous (using water soluble dyes) solutions.[8] The CMC determinated from the color, absorption spectra changes, or change of the amount of the solubilizate is mainly used in industry. The measurement results can be affected by the indicator effect upon the micellization process and also by indicator-surfactant chemical reactions. The dye and surfactant ions can form a salt, insoluble bellow the CMC. Above it, this salt is solubilized in micelles. Generally, compounds solubilized in micelles significantly lower the CMC values. And that is the main reason why measured CMC values using solubilization method are lower than values obtained by other experimental techniques.[15] The spectra of dyes added to the surfactant solution in a small amount (usually the concentration range from 10^{-4} to 10^{-5} M, limited by the spectrophotometer sensitivity) differ in premicellar and micellar region.
Dye micellization methods are based on this dependence. Interaction between dye and micelle causes the shift in absorption spectra. The CMC is evaluated from the absorbance at the certain wavelength versus concentration plot. Dyes used for this method have a large extinction coefficients and a large sensitivity to the particular microenvironment. For example Fluorescein, Erythrosin, Crystal Violet, Methyl Orange etc.[8,92,115,135]

Short description of others methods

Fluorescence for the study of micellization, the fluorescence probe adding into the solution is necessary. The most often used is the pyrene probe.[101-107,136] Among others fluorescence probes could be mentioned, pyrene-3-carboxaldehyde[106] or 1,6-diphenyl-1,3,5-hexatriene (DPH)[108], 8-anilinonaphthalenesulfonic acid magnesium salt (ANS)[109] and monoazacryptand-Ba^{2+} complex[110].

Partial molal volume – this method involves a precise measurement of the solution density and concentration of the surfactant. The accuracy of this method is strongly affected by temperature, which is recommend to be kept constant. A change of the partial molal volume is reflected by the change of density of the solution. This method can be used for all kinds of surfactant in aqueous and also in nonaqueous environment.[4,8,77,87-89]

Molecular absorption – it is known that absorption spectra differ in the monomer and the micellar state. The absorbance dependence, measured by UV-VIS spectrometry, upon concentration at the certain wavelength shows the slope change, taken as the CMC.[8]

Refractive index is an experimental method applicable on any kind of surfactant or solvent. But it is really necessary to keep the temperature constant and previous precise determining of the surfactant concentration in the solution.[8,39]

Sound velocity – in a liquid system, the sound velocity is related to the molecular weight through the equation, which involves density, refractive index and two empirical constants. The CMC value can be determined as the breakpoint on the speed of sound against concentration curve.[8,90]

Voltammetry and polarography – Ma[94] determined the first and second CMCs of SDS and CTAB by adsorptive voltammetry with "neutral red" (3-Amino-6-dimethylamino-2-methylphenazine hydrochloride) as an electrochemical probe.
The polarography method was also used. For example Colichman[98,99] measured the CMC of TritonX-100 and other surface active agents by this technique.

Calorimetry – Stodghill[84] carried out calorimetric measurements using the isothermal titration calorimetry (ITC). The thermodynamics of micellar systems can be studied within this method. The CMC can be determined as the inflection point of the line between the low-concentration plateau and the high-concentration plateau. Király[81], Majhi[82] also used this method for determination of the CMC of various types of surfactants.

Vapor pressure osmometry – The solvent changes its vapor pressure in the presence of any surfactant. The technique is based on the comparison of the solution drop and the solvent drop temperature. Thus, measurements of the pressure-concentration dependence can be used for the CMC evaluation.[8]

6. Micellar systems applications in the catalysis and separation methods

Micellar catalysis

The catalytic efficiency can be included in the chemical properties of surfactants.[7] Chemical processes can be kinetically modified in the presence of surfactant micelles. If micelles associate with reactants or products, then reaction rate or distribution of products can be modified. It is supposed, micellar environment can affect transition states of reactions and alter reaction rates. The hydrophobic cores of micelles represent the driving power for substrate associating with a micelle. In the micellar pseudo-phase, reactants of the hydrophobic nature can be preferentially solubilized and their concentration is controlled here. Both the electrostatic and the geometric factor are important in the micellar catalysis. For example, hydrophilic part of the amphiphile, its charge, volume and hydration influence the catalytic power of the micelle. Hydrophilic parts function in the transition states modification can be contradictory to the function of hydrophobic cores associating the substrate. The most important effect in the micellar catalysis is related to the control of local concentrations of components in bimolecular reactions.[5,6]
The effect of micelles onto the monomolecular reaction is analogous to the enzymatic catalysis.[137] If micellar and enzymatic catalysis are compared, the substrate specifity of the micellar one is much lower and thus the rate increase is also much smaller. The substrate concentration in the enzymatic catalysis is much smaller than the enzyme concentration, whereas the micelle concentration in the micellar catalysis is usually of the same order as at least one of the reactants.

Separation methods

The unique properties of the surfactants can be utilized for modification and improvement of separation techniques in a liquid phase, in detail for the case of liquid chromatography and capillary electrophoresis.[138]

Capillary electrophoresis (CE)

A thin capillary is filled with the electrolyte solution and the electric potential is applicated. Thanks to the combination of electrophoretic migration and electroosmotic flow effects, the process of transport and separation of the solutes occurs. The solutes without charge do not separate.[15]

Jacquier[139] presented the publication of the theoretical background for the CMC determining of surfactants, using CE methods. Lin published a study[140] that is focused on determination of the CMC of the cationic surfactants by the capillary electrophoresis first. Five years later, he extended it to the comprehensive review[141] about CE method and its modifications as MECC applications in the determining of the CMC values of charged and also of the discharged surfactants in aqueous and in non-aqueous media.

Micellar liquid chromatography (MLC)

This method uses surfactants for partial or complete substitution of the polar organic component in aqueous mobile phase. The theoretical background have been developed working on HPLC.[15] Armstrong and Nome extended the partition theory to MLC.[142]

The principle of MLC method is based on the analyte separation between the aqueous phase, micellar pseudophase and the stationary phase covered with surfactant. Thus the use of the secondary chemical equilibrium is taken in this case; concretely the analyte separates between water and the micellar phase.[138]

By combining of CE and MLC methods principles, the **micellar electrokinetic capillary chromatography (MECC)** has been invented. As in all CE methods, also in MECC the separation occurs in thin capillaries where a great electrical field is applicated on.[143] Thanks to the principle of this experimental technique, electrophoretic separation of uncharged compounds is possible, whereas classical CE cannot be used so. And moreover, the selectivity is improved for determining of charged solutes.[144] Micelles behave as a liquid "pseudostationary phase". Ionic micelles presented in the flowing buffer solution migrate with a different rate than the electrolyte solution in the bulk.

In traditional liquid chromatography, the retention of each analyte is driven by solute-solvent interactions and the secondary arising contributions from solute-stationary phase interactions. In micellar chromatography, there is a more complex distribution pattern of solutes among micellar aggregates, the bulk solution and the stationary phase.

The advantages of these reverse-phase systems were presented in some reviews [145,146].

If the MECC is carrying out in the capillary whose walls are covered with a suitable polymer, the electroosmotic flow is eliminated. In this case, we can talk about **micellar electrokinetic capillary chromatography with reduced electroosmotic flow**

(RF-MECC). This method resolve the problem of compounds of the hydrophobic character, strongly bound on the micelles. Their retention factor is high and the separation is incomplete.

The newest research developed a method based on the MECC and the ligand exchange. It is **ligand exchange-micellar electrokinetic chromatography (LE-MECC)** and Chen[83] used it for the CMC of anionic surfactants determination.

7. Conclusion

The presented review summarises the experimental methods used for the CMC measuring and describes the effects of the added compounds on the surfactant solution behaviour. It is understood that although the CMC value is a very important parameter the effect of additives and electrolytes of various types has not been recognised in details up to the present. Especially for this particular reason and in context with the increasing number of applications, particularly in analytical chemistry, it is necessarily to continue in the research of these regularities. The use of experimental techniques such as e.g. DLS, NMR etc., for this purpose, enables more detailed insight into the composition of the systems.

References

1. Maibaum L., Dinner A.R., Chandler D., *J. Phys. Chem. B* **108**, 6778 (2004)
2. McBain J. W., *Trans. Faraday Soc.* **9**, 99 (1913)
3. Davies J.T., Bury C. R., *J. Chem. Soc.*, 2263 (1930)
4. Hartley G. S.: *Aqueous Solutions of Paraffin Chain Salts*, Hermann, Paris (1936)
5. Meyers R.: *Encyclopedia of Physical Science and Technology*, California (2002)
6. Moore J. H., Spencer N. D.: *Encyclopedia of Chemical Physics and Physical Chemistry*, Institute of Physics (2001)
7. Blažej A.: *Tenzidy*, ALFA, Bratislava (1977)
8. Holmberg K.: *Handbook of applied surface and colloid chemistry*, J. Wiley (2002)
9. Patist A., Oh S. G., Leung R., Shah D. O., *Colloid Surfaces A* **176**, 3 (2001)
10. Drummond C. J., Fong C., *Curr. Opin. Colloid Interface Sci*. **4**, 449 (2000)
11. Abbott N. L., MacKay R. A., *Curr. Opin. Colloid Interface Sci.* **4**, 323 (1999)
12. John V. T., Simmons B., McPherson G. L., Bose A., *Curr. Opin. Colloid Interface Sci.* **7**, 288 (2002)
13. Bognolo G., *Adv. Colloid and Interface Science* **106**, 169 (2003)
14. Nalwa H. S.: *Handbook of Surfaces and Interfaces of Materials*, Vol. **3**, 405, London (2001)
15. Weber S. G.: *Surfactants in Analytical Chemistry – Applications of Organized Amphiphilic Media*, Elsevier, Amsterdam (1996)
16. Flockhart B. D., *J. Colloid Interface Sci.* **16**, 484 (1961)
17. La Mesa C., *J. Phys. Chem.* **94**, 323 (1990)
18. Schick M. J., *J. Phys. Chem.* **67,** 1796 (1963)
19. Vojtekova M., Kopecký F., Greksakova O., Oremusova J., *Collect. Czech. Chem. Commun.* **59**, 99 (1994)
20. Crook E. H., Trebbi G. F., Fordyce D. B., *J. Phys. Chem.* **68**, 3592 (1964)
21. Chen L. J., Lin S. Y., Huang C. C., Chen E. M., *Colloids and Surfaces A* **135**, 175 (1998)
22. Bales B. L., Zana R., *Langmuir* **20**, 1579 (2004)
23. Kumar S., Sharma D., Ud-Din K., *Langmuir* **16**, 6821 (2000)
24. Kumar S., Sharma D., Khan Z. A., Ud-Din K., *Langmuir* **17**, 5813 (2001)

25. Kumar S., Aswal V. K, Naqvi A. Z., Goyal P. S., Ud-Din K., *Langmuir* **17**, 2549 (2001)
26. Kumar S., Sharma D., Khan Z. A., Ud-Din K., *Langmuir* **18**, 4205 (2002)
27. Kumar S., Sharma D., Ud-Din K., *Langmuir* **19**, 3539 (2003)
28. Brown W., Rymdik R., van Stam J., Almgren M., Svensk G., *J. Phys. Chem.* **93**, 2512 (1989)
29. Corti M., Minero C., Degiorgio V., *J. Phys. Chem.* **88**, 309 (1984)
30. Komaromy-Hiller G., Von Wandruszka R., *J. Colloid Interface Sci.* **177**, 156 (1996)
31. Goel S. K., *J. Colloid Interface Sci.* **212,** 604 (1999)
32. Tanford C., *J. Phys. Chem.* **76**, 3020 (1972)
33. Shinoda K., Hutchinson E., *J. Phys. Chem.* **66**, 577 (1962)
34. Mukerjee P., *J. Phys. Chem.* **66**, 1375 (1962)
35. Yu Z.J., Xu G., *J. Phys. Chem.* **93**, 7441 (1989)
36. Rusanov A. I., *Adv. Colloid Interface Sci.* **45**, 1 (1993)
37. Monduzzi M., *Curr. Opin. Colloid Interface Sci.* **3**, 467 (1998)
38. Matsuoka K., Moroi Y., *Curr. Opin. Colloid Interface Sci.* **8**, 227 (2003)
39. Klevens H. B., *J. Phys. Chem.* **52**, 130 (1948)
40. Dutkiewicz E., Jakubowska A., *Colloid Polym Sci.* **280**, 1009 (2002)
41. Esposito C., Colicchio P., Facchiano A., Ragone R., *J. Colloid Interface Sci.* **200**, 310 (1998)
42. Srinivasan V., Blankschtein D., *Langmuir* **19**, 9932 (2003)
43. Srinivasan V., Blankschtein D., *Langmuir* **19**, 9946 (2003)
44. Mukerjee P., Mysels K. J., Kapauan P., *J. Phys. Chem.* **71**, 4166 (1967)
45. Alargova R., Petkov J., Petsev D., Ivanov I. B., Broze G., Mehreteab A., *Langmuir* **11**, 1530 (1995)
46. Alargova R. G., Danov K. D., Kralchevsky P. A., Broze G., Mehreteab A., *Langmuir* **14**, 4036 (1998)
47. Alargova R. G., Ivanova V. P., Kralchevsky P. A., Mehreteab A., Broze G., *Colloids and Surfaces A* **142**, 201 (1998)
48. Nowakowska M., Szczubiałka K., Gręboszm M., *J. Colloid Interface Sci.* **265**, 214 (2003)
49. Nagarajan R., *Langmuir* **1**, 331 (1985)
50. Thomas H. G., Lomakin A., Blankschtein D., Benedek G. B., *Langmuir* **13**, 209 (1997)
51. Hines J. D., *Curr. Opin. Colloid Interface Sci* **6**, 350 (2001)
52. Kang K. H., Kim H. U., Lim K. H., Jeong N. H., *Bull. Korean Chem. Soc.* **22**, 1009 (2001)
53. Garamus V. M., *Langmuir* **19**, 7214 (2003)
54. Muñoz M., Rodríguez A., Graciani M. M., Moyá M. L., *Langmuir* **20**, 10858 (2004)
55. Sharma K. S., Rodgers C., Palepu R. M., Rakshit A. K., *J. Colloid Interface Sci.* **268**, 482 (2003)
56. Aswal V. K., *Chem. Phys. Lett.* **371**, 371 (2003)
57. Attwood D., Patel H. K., *J. Colloid Interface Sci.* **129**, 222 (1989)
58. Treiner C., Makayssi A., *Langmuir* **8**, 794 (1992)
59. Bury R., Treiner C., Chevalet J., Makayssi A., *Anal. Chim. Acta* **251**, 69 (1991)
60. Moulik S. P., Haque E., Jana P. K., Das A. R.**,** *J. Phys. Chem.* **100**, 701 (1996)
61. Yang X. Y., Tan X. L., Cheng G. Z., Yuan H. Z., Mao S. Z., Zhao S., Yu J. Y., Du Y. R., *J. Colloid Interface Sci.* **279**, 533 (2004)
62. Mukerjee P., Mysels K.: *Critical Micelle Concentrations of Aqueous Surfactant Systems,* National Standards Reference Data Series, Vol. 36, National Bureau of Standards, Washington DC. (1971)
63. Van Os N. M. et al.: *Physico-Chemical Properties of Selected Anionic, Cationic and Nonionic Surfactants*, Elsevier, Amsterdam (1993)
64. Wright K. A., Abbott A. D., Sivertz V., Tartar H. V., *J. Am. Chem. Soc.* **61**, 549 (1939)
65. Schick M. J., Atlas S. M., Eirich F. R., *J. Phys. Chem.* **66,** 1326 (1962)
66. Eastoe J., Dalton J. S., Rogueda P. G. A., Crooks E. R., Pitt A. R., Simister E. A., *J. Colloid Interface Sci.* **188**, 423 (1997)
67. Hsiao L., Dunning H. N., Lorenz P. B., *J. Phys. Chem.* **60,** 657 (1956)
68. Crook E. H., Fordyce D. B., Trebbi G. F., *J. Phys. Chem.* **67**, 1987 (1963)
69. Debye P., Light Scattering in Soap Solutions, *J. Phys. Chem.* **53**, 1 (1949)
70. Phillips J. N., Mysels K. J., *J. Phys. Chem*. **59,** 325 (1955)
71. Mysels K.J., Princen L.H., *J. Phys. Chem.* **63**, 1699 (1959)
72. Manabe M., Kawamura H., Yamashita A., Tokunaga S., *J. Colloid Interface Sci.* **115**, 147 (1987)
73. Sugihara G., Era Y., Funatsu M., Kunitake T., Lee S., Sasaki Y., *J. Colloid Interface Sci.* **187**, 435 (1997)
74. García-Mateos I., Velázquez M. M., Rodríguez L. J., *Langmuir* **6**, 1078 (1990)

75. Pérez–Rodríguez M., Prieto G., Rega C., Varela L. M., Sarmiento F., Mosquera V., *Langmuir* **14**, 4422 (1998)
76. Carpena P., Aguiar J., Bernaola-Galván P., Carnero Ruiz C., *Langmuir* **18**, 6054 (2002)
77. Castillo J.L., Czapkiewicz J., González Pérez A., Rodríguez J.R., *Colloids and Surfaces A* **166**, 161 (2000)
78. Kay R. L., Lee K. S., *J. Phys. Chem.* **90**, 5266 (1986)
79. Benito I., Garcia M.A., Monge C., Saz J.M., Marina M.L., *Colloids and Surfaces A* **125**, 221 (1997)
80. Voeks J. F., Tartar H. V., *J. Phys. Chem.* **59**, 1190 (1955)
81. Cifuentes A., Bernal J. L., Diez-Masa J.C., *Anal. Chem.* **69**, 4271 (1997)
82. Terabe S., *Anal. Chem.* **57**, 834 **(**1985)
83. Chen Z., Lin J. M., Uchiyama K., Hobo T., *Anal. Chim. Acta.* **403**, 173 (2000)
84. Stodghill S. P., Smith A. E., O'Haver J. H., *Langmuir* **20**, 11387 (2004)
85. Király Z., Dekány I., *J. Colloid Interface Sci.* **242,** 214 (2001)
86. Majhi P. R., Moulik S. P., *Langmuir* **14**, 3986 (1998)
87. Wright K. A., Tartar H. V., *J. Am. Chem. Soc.* **61**, 544 (1939)
88. Grindley B. J., Bury C. R., *J. Chem. Soc.,* 679 (1929)
89. Bury C. R., Parry, *J. Chem. Soc.*, 626 (1935)
90. Junquera E., Tardajos G., Aicart E., *Langmuir* **9**,1213 (1993)
91. Poskanzer A. M., Goodrich F. C., *J. Phys. Chem.* **79**, 2122 (1975)
92. Vulliez-Le Normand B., Eiselé J. L., *Anal. Biochem.* **208**, 241 (1993)
93. Müller N., Pellerin J. H., Chen W. W., *J. Phys. Chem.* **76**, 3012 (1972)
94. Ma C., Li G., Xu Y., Wang H., Ye X., *Colloids and Surfaces A* **143**, 89 (1998)
95. Mandal A. B., Nair B. U., Ramaswamy D., *Langmuir* **4**, 736 (1988)
96. Texter J., Horch F. R., *J. Colloid. Interface Sci.* **135**, 263 (1990)
97. Kjellin U. R. M., Reimer J., Hansson P., *J. Colloid Interface Sci.* **262**, 506 (2003)
98. Colichman E. L., *J. Am. Chem. Soc.* **72**, 4036 (1950)
99. Colichman E. L., *J. Am. Chem. Soc.* **73**, 1795 (1951)
100. De Vendittis E., Palumbo G., Parlato G., Bocchini V., *Anal. Biochem.* **115**, 278 (1981)
101. Aguiar J., Carpena P., Molina-Bolívar J.A., Carnero Ruiz C., *J. Colloid Interface Sci.* **258**, 116 (2003)
102. Frindi M., Michels B., Zana R.**,** *J. Phys. Chem.* **96**, 8137 (1992)
103. Zana R., Lévy H., Kwetkat K., *J. Colloid Interface Sci.* **197**, 370 (1998)
104. Regev O., Zana R., *J. Colloid Interface Sci.* **210**, 8 (1999)
105. Sugioka H., Matsuoka K., Moroi Y., *J. Colloid Interface Sci.* **259**, 156 (2003)
106. Ananthapadmanabhan K. P., Goddard E. D., Turro N. J., Kuo P. L., *Langmuir* **1**, 352 (1985)
107. Hara H., Suzuki H., Takisawa N., *J. Phys. Chem.* **93**, 3710 (1989)
108. Zhang X., Jackson J. K., Burt H. M., *J. Biochem. Biophys. Methods* **31**, 145 (1996)
109. De Vendittis E., Palumbo G., Parlato G., Bocchini V., *Anal. Biochem.* **115**, 278 (1981)
110. Nakahara Y., Kida T., Nakatsuji Y., Akashi M., *Langmuir* **21**, 6688 (2005)
111. Mukerjee P., Mysels K. J., *J. Am. Chem. Soc.* **77**, 2937 (1955)
112. Becher P., *J. Phys. Chem.* **66**, 374 (1962)
113. Kapoor R. C., Chand P., Aggarwala V. P., *Anal. Chem.* **44**, 2107 (1972)
114. Ledbetter Jr., J. W., Bowen J. R., *Anal. Chem.* **43**, 773 (1971)
115. Corrin M. L., Harkins W. D., *J. Am. Chem. Soc.* **69,** 679 (1947)
116. Corrin M.L., Harkins W., *J. Am. Chem. Soc.* **69,** 683(1947)
117. Ogita M., Nagai Y., Mehta M.A., Fujinami T., *Sensors and Actuators B* **64**, 147 (2000)
118. Singh C.D., ShibataY., Ogita M., *Sensors and Actuators B* **96**, 130 (2003)
119. Dearden L. V., Woolley E. M., *J. Phys. Chem.* **91**, 4123 (1987)
120. Yang J. T. , Foster J. F., *J. Phys. Chem.* **57**, 628 (1953)
121. Perkowski J. , Mayer J., Ledakowicz S., *Colloids and Surfaces A* **101**, 103 (1995)
122. Blandamer M. J., Cullis P. M., Soldi L. G., Engerts J. B. F. N., Kacperska A., Van Os N. M., Subha M. C. S., *Adv. Colloid Interface Sci.* **58**, 171 (1995)
123. Teipel U., Aksel N., *Chem. Eng. Technol.* **24**, 393 (2001)
124. Yang C., Gu Y., *Langmuir* **20**, 2503 (2004)
125. Mysels K. J., *Langmuir* **2**, 423 (1986)
126. Debye P., Anacker E. W., *J. Phys. Chem.* **55**, 644 (1951)

127. Richtering W. H., Burchard W., Jahns E., Finkelmann H., *J. Phys. Chem.* **92**, 6032 (1988)
128. Moroi Y., Yoshida N., *Langmuir* **13**, 3909 (1997)
129. Dev S., Gunaseelan K., Ismail K., *Langmuir* **16**, 6110 (2000)
130. Gunaseelan K., Ismail K., *J. Colloid Interface Sci.* **258**, 110 (2003)
131. Cappelaere E., Cressely R., Decruppe J.P., *Colloids and Surfaces A* **104**, 353 (1995)
132. Berret J. F., *Langmuir* **13**, 2227 (1997)
133. Angelescu D., Khan A., Caldararu H., *Langmuir* **19**, 9155 (2003)
134. Ud-Din K., David S. L., Kumar S., *J. Chem. Eng. Data* **42**, 1224 (1997)
135. Mandal A.S., Nair B. U., *J. Phys. Chem.* **95**, 9008 (1991)
136. Anthony O., Zana R., *Macromolecules* **27**, 3885 (1994)
137. Menger F. M., Portnoy C. E., *J. Am. Chem. Soc.* **89**, 4698 (1967)
138. Fischer J., Jandera P.: Využití tenzidů v separačních metodách, str. 11. In Sborník přednášek z XXXV. semináře o tenzidech a detergentech, Ed. Kalous J. a Vytřas K., Lázně Bohdaneč 2001.
139. Jacquier J.C., Desbéne P.L., *J. Chromatogr. A* **718**, 167 (1995)
140. Lin C. E., Wang T. Z., Chiu T. C., Hsueh C. C., *J. High Resol. Chromatogr.* **22**, 265 (1999)
141. Lin C. E., *J. Chromatogr. A* **1037**, 467 (2004)
142. Armstrong D. W., Nome F., *Anal. Chem.* **53**, 1662 (1981)
143. Jörgenson J. W., Lukacs K. D., *Anal. Chem.* **5**, 1298 (1981)
144. Terabe S., *Anal. Chem.* **56**, 111 (1984)
145. Khaledi M. G., *Trends Anal. Chem.* **7**, 293 (1988)
146. Borgerding M. F., Willams R. L., Hinze W. L., Quina F. H., *J. Liq. Chromatogr.* **12**, 1367 (1989)

Acta Univ. Palacki. Olomuc.
Fac. rer. nat. 2005
Chemica 44, 7 - 23

ACTA UNIVERSITATIS PALACKIANAE OLOMOUCENSIS
FACULTAS RERUM NATURALIUM (2005) CHEMICA 44

SURFACE ENERGY – EFFECTS OF PHYSICAL AND CHEMICAL SURFACE PROPERTIES

Jana Vojtěchovská*, Libor Kvítek

Department of Physical Chemistry, Palacký University, Tř. Svobody 8, 771 47 Olomouc, Czech Republic, E-mail: jvojtechovska@volny.cz

Received May 19, 2005.
Accepted August 30, 2005.

Abstract

Contact angle can be an important value in industry and science. However, making meaningful contact angle measurements and interpreting these measurements is a complex problem. For years, researchers have produced a wide variety of issues concerning contact angles, some questions have been answered, and the others have still remained open. The aim of this article is focused on the appropriate definitions and use of contact angle and solid surface energy. Interfacial solid – liquid interactions play a crucial role in wetting and adhesion processes. Contact angle measurements are commonly utilized for the determination of solid surface energy and its components. This paper offers a brief review of the fundamental theories and approaches that have been proposed in literature, but formulation of surface and interfacial free energy, as regards its components, is still questionable.

Key words: *contact angle, solid surface energy, contact angle hysteresis*

Introduction

Knowledge about mutual interactions between phases and possibility to determine free surface energy values of materials is required in many industrial applications and it is also useful for finding optimal functions and utilization of materials. Pharmaceutical and cosmetic industries are well known fields where surface chemistry is used. Surface free energies and its components between two interacting surfaces are critically important for processes like stabilization of aqueous colloidal suspensions, control of the dynamics of molecular self-assembly[1, 2], wetting, spreading of liquids on solid surface, adhesion of materials etc.[3, 4] Determination of interfacial

* Author for correspondence

tensions (energies) solid – vapour (γ_{sv}) and solid – liquid (γ_{sl}) is therefore widely used in applied chemistry, biochemistry, and industry.

1. Surface energy

Sources of interfacial surface energy are cohesive (between molecules of one type of material) and adhesive forces (between two different materials). These forces are the result of unlike charge attractions among molecules. The most important forces relative to adhesion and surface energy are the van der Waals forces.[5, 6]

Forces acting on surface molecules are not compensated like in the bulk of the phase. Hence the energy of surface or interface layer is different from the bulk. The existence of liquids surface energy is simply demonstrated by the fact that a drop of liquid tends to go to its lowest energy state, i.e. it assumes a spherical shape in the absence of gravitational distortion. Considering the fact that forces acting on surface molecules in the direction from the liquid are negligible, surface energy [mJ/m^2] of pure liquids is equalled to its surface tension γ_{lv} [mN/m]. For a solid surface, surface energy and surface tension are not the same. It is an easy matter to measure the surface tension of a liquid in equilibrium with its vapour (γ_{lv}) with a duNouy ring or Wilhelmy plate.[7-9] This kind of direct measurements for solid surface energies are mostly use near the melting point, whereas the majority of surface phenomenon is observable below room temperature. Hence the surface free energies of solids are indirectly estimated through contact angle methods[10-13], capillary penetration into columns of powder material[14-16], particles sedimentation[17], Lifshitz theory of van der Waals forces[18], AFM-microscopy[19-20] etc. The contact angle measurement, as one of the mentioned methods, is experimentally believed to be the simplest one, which allows determination of a solid surface energy.

2. Contact angle

There is no doubt that the understanding of surface phenomena and especially wetting is very important for improvement and further development in the processes related to the surface chemistry. First studies about wetting were published by Laplace and Poisson during the eighteenth and early nineteenth century. Their results played an important role in establishing of the fundamental background for capillarity.[21, 22] Surface energy and surface tension are closely connected with one very important parameter used in surface chemistry, *contact angle* θ . Approximately 200 years ago, Thomas Young (1805) proposed contact angle of liquid as a mechanical equilibrium of the drop resting on a plane solid surface at the three-phase boundary.[23] This concept was then thermodynamically proved on more rigorous basis by Gibbs. Since that time it has been known that the behaviour of liquid on a solid surface is controlled by competition between the interfacial energies of the liquid – vapour γ_{lv}, solid – liquid γ_{sl} and solid – vapour γ_{sv} interfaces (Fig.1).

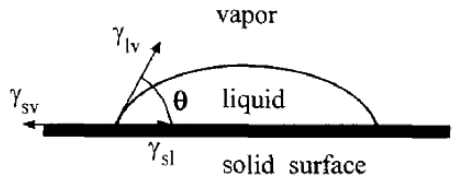

Figure 1. Illustration of an equilibrium sessile drop system

This relation of interfacial energies is generally known as Young equation:

$$\gamma_{lv}\cos\theta_Y = \gamma_{sv} - \gamma_{sl} \quad (1)$$

where γ_{lv} is surface energy on a liquid – vapour interface, γ_{sv} is surface energy on a solid – vapour interface and γ_{sl} is surface energy on a solid – liquid interface, θ_Y is Young's contact angle, which is formed in contact point of liquid drop and solid. It is obvious that experimental values of contact angles θ are not necessary equal those ideal Young's contact angle θ_Y. Equation (1) is of limited practical significance. It can be applied only for solids with homogeneous surfaces, perfectly plane and smooth, rigid and which are not attacked by the probing liquid or liquid components (chemical reaction, dissolution, swelling). In the rest of the real cases, where heterogeneity and roughness are present, infinite metastable states exist, so that it is not possible to measure a single equilibrium contact angle, but a wide set, comprised between two extremes. The highest value is called the *advancing* contact angle θ_a and the lowest one *receding* contact angle θ_r. Their difference is called *contact angle hysteresis H*:[5, 24, 25]

$$H = \theta_a - \theta_r \quad (2)$$

From the equation (1) it can be understood that the contact angle can reach values only in the interval from 0° to 180°. The rage of values between 0 – 90° refer about good wettability of solid, the values of contact angles in the interval from 90° to 180°) 90 – 180° indicate a bad solid wettability. Although a zero contact angle is frequently observed in practice (complete wetting or spreading), the contact angle 180° is not realistic. There does not exist any such system in nature, or created by man, which exhibits no interaction. A spontaneous and complete spreading of liquid occurs over the solid surface when the *spreading coefficient* S_{slv} is positive or at least zero.[9, 26] The spreading coefficient is expressed by the following equation (3):

$$S_{slv} = \gamma_{sv} - \gamma_{sl} - \gamma_{lv} \quad (3)$$

If S_{slv} is negative, the solid – vapour interface will have the lower free energy, i.e. the liquid does not spread and partial wetting occurs. In this case, the liquid drop deposited on a solid surface will form an equilibrium shape. There occurs a spontaneous spreading in the case of positive S_{slv} and the equilibrium state corresponds to a complete coverage of the solid by a liquid film.

The solid surface in a solid – vapour system can be modified by adsorption from the vapour phase. Depending on the nature of the liquid (non-volatile or volatile) the difference of "dry" wetting and "moist" wetting must be distinguished, corresponding to two extreme situations. In the case of dry wetting, the vapour pressure of the liquid is negligible and it is assumed that the liquid molecules, adsorbed on the solid surface, do not significantly change the surface properties in the process of) wetting. If moist wetting occurs, the drop will be in equilibrium with the vapour of the liquid and usually a film of liquid is adsorbed on the solid surface. The film can be thick and even macroscopic in the case of complete wetting. This effect of adsorption can be expressed by the following equation for interfacial tension γ_{sv} of the modified solid surface:

$$\gamma_{sv} = \gamma_s^0 - \pi_e \qquad (4)$$

where γ_s^0 is the surface tension of the bare solid and π_e is the so-called *film pressure* (Fig.2). Combination of equations (4) and (1) results in:

$$\gamma_{lv}\cos\theta = \gamma_s^0 - \pi_e - \gamma_{sl} \qquad (5)$$

Since adsorption is a spontaneous process, the interfacial tension γ_{sv} after adsorption is lower than that of the bare solid.

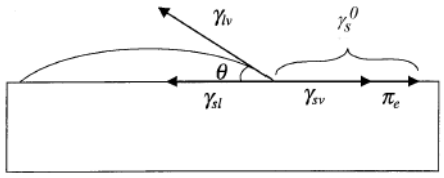

Figure 2. Contact angle of a sessile drop accounting for spreading pressure[74]

It is assumed that the term π_e is usually unimportant for non-wetting liquids, but it can be quite important for more hydrophilic surfaces, particularly if $\gamma_{sv} \approx \gamma_{lv}$ or $\gamma_{lv} \langle \gamma_{sv}$.[3,

[5, 9, 27] According to some authors π_e can be neglected if contact angle values are $\theta \rangle 10°$.[28] Parameter π_e can be measured due to thickness of adsorbed layer by ellipsometry.[29]

2.1. Contact angle hysteresis

The results of contact angle measurements are often hysteresis loops (Fig.3). Contact angle hysteresis can have several reasons that can be divided into the thermodynamic and kinetic ones.[30] In the case of thermodynamic hysteresis the advancing and the receding contact angle values have to be stable, independent on time or number of cycles. There are two main accounts for this type of hysteresis; surface roughness and surface chemical heterogeneity. In contrast to the thermodynamic hysteresis, kinetic hysteresis is time-dependent and the main reasons are swelling, deformation of elastomeric material surfaces and adsorption from liquid phase.[3, 5, 9]

Almost all solid samples exhibit surface heterogeneity. Solid surface characteristics are influenced by the procedure of preparation and by its environment. In particular metal surfaces are difficult to protect against chemical (corrosion reactions) and physical (adsorption of the gas components) interactions with the atmosphere. High-energy solid surfaces (γ_{sv} >100 mJ/m^2) such as mineral[31-35] and metal surfaces are energetically less stable than low-energy surfaces (γ_{sv} <100 mJ/m^2, polymers), and thus they are sensitive to environmental contaminations. Surface heterogeneity, its magnitude, shape and distribution involve contact angle values, but a complete theory for such impacts is not available yet because the existing models supply only a partial explanation of the hysteresis.

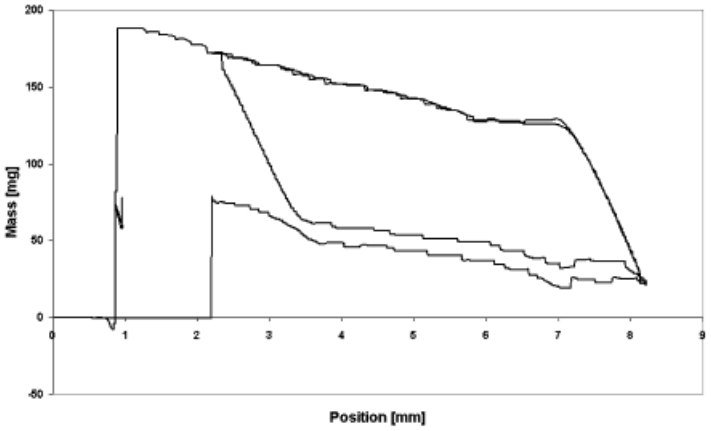

Figure 3. Double hysteresis loop – Wilhelmy experiment

Johnson and Dettre (1964) have characterized some of the general properties of the hysteresis by analysing some model surfaces with a well-defined roughness or heterogeneity they were aware of its magnitude, geometry and distribution, it is noticeable that they didn't study contact angle hysteresis on surfaces which are both heterogeneous and rough.[36, 37] It seems to be only one apparent contact angle on chemically homogeneous rough surface, but due to geometric structure, there are at least two experimental values, in detail the advancing and the receding contact angle. The first one is in general larger and the second one smaller than the Young angle θ_Y . Moreover, the widely accepted concept shows that the increase in roughness generally enhances this phenomenon and thus the hysteresis.[25, 38, 39]

Advancing contact angle data are very often presented as equilibrium or Young contact angles in routine practice, there could be found many static (it has not been studied time dependence of contact angle) or advancing contact angles of various liquids measured on various solid surfaces, which are considered as Young equilibrium contact angles.[24, 39-42] It is useful to remember that static angles are not necessarily the "equilibrium" values. They generally correspond to metastable or stationary states. Then the advancing and the receding angles must be measured for general characteristic of a solid surface.

As it was mentioned, Young's equation is applicable only on ideal solid surface (smooth, rigid, chemically homogeneous), but not on a rough one. R. N. Wenzel proposed a model describing the contact angle on a rough surface and he modified Young's equation as follows:

$$\cos\theta_W = r\left(\gamma_{sv} - \gamma_{sl}\right)/\gamma_{lv} = r\cos\theta_Y \quad (6)$$

In Eq. (6), r is a factor of roughness, defined as the ratio of the actual area of a rough surface to the geometric projected area, θ_W is Wenzel's contact angle (actual contact angle measured on rough surface) and θ_Y is equilibrium Young's angle measured on chemically identical but smooth surface. Since always $r \geq 1$, influence of roughness is expressed as follows: contact angle increase if $\theta_Y > 90°$ and contact angle decrease if $\theta_Y < 90°$. So the surface roughness enhances both the hydrophilicity of hydrophilic surfaces and hydrophobicity of hydrophobic ones.[5, 7-9, 43]

Application of Wenzel's equation is not so simple and is often criticized by modern authors. The main reason is that the Wenzel's equation (6) is deduced from the same principles as the Young's equation (1) and both assumed that there exists only one equilibrium contact angle. But there exists a contact angle hysteresis on real surfaces. In 1850s Bartell and Shepard were studying θ_a and θ_r of liquids on rough paraffin surfaces and they have determined that dependence of θ_a on surface roughness is quite different than dependence of θ_r [44-46]. Kamusewitz had been working on similar problem, too.[47] T. S. Meiron *et al.*[48] proposed other possible approach, which is searching for

apparent contact angle corresponding to the global energy minimum (GEM, the lowest energy out of all possible metastable states, they used loudspeaker vibrations for finding this minimum). This contact angle value can be, in principle, correlated with the ideal Wenzel's contact angle θ_W. Experiments carried out by Wolansky and Marmur[49] demonstrated that Wenzel's equation is valid only in specific cases when surface roughness is very small and the liquid drop size is comparable with dimensions of surface roughness (they used axisymmetric drop shape analysis for their experiments).

Composite smooth solid surfaces with varying degrees of heterogeneity were analysing by A. B. D. Cassie (1948). He derived an equation describing contact angle changes for two-component surfaces as follows:[50]

$$\cos\theta_C = f_1 \cos\theta_1 + f_2 \cos\theta_2 \quad (7)$$

where f_1 is the fractional area of the surface with contact angle θ_1 and f_2 is the fractional surface area with contact angle θ_2, θ_C is the Cassie's contact angle. Cassie's equation (7) reduces to the Cassie – Baxter's equation for porous surfaces such as a mash or screen surfaces:

$$\cos\theta_C = f_1 \cos\theta_1 - f_2 \qquad (8)$$

where in this case, f_2 is the fraction of open area in contact with the liquid. Cassie and Baxter assumed that water contact angle for air is 180°.[5, 7, 43]

Wenzel's equation as well as Young's equation are not unambiguous valid on real surfaces. Bain *et al*.[44, 45] studied self-assembled monolayers of alkanethiols with different functional groups adsorbed onto gold. They found that the Cassie's equation is applicable only for system where intermolecular forces between solid surface and probe liquid are dispersive. Paterson, Robin *et al*.[53] compared surfaces with random and regular arranged surface fractions with different chemical properties and they have found that Cassie's equation is valid only for surfaces with random surface chemical structure.

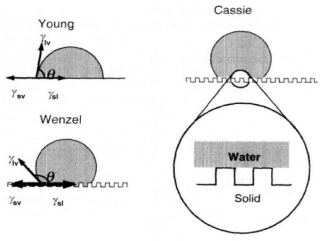

Figure 4. Illustration of solid surface roughness effect on the contact angle[43]

Another problem, which has not been solved yet, is the fact that the interfacial tensions that appear in Young's equation are those evaluated far from the contact line. Young's equation ignores the three-phase molecular interactions at the line between the solid, liquid and vapour phase. The interfacial tensions at the contact point and in the near vicinity (*core region*) can have different values. The introduction of the so-called *line tension* as a correction term that accounts for the three-phase molecular interactions was an attempt to solve this problem.[54] Several theoretical approaches[55, 56] showed that the line tension value should be around $1 \cdot 10^{-12}$ - $1 \cdot 10^{-10}$ J/m. Experimental results[57, 58] give a magnitudes of line tension around $1 \cdot 10^{-8}$ -$1 \cdot 10^{-9}$ J/m. Even such tiny energetic effects in the region of three-phase contact line can have a significant impact on the contact angle. To discuss this phenomenon, there is a need to accommodate the line tension into Young's equation as follows:

$$\gamma_{lv} \cos\theta = \gamma_{sv} - \gamma_{sl} - \gamma_{slv} \kappa_{gs} \quad (9)$$

where γ_{slv} is the line tension and κ_{gs} is the geodesic curvature of the three-phase contact line. For the ideal case when liquid drop is axisymmetric and three-phase boundary is circular ($\kappa_{gs} = 1/R$), equation (9) reduces to:

$$\gamma_{lv} \cos\theta = \gamma_{sv} - \gamma_{sl} - \frac{\gamma_{slv}}{R} \qquad (10)$$

In the case where $R \to \infty$ the line tension is negligible and Young's equation is valid.

Eq. (10) shows that the contact angle will vary with drop size, or more explicitly, with radius of three-phase line and is a linear function of $1/R$ (provided that both line tension and liquid surface tension are constant). The slope of this line is γ_{slv}/γ_{lv} . Since liquid surface tension is always positive then if the line tension is positive, too, the linear relation $\cos\theta = f(1/R)$ will have a negative slope. In the other words, the contact angle will decrease as the radius of the three-phase line increases. If the line tension is negative, then the linear relation $\cos\theta = f(1/R)$ will have a positive slope, or the contact angle will increase as the radius of the three-phase line increases.[60, 61] There exists many difficulties both in theory and experiments when the drop size dependence of contact angle is interpreted in terms of line tension, there could be found a lot of literature about this theme.[62-64]

When a liquid is in contact with heterogeneous surface composed of chemically distinct patches, the three-phase contact line is distorted (Fig.5). The radius of curvature for local deformation of the three-phase contact line depends on the size, shape, distribution and wetting properties of the heterogeneous pattern. In general, if this radius is less than a few micrometers, the correction for the local (microscopic) contact angle is

required. Modified Cassie's equation for a smooth and horizontal surface composed of two components uniformly distributed with circular curvatures of the three-phase contact line is as follows:[54]

$$\cos\theta_{MC} = f_1 \cos\theta_1 + f_2 \cos\theta_2 - \left(\frac{1}{\gamma_{LV}}\right)\left(\frac{f_1\gamma_{SLV1}}{r_1} - \frac{f_2\gamma_{SLV2}}{r_2}\right) \quad (11)$$

where r_i is the radius of the three-phase contact line at the *i* – component of the surface, θ_{MC} is the modified Cassie's contact angle and the other nomenclature is the same as used in previous equations.

The difference between θ_{MC} and θ_C is illustrated in Fig.5. In this particular system, the solid surface is composed of alternating and parallel strips differing in surface properties. A pure liquid at each surface strip forms an intrinsic contact angle (θ_1 and θ_2), which satisfies the modified Cassie's equation (11). If the dimensions of the heterogeneous mosaics are too large, the contribution of the line tension to the total free energy of the three-phase system is negligible and the modified Cassie's equation (11) is reduced to the original Cassie's equation (10).

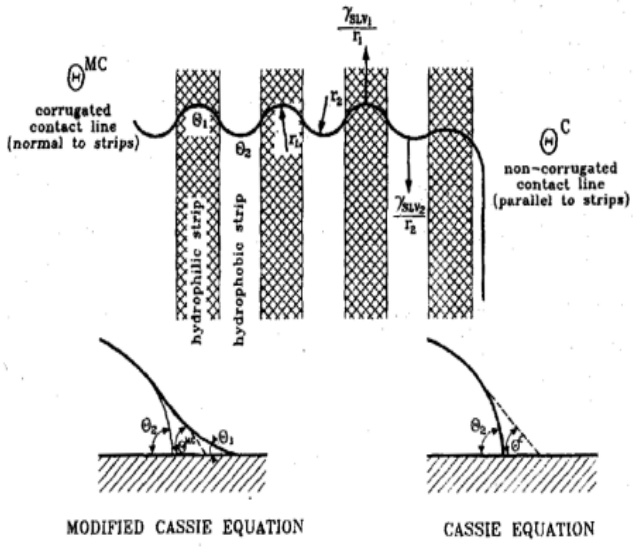

Figure 5. Model heterogeneous solid surface composed of hydrophobic and hydrophilic strips[54]

3. Solid surface energy – contact angle interpretation

From the four quantities in Young's equation, only γ_{lv} and θ are direct measurable. Historically, the interpretation of contact angles in terms of solid surface energetic started with W. A. Zisman *et al*.[65-70] He introduced the concept of *critical surface tension* γ_c as a method of determining the wettability of solid surfaces. Subsequent to Zisman's work, two major approaches of solid surface energy determination evolved: microscopic and macroscopic theories. The microscopic ones are based on surface tension components approach[71], energetic attributions of these components are additive. F.M.Fowkes is the author of this theory. The well known macroscopic theory is thermodynamic equation of state for interfacial boundary.[72]

Molecules are held in larger structures (liquids and solids) by cohesive and adhesive forces, for more than 20 types of intermolecular forces have been identified[73], but only a minority of them is significant.

3.1. Zisman approach

Zisman was the first one who found out that very frequently there is a linear relation between $\cos\theta$ and γ_{lv} .[65-70] Zisman's approach is based on plotting the cosine of contact angle vs. surface tensions of a series of liquids (alcohols, n-alkanes):

$$\cos\theta = f(\gamma_{lv}) \quad (12)$$

The point at which the resulting curve intercepts the line at $\cos\theta = 0$ is called critical surface tension γ_c. The liquids with surface tension γ_{lv} below the γ_c value of solid simply spread on the solid. Value of critical surface tension characterizes molecules on solid surface (on solid – liquid interface), but it is not equal to solid surface energy. Certain high-energy solids exhibit curvature, in this relation, for liquids with surface tension above 50 mN/m. This is because because of weak hydrogen bonds form between molecules of liquid and those in the solid.

Then it is possible to obtain the total solid surface energy of an apolar solid by using series of homologous apolar liquids, e.g. n-alkanes. And it is possible to find only dispersive force component γ_s^d of the total surface energy of a polar solid by using series of apolar liquids, too. On the other hand, it is not possible to determine any polar component of solid surface energy by using polar liquids.[74, 75]

3.2. Fowkes approach

Fowkes approach[76] forms a basis of all the surface tension component approaches used today and the dispersion component of the total surface energy is still calculated by using this approach. He considered the surface tension γ to be a measure of the attractive forces between surface layer and liquid phase, and such forces and their contribution to the free energy are additive:

$$\gamma = \gamma^d + \gamma^h + \gamma^k + \gamma^i + \gamma^{ab} + \ldots \qquad (13)$$

where superscript *d* indicates the dispersive (London) interactions, *k* marks polar Keesom interactions, *h* hydrogen bonds, *i* Debye inductive forces and superscript *ab* is due to acid/base interactions.

Because of the operative accounts, total surface energy is divided only into two components: dispersive γ^d and non-dispersive (polar) γ^p, that includes all the other contributions of intermolecular interactions to total surface energy (Keesom, Debye forces, hydrogen bonds):

$$\gamma = \gamma^d + \gamma^p \qquad (14)$$

According to Fowkes approach work of adhesion between two materials 1 (liquid) and 2 (solid) is defined by interactions that affect on interface between phases (Fig.6), and there are particularly dispersive forces.

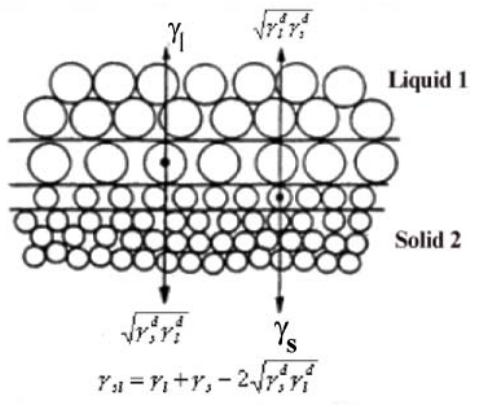

Fig. 6 Illustration of dispersive forces on solid – liquid interface[76]

The interface between two phases with only dispersive force interactions is composed of two monolayers as indicated Fig. 6. Then the decrease in tension in the interfacial monolayer of each phase resulting from the presence of other phase is $\sqrt{\gamma_1^d \gamma_2^d}$. A geometric mean relationship was postulated for both, solid – liquid and liquid – liquid interfacial tensions. At the solid – liquid interface the Fowkes relation looks as follows:

$$\gamma_{sl} = \gamma_{sv} + \gamma_{lv} - 2\sqrt{\gamma_s^d \gamma_l^d} \qquad (15)$$

where γ_s^d and γ_l^d are dispersion components of solid and liquid surface energy. Combining this equation with Young´s equation (1), results in the below mentioned equation:

$$W_a = \gamma_{lv}\left(\cos\theta_Y + 1\right) = 2\sqrt{\gamma_s^d \gamma_l^d} \qquad (16)$$

When only apolar liquids are used, for which hold $\gamma_{lv} = \gamma_l^d$, then a plot of $\cos\theta$ vs. $\sqrt{\gamma_l^d}\,/\gamma_{lv}$ gives a straight line with the origin at $\cos\theta = -1$ and slope $2\sqrt{\gamma_s^d}$. Since the origin is fixed, one contact angle measurement is sufficient to determine the dispersive force component of the solid surface energy. It is needed to point out that equations (15) and (16) are valid only in cases when both liquid and solid are apolar. Fowkes, himself, assigned that polar components cannot be determined through the rule of geometric mean.[77]

3.3. Owens – Wendt – Kaelble approach

D. K. Owens and R. C. Wendt extended Fowkes' concept by cases where both dispersive and polar (hydrogen bonding) forces operate on interface between phases (liquid and solid are polar).[78] They assumed that there are interactions between dispersive components and polar components of both phases, but there are no interactions between dispersive and polar surface energy components. The total surface energy consists of two types components, polar and dispersive, (Eq. (14) $\gamma = \gamma^d + \gamma^p$). Hence for solid – liquid interfacial energy applies:

$$\gamma_{sl} = \gamma_{sv} + \gamma_{lv} - 2\sqrt{\gamma_s^d \gamma_l^d} - 2\sqrt{\gamma_s^p \gamma_l^p} \qquad (17)$$

combining this equation with Young's Eq. (1):

$$W_a = \gamma_{lv}\left(\cos\theta_Y + 1\right) = 2\sqrt{\gamma_s^d \gamma_l^d} + 2\sqrt{\gamma_s^p \gamma_l^p} \qquad (18)$$

Nearly at the same time, D. H. Kaelble also published a very similar equation in terms of dispersive and polar forces.[79] Thus, Eq. (18) is often called the Owens – Wendt – Kaelble equation. Since Eq. (18) has two unknowns (γ_s^d and γ_s^p) of the solid, the contact angle data from at least two liquids are needed on one and the same solid surface. In general the liquids used are water and diiodomethane, because their values of γ_l^d and γ_l^p are known from literature.[10, 24, 80-83] Experimental results obtained with this method are not so

satisfactory, because different choices of the liquids pairs yield different surface tension components of the solid surface.[11, 24, 84, 85] It is probably caused by inclusion of all non-dispersive interactions between polar, included asymmetric donor – acceptor interactions.

3.4. Harmonic mean approach

S. Wu assumed that total surface energy consists of two components, too, Eq. (14). He proposed the harmonic mean to combine the polar and dispersion components of the solid and liquid surface energies in order to obtain the solid – liquid interfacial energy[86]:

$$\gamma_{sl} = \gamma_{sv} + \gamma_{lv} - 4\left[\frac{\gamma_s^d \gamma_l^d}{\gamma_s^d + \gamma_l^d} + \frac{\gamma_s^p \gamma_l^p}{\gamma_s^p + \gamma_l^p}\right] \qquad (19)$$

Combining this to Young's equation, the following relation is obtained:

$$\left(1 + \cos\theta_Y\right) = \frac{4}{\gamma_{lv}}\left[\frac{\gamma_s^d \gamma_l^d}{\gamma_s^d + \gamma_l^d} + \frac{\gamma_s^p \gamma_l^p}{\gamma_s^p + \gamma_l^p}\right] \qquad (20)$$

Similarly to the previous theory, it is needed to measure contact angle data from two different liquids to estimate polar and dispersive component of solid surface. It is possible to use the combination of geometric and harmonic mean, too:

$$\left(1 + \cos\theta_i\right) = 2\sqrt{\gamma_s^d \gamma_{li}^d} + 4\frac{\gamma_s^p \gamma_{li}^p}{\gamma_s^p + \gamma_{li}^p} \qquad (21)$$

or

$$\left(1 + \cos\theta_i\right) = 2\sqrt{\gamma_s^p \gamma_{li}^p} + 4\frac{\gamma_s^d \gamma_{li}^d}{\gamma_s^d + \gamma_{li}^d} \qquad (22)$$

subscript *i* adverts to measuring contact angles with several different liquids. Equations (21) and (22) give good results for, primarily, high-energy surfaces like glass, metals and oxides.[87, 88]

E. N. Dalal performed a comparative study of two approaches, geometric mean and harmonic mean, on 12 common polymers using the published data with six liquids.

He has found that the total surface energies of the solids obtained by the two conceptually different equations are comparable. Dalal developed a method for the best-fit solution of simultaneous equations, which are obtained when more than two contact angle liquids are used.[89]

3.5. Lifshitz – van der Waals / Acid – base (van Oss) approach

Lifshitz – van der Waals / Acid – base (van Oss) approach[71, 75] was claimed to be a generalization of the Fowkes approach, by considering acid – base interactions at the interface. van Oss *et al*. divided the surface tension into so-called Lifshitz – van der Waals (LW), acid (+) and base (-) components (AB), such the total surface tension is given by:

$$\gamma_i = \gamma_i^{LW} + \gamma_i^{AB} \qquad (23)$$

where *i* denotes either solid or liquid phase, γ_i^{LW} is contribution of non-polar (dispersive) Lifshitz – van der Waals forces (it includes London, Keesom and Debye interactions) and the second polar part of surface energy is composed of acid – base interactions γ_i^{AB}, that is caused by the moving electrons. The most common interactions of this type are hydrogen bonds. This polar part is furthermore divided into electron – acceptor (γ^+) and electron – donor (γ^-) functionality. Then it can be written by the following equation:

$$\gamma_i^{AB} = 2\sqrt{\gamma_i^+ \gamma_i^-} \qquad (24)$$

by appointing Eq. (24) into Eq. (23):

$$\gamma_i = \gamma_i^{LW} + 2\sqrt{\gamma_i^+ \gamma_i^-} \qquad (25)$$

On the basis of this theory, for solid – liquid interfacial tension, with equations (15), (23) and (25) usage, the following equation was postulated:

$$\gamma_{sl} = \gamma_{sv} + \gamma_{lv} - 2\left(\sqrt{\gamma_{sv}^{LW}\gamma_{lv}^{LW}} + \sqrt{\gamma_s^+\gamma_l^-} + \sqrt{\gamma_s^-\gamma_l^+}\right) \qquad (26)$$

combining Eq. (26) with Young's Eq. (1):

$$(1+\cos\theta)\gamma_{lv} = 2\left(\sqrt{\gamma_{sv}^{LW}\gamma_{lv}^{LW}} + \sqrt{\gamma_s^+\gamma_l^-} + \sqrt{\gamma_s^-\gamma_l^+}\right) \quad (27)$$

Eq. (27) is known as van Oss – Chaudhury – Good's equation.[71, 75, 81, 90] Equation (27) is often used to determine the solid surface components ($\gamma_{sv}^{LW}, \gamma_s^+, \gamma_s^-$) from contact angles, using three simultaneous equations inserting properties of calibration liquids that have known surface properties ($\gamma_{lv}^{LW}, \gamma_l^+, \gamma_l^-$).[91, 92] As calibration liquids are often used water (W), glycerol (G), formamide (F), diiodomethane (DM), ethylene glycol (EG), 1-bromnaphtalene (B), dimethyl sulfoxide (DMSO) and in the main their combinations for calculation solid surface energy (D-W-F, D-W-G, D-W-EG, B-W-F, B-W-DMSO etc.). Studies and experiments based on this approach can be found in literature.[39, 74, 93, 94] This approach has one fatal failure. Experimental results showed that value of solid surface energy strongly depends on liquid triplets, which were measured.[95, 96] Later C. Della Volpe and S. Siboni have proposed using a matrix of the measured contact angles for many probe liquids to determine averaged apolar and polar components for the tested solid. They made a suggestion of mathematical method for selection of appropriate liquid triplets.[97, 98]

3.6. Equation of state for interfacial tensions of solid – liquid systems

Another, quite different, method for solid surface energies determination is based on macroscopic model of thermodynamic equation of state. A. W. Neumann *et al.* were the first who evolved equation of state for determination solid surface tension from contact angle data. With usage of the thermodynamic accounts, they have found that on ideal solid – liquid – vapour interface (homogeneous, smooth solid, no adsorption etc.) interfacial energy (tension) is dependent only on values of liquid and solid surface energy (assuming thermodynamic equilibrium)[72]:

$$\gamma_{sl} = f(\gamma_{lv}, \gamma_{sv}) \quad (28)$$

They proved experimentally that relation $\gamma_{lv}\cos\theta$ vs. γ_{lv} yields smooth curves if there is no liquid adsorption, γ_{lv} decreases with increasing value of $\gamma_{lv}\cos\theta$ (assuming that γ_{sv} is constant), slope $d(\gamma_{lv}\cos\theta)/d\gamma_{lv}$ is zero at the point $\theta = 0$, which correspond to $\gamma_{lv}\cos\theta = \gamma_{sv}$. And subsequent Neumann and Ward have derived an empirical equation of state, based on a wide variety of contact angle data on low-energy polymeric surfaces:

$$\gamma_{sl} = \frac{\left(\sqrt{\gamma_{sv}} - \sqrt{\gamma_{lv}}\right)^2}{1 - 0.015\sqrt{\gamma_{sv}\gamma_{lv}}} \qquad (29)$$

combining this equation with Young's equation gives:

$$\cos\theta = \frac{\left(0.015\gamma_{sv} - 2.00\right)\sqrt{\gamma_{sv}+\gamma_{lv}} + \gamma_{lv}}{\gamma_{lv}\left(0.015\sqrt{\gamma_{sv}\gamma_{lv}} - 1\right)} \qquad (30)$$

However, there is some imperfection with this formulation of equation of state. When the product $\left(\gamma_{sv}\gamma_{lv}\right)$ is large enough, the denominator of Eq. (30) will tend to zero, so that the function becomes discontinuous. Hence, the equation of state had to be reformulated.

D. Li and A. W. Neumann (1992) came with a quite different derivation and a new formulation of equation of state.[99] In the analogy of Berthelot's rule, the work of adhesion W_{sl} can be expressed as the geometric mean of cohesion work of the solid pair W_{ss}, and the cohesion work of the liquid pair W_{ll} [100]:

$$W_{sl} = \sqrt{W_{ss}W_{ll}} \qquad (31)$$

By the definitions $W_{ss} = 2\gamma_{sv}$ and $W_{ll} = 2\gamma_{lv}$, Eq. (31) becomes:

$$W_{sl} = 2\sqrt{\gamma_{sv}\gamma_{lv}} = \gamma_{sv} + \gamma_{lv} - \gamma_{sl} \qquad (32)$$

However, it has been found that the simple Eq. (32) works only for situations where γ_{lv} values are close to the values of γ_{sv} (this is because of Berthelot's rule, which works best for the like-pair interactions, where holds $W_{ss} \approx W_{ll}$).[24, 100-103] Girifalco and Good introduced a modifying factor Φ, called *interaction parameter*, to modify the geometric mean combining rule.[100] Interaction parameter Φ is defined as:

$$W_{sl} = \Phi\sqrt{W_{ll}W_{ss}} = 2\Phi\sqrt{\gamma_{sv}\gamma_{lv}} \qquad (33)$$

It has been found that value of Φ is $\Phi \leq 1$ ($\Phi = 1$ holds for an ideal surface) and this implies that the geometric mean combining rule generally overestimates the value of W_{sl}.

In general, the above mentioned pattern also applies for a bulk system. In the theory of intermolecular interactions and the theory of mixtures, the combining rule is used to evaluate the parameters of unlike-pair interactions in terms of those of the like interactions. In the cases of large difference between γ_{sv} and γ_{lv}, the combining rule for the free energy of adhesion of solid – liquid pair can be written as:

$$W_{sl} = \sqrt{W_{ss} W_{ll}}\, e^{-\alpha(W_{ll} - W_{ss})^2} \qquad (34)$$

or more explicitly, by using Eq. (32):

$$\gamma_{sl} = \gamma_{sv} + \gamma_{lv} - 2\sqrt{\gamma_{sv}\gamma_{lv}}\, e^{-\beta(\gamma_{sv} - \gamma_{lv})^2} \qquad (35)$$

In the above Eq. (34), (35), α and β are as yet unknown constants. Clearly, when the values of γ_{sv} and γ_{lv} are close to each other, Eq. (35) reverts to Eq. (31), the geometric mean combining rule. It should be mentioned that the exponential form of the modifying factor in the modified combining rule is chosen simply because it produces a good fit to all the experimental data. Combining Eq. (35) with Young's equation will yield:

$$\cos\theta = -1 + 2\sqrt{\frac{\gamma_{sv}}{\gamma_{lv}}}\, e^{-\beta(\gamma_{sv} - \gamma_{lv})^2} \qquad (36)$$

which will enable determination of the solid surface tension γ_{sv} from the experimental data for liquid surface tension γ_{lv} and the contact angle θ.

Li and Neumann determined a specific value for constant β in the equation of state from the experimental data. For a given set of γ_{lv} and θ data measured on the solid surfaces of the same type, the constant β and γ_{sv} values can be determined by a least-square analysis technique. And the mean value of β is:

$$\beta = 0.0001247\left(m^2/mJ\right)^2 \qquad (37)$$

Experiments were performed on polymer surfaces (fluoropolymer FC-721); contact angles were measured by method of axisymmetric drop shape analysis – profile (ADSA – P)[99, 104, 105] and capillary rise methods (Wilhelmy and Washburn technique).[106, 107]

D. Y. Kwok and A. W. Neumann (1998) modified Berthelot's rule again, with a help of similar accounts as Li and Neumann (1992). They have found this modified formulation of Young's equation:

$$\cos\theta = -1 + 2\sqrt{\frac{\gamma_{sv}}{\gamma_{lv}}}\left(1 - \beta\left(\gamma_{lv} - \gamma_{sv}\right)^2\right) \quad (38)$$

A value of $\beta = 0.0001057\left(m^2/mJ\right)^2$ was obtained by using the same least-square method (as used Li and Neumann) to fit the new contact angle data obtained by various liquids on 15 homogeneous and smooth solids.

This approach of equation of state for interfacial tensions denies Fowkes approach of surface tension components. According to the equation of state the intermolecular forces do not have additional and independent effects on the contact angles. Experiments show that various liquids with the same liquid tension value γ_{lv} have, on the on the given solid surface, the same contact angle value.[11, 74, 99, 103,108]

3.7. Determination of surface energy from contact angle hysteresis

As it was mentioned, contact angle hysteresis is caused by influence of surface roughness, chemical heterogeneity of solid or surface-active impurities of probe liquid. E. Chibowski *et al*. suggested a quantitative interpretation of the contact angle hysteresis based on assumption that the liquid film is left behind the drop if its contact line has retreated. In consequence, an equation relating the advancing and the receding contact angles with total surface energy of the solid was proposed. Thus, having measured the advancing and the receding contact angles for a probe liquid total surface free energy can be evaluated.[109]

Now, assume that a film of the liquid is left behind the drop, the surface free energy of the solid is altered, but still the Young equation in a modified form can be utilized to describe this system:

$$\gamma_s = \gamma_{sl} + \gamma_l \cos\theta_a \quad (39)$$

$$\gamma_{sf} = \gamma_{sl} + \gamma_l \cos\theta_r \quad (40)$$

where γ_{sf} is the film-covered solid surface energy, γ_s, γ_l are total surface free energies of solid and liquid, and θ_a, θ_r are advancing and receding contact angles. Then, with using Eq. (5), (39) and (40), the film-covered surface energy can also be expressed as:

$$\pi = \gamma_l\left(\cos\theta_r - \cos\theta_a\right) = W_a^R - W_a^A \quad (41)$$

where π is the film pressure and W_a^R, W_a^A are works of liquid adhesion in advancing and receding mode. Eq. (41) points out that the solid surface energy could be evaluated based on three parameters, film pressure, the advancing and the receding contact angle, (π, θ_a, θ_r). So they availed advantage of Girifalco – Good's interaction parameter Φ, Eq. (33) and expressed works of adhesion as follows:

$$\frac{W_a^A}{W_a^R} = \frac{2\Phi\sqrt{\gamma_s \gamma_l}}{2\Phi\sqrt{\gamma_{sf} \gamma_l}} = k \qquad (42)$$

$$k^2 = \frac{\gamma_s}{\gamma_{sf}} = \frac{\gamma_s}{\gamma_s + \pi} \qquad (43)$$

then the total surface free energy of the solid can be described by two contact angles and liquid surface tension, $\gamma_l, \theta_a, \theta_r$. All these parameters are readily measurable:

$$\gamma_s = \gamma_l (\cos\theta_r - \cos\theta_a) \frac{(1+\cos\theta_a)^2}{(1+\cos\theta_r)^2 - (1+\cos\theta_a)^2} \qquad (44)$$

It should be noted that equation (44) works also for zero receding contact angle, but it has a limitation when no hysteresis appears ($\theta_a = \theta_r$). E. Chibowski *et al.* proved Eq. (44) by experiments with low-energy solids, where hysteresis appears in all cases.[109-111]

4. Contact angle measurement on powdered solids

Many naturally obtained solids, which are of a great interest, like soils, clays, pigments, pharmaceutics, and others, can be obtained only as powders and no flat and smooth surface of them can be prepared. For such solids, the contact angles cannot be measured directly. Measurements of contact angles on compressed pellets are charged with some error. The pellets are usually rough and porous, which causes that a smaller contact angle is measured, than it would be obtained on a smooth specimen of this solid. Since porous materials are often highly absorbent, attempts to obtain contact angle values by an optical method have been largely unsuccessful. A technique called *thin layer wicking* is sometimes used – especially when the thin layer of the studied solid powder is deposited on glass slide and the contact angle measurement is made by Wilhelmy method.[112, 113] At present, however, the methods based on liquid imbibition into porous columns, so-called Washburn method, are used.[114] Powder sample is placed into a glass tube with fritted glass bottom, glass material was chosen for its high surface energy. This allows the liquid penetrate through frit quickly and will not impede the

liquid adsorption into powder. Once the sample is immersed in the liquid, there will be a weight change, which is called the wicking process. Very often the wetted powder is shrinking. This could be caused by a gap between the wetted and dry powder. Therefore, a special weight is placed on top of the powder sample to improve contact between the wetted and the dry powder, during the experiment.

Lucas and Washburn, who modelled the porous solid as a bundle of round capillary tubes, each with radius *r*, first described the wicking process. With help of this approximation, they expressed relation between the contact angle and the distance that liquid in powder column travelled. This relation is generally known as Lucas – Washburn equation:

$$\frac{\mathrm{d}h}{\mathrm{d}t} = \frac{r\gamma_{lv}\cos\theta}{4\eta h} + \frac{r^2\rho g\cos\beta}{8\eta} \qquad (45)$$

where h is the distance covered by the liquid from the reservoir, r is the effective pore radius, θ is the liquid – solid – vapour contact angle and η, γ_{lv}, ρ is the viscosity, surface tension and density of the probe liquid. β is the angle between direction of flow and the gravitational acceleration g. When the direction of imbibition is horizontal ($\beta = 0$) or r is very small ($r \leq 10\mu m$), the second term in Eq. (45) drops out, leaving:

$$\frac{\mathrm{d}h}{\mathrm{d}t} = \frac{r\gamma_{lv}\cos\theta}{4\eta h} \qquad (46)$$

for initial conditions of experiment, when $h = 0$ and $t = 0$, applies:

$$h^2 = \frac{r\gamma_{lv}\cos\theta}{2\eta}t \qquad (47)$$

Assuming a uniform cross-section area A of pores in the sample, the Eq. (47) can be expressed as follows:

$$w^2 = \frac{A^2 r\gamma_{lv}\rho^2\cos\theta}{2\eta}t \qquad (48)$$

where w is the weight of the liquid travelled into the powder column, ρ is the density of the liquid. Rearrangement of Eq. (48) gives:

$$\cos\theta = \frac{w^2}{t} \times \frac{\eta}{\rho^2 \times \gamma_{lv} \times C} \qquad (49)$$

where C is the *dimension constant* of the sample. All parameters on the right side of Eq. (49), except for the constant C, can be measured or are known from literature. Constant C can be obtained by using a standard calibration liquid with a low surface tension (n-alkanes). There is a necessary condition that the standard liquid has to fulfil – to wet a powder sample completely ($\theta = 0$) and cannot react with the sample. The ratio w^2/t is obtained from experimental data. For each powder sample, at least two wicking experiments are needed in order to use Washburn equation to obtain contact angle value for a given liquid.[115]

Experimentation with the Washburn method seems to be relative simple. But there is one big complication with powder sample packing into glass tube. It is clear that some reproducible manner should be chosen, because of the dimension constant C, which is determined through standard liquid. And it is used for calculations of contact angles with probe liquid. A various methods of sample preparation are used. Either every time the same amount of sample is weighed and then mechanically shaked to given column height, or the powder sample is for a given time exposed to vibrations. There does not exist any universal way how to pack a powder sample, which is needed for each experiment. It is very important to perform enough experiments and check availability of powder packing approach. A complication can be a powder sample itself. Packing approach that is suitable for one powder type needn't be acceptable for another powder type. This field of surface chemistry engaged in powders has not been explored in such extend and described as the field of solids and liquids. But powders wetting is, at present, very intensively exploring because of large practical applications in pharmaceutics industry.

5. Conclusion

In conclusion, it has been clearly shown that the wettability of a solid surface is a property, which can be affected by various other surface properties, like heterogeneity, roughness and its shape, size and distribution. The combined effect of roughness and heterogeneity is a complex subject in the field of contact angles measurements and interpretation. There is, however, no universal theoretical model, which describes all possible cases. Still even Cassie´s and Wenzel´s well known equations cannot predict the angle hysteresis. Therefore, a new universal model is needed.

Surface energy is another very important parameter, in wettability characterization, influencing adhesion of solids surfaces. Contact angle measurements with different liquids with known surface tension are fundamental for calculation of solid surface energy values. It was mentioned, in this review, that the resultant values of solid surface energy are different and are dependent on the approach followed. In so far there still exist many remaining unsolved questions relating to the measurement and interpretation of contact angle data. Measurement and contact angle interpretation in the

cases of powdered solids is an individual complex section of surface chemistry. Therefore, studies on new approaches and experimental procedures to solve the problems with packing the powder samples into the sample holder are still needed and moreover, the field of heterogeneous and rough solid surfaces has not been also completely solved.

References

1. Eriksson L. G. T., Claesson P. M., Eriksson J. C., Yaminsky V. V.: *J. Colloid Interface Sci.* **181,** 476 (1996)
2. Svitova T. F., Wetherbee M. J., Radke C. J.: *J. Colloid Int. Sci.* **261**, 170 (2003)
3. Holmberg K., Shah D.O., Schwuger M. J.: *Handbook of applied surface and colloid chemistry,* Volume 2, John Wiley & Sons Ltd., Chichester 2002
4. Jańczuk B., Wójcik W., Zdziennicka A.: *J. Colloid Interface Sci.* **157**, 384 (1993)
5. Holmberg K., Shah D.O., Schwuger M. J.: *Handbook of applied surface and colloid chemistry*, Volume 1, John Wiley & Sons Ltd., Chichester 2002
6. Petrie E. M.: *Handbook of Adhesives and Sealants*, McGraw – Hill 2000, electronic version (www.knovel.com)
7. Adamson A. W., Gast A. P.:*Physical chemistry of surfaces*, sixth edition, John Wiley & Sons 1997
8. Pashley R. M., Karaman M. E.: *Applied Colloid and Surface Chemistry*, John Wiley & Sons Ltd., Chichester 2004
9. Hiemenz P. C.: *Principles of Colloid and Surface Chemistry*, Marcel Dekker, Inc., New York and Basel 1986
10. León V., Tusa A., Araujo C.: *Colloids and Surfaces A* **155**, 131 (1999)
11. Kwok D. Y., Neumann A. W.: *Colloids and Surfaces A* **161**, 31 (2000)
12. Muster T. H., Neufeld A. K., Cole I. S.:*Corrosion Science* **46**, 2337 (2004)
13. Knorr S. D., Combe E. C., Wolf L. F.,Hodges J. S.: *Dental Materials* **21**, 272 (2005)
14. Kiesvaara J., Yliruusi J.: *Int. J. Pharm.* **92**, 81 (1993)
15. Prestidge C. A., Tsatouhas G.: *Int. J. Pharm.* **198**, 201 (2000)
16. Prestidge C. A., Ralston J.: *Minerals Engineering* **9**, 85 (1996)
17. Vargha – Butler E. I., Zubovits T. K., Neumann A. W., *Chem. Eng. Comm.* **33**, 255 (1985)
18. van Giessen A. E., Bukman D. J., Widom B.: *J. Colloid Interface Sci.* **192**, 257 (1997)
19. Drechsler A., Petong N., Zhang J., Kwok D. Y., Grundke K.: *Colloids and Surfaces A* **250**, 357 (2004)
20. Eske L. D., Galipeau D. W.: *Colloids and Surfaces A* **154** 33 (1999)
21. de Laplace P. S.: *Mecanique Celeste,* Suppl. Au Xieme Livre, Lourier, Paris 1805
22. Poisson S. D.: *Nouvelle Theorie de L'action Capillaire,* Paris 1831
23. Young T.: *Phil. Trans.* **95**, 65 (1805)
24. Kwok D. Y., Neumann A. W.: *Adv. Coll. Int. Sci.* **81**, 167 (1999)
25. Della Volpe C., Penati A., Peruzzi R., Sioni S., Toniolo L., Colombo C.: *J. Adhesion Sci. Technol.* **14**, 273 (2000)
26. Drelich J., Leliński D., Miller J. D.: *Colloids and Surfaces A* **116**, 211 (1996)
27. Ščukin E. D., Percov A. V., Amelinová E. A.: *Koloidní chemie*, Academia, Praha 1990
28. Kloubek J.: *Adv. Coll. Int. Sci.* **38**, 99 (1992)
29. Lukeš F.: *Československý časopis pro fyziku* **33**, 545 (1983)
30. Marmur A.: *Adv. Coll. Int. Sci.* **50**, 121 (1994)
31. van Oss C. J., Giese R. F.: *J. Disper. Sci. Technol.* **24**, 363 (2003)
32. Giese R. F., van Oss C. J.: *Colloid and Surface Properties of Clays and Related Minerals*, Marcel Dekker, Inc, New York 2002 (electronic version: http://site.ebrary.com)
33. Giese R. F., Wu W., van Oss C. J.: *J. Disper. Sci. Technol.* **17**, 527 (1996)
34. Girifalco L. A., Good R. J.*: J. Phys. Chem.* **61**, 904 (1957)
35. Nishino T., Meguro M., Nakamae K., Matsushita M., Ueda Y.: *Langmuir* **15**, 432 (1999)
36. Johnson R. E., Dettre R. H.: *J. Phys. Chem.* **68**, 1744 (1964)
37. Johnson R. E., Dettre R. H.: *J. Phys. Chem.* **69,** 1507 (1965)

38. Chibowski E., *Adv. Coll. Int. Sci.* **103**, 149 (2003)
39. van Oss C. J., Giese R. F.: *J. Disper. Sci. Technol.* **24**, 363 (2003)
40. Nguyen D. T.:, *Colloids and Surfaces A* **116**, 145 (1996)
41. Michalski M. – C., Saramago B. J. V.: *J. Colloid Interface Sci.* **227**, 380 (2000)
42. Kamusewitz H., Possart W., Paul D.: *Colloids and Surfaces A* **156**, 271 (1999)
43. Nakajima A., Hashimoto K., Watanabe T.: *Monatshefte für Chemie* **132**, 31 (2001)
44. Bartell F. E., Shepard J. W.: *J. Phys. Chem.* **57**, 211 (1953)
45. Bartell F. E., Shepard J. W.: *J. Phys. Chem.* **57**, 455 (1953)
46. Bartell F. E., Shepard J. W.: *J. Phys. Chem.* **57**, 458 (1953)
47. Kamusewitz H., Possart W., Paul D.: *Colloids and Surfaces A* **156**, 271 (1999)
48. Meiron T. S., Marmur A., Saguy I. S.: *J. Colloid Interface Sci.* **274** 637 (2004)
49. Wolansky G., Marmur A.: *Colloids and Surfaces A* **156**, 381 (1999)
50. Cassie A. B. D.: *Discussion in Faraday Society* **3**, 11 (1948)
51. Bain C. D., Evall J., Whitesides G. M.: *J. Am. Chem. Soc.* **111**, 7155 (1989)
52. Bain C. D., Whitesides G. M.: *J. Am. Chem. Soc.* **111**, 7164 (1989)
53. Paterson A., Robin M., Fermigier M., Jenffer P., Hulin J. P.: *J. Petroleum Sci. Eng.* **20**, 127 (1998)
54. Drelich J.: *Polish Journal of Chemistry* **71**, 525 (1997)
55. Toshev B. V., Avramov M. Z.: *Colloids and Surfaces A* **100**, 203 (1995)
56. Koch W., Dietrich S.: *Physical Review E* **51**, 3300 (1995)
57. Aveyard R., Clint J. H.: *J. Chem. Soc. – Far. Trans.* **92**, 85 (1996)
58. Vitt E., Shull K. R.: *Macromolecules* **28**, 6349 (1995)
59. Boruvka L., Neumann A. W.: *J. Chem. Phys.* **66**, 5464 (1977)
60. Li D.: *Colloids and Surfaces A* **116**, 1 (1996)
61. Amirfazli A., Hänig S., Müller A., Neumann A. W.: *Langmuir* **16**, 2024 (2000)
62. Drelich J., Miller J. D., Kumar A., Whitesides G. M.: *Colloids and Surfaces A* **93**, 1 (1994)
63. Drelich J., Miller J. D.: *J. Colloid Interface Sci.* **164**, 252 (1994)
64. Amirfazli A., Kwok D. Y., Gaydos J., Neumann A. W.: *J. Colloid Interface Sci.* **205**, 1 (1998)
65. Zisman W. A.: *Ind. Eng. Chem.* **55**, 18 (1963)
66. Ellison A. H., Zisman W. A.: *J. Phys. Chem.* **58**, 503 (1954)
67. Hare E. F., Shafrin E. G., Zisman W. A.: *J. Phys. Chem.* **58**, 236 (1954)
68. Ellison A. H., Zisman W. A.: *J. Phys. Chem.* **58**, 260 (1954)
69. Shafrin E. G., Zisman W. A.: *J. Phys. Chem.* **61**, 1046 (1957)
70. Shafrin E. G., Zisman W. A.: *J. Phys. Chem.* **66**, 740 (1962)
71. van Oss C. J., Chaudhury M. J., Good R. J.: *Chemical Review* **88**, 927 (1988)
72. Neumann A. W., Good R. J., Hope C. J., Sejpal M.: *J. Colloid Interface Sci.* **49**, 291 (1974)
73. Woodward R. P.: http://www.firsttenangstroms.com/
74. Sharma P.K., Hanumantha Rao K.: *Adv. Coll. Int. Sci.* **98**, 341 (2002)
75. van Oss C. J.: *Colloids and Surfaces A* **78**, 1 (1993)
76. Fowkes F. M.: *Ind. Eng. Chem.* **56**, 40 (1964)
77. Fowkes F. M.: *Journal of Adhesion* **4**, 155 (1972)
78. Owens D. K., Wendt R. C.: *J. Appl. Pol. Sci.* **13**, 1741 (1969)
79. Kaelble D. H.: *Journal of Adhesion* **2**, 66 (1970)
80. van Oss C. J., Giese R. F., Wu W.: *Journal of Adhesion* **63**, 71 (1997)
81. van Oss C. J., Good R. J., Chaudhury M. K.: *Langmuir* **4**, 884 (1988)
82. Lee L.-H.: *Langmuir* **12,** 1681 (1996)
83. Radelczuk H., Hołysz L., Chibowski E.: *J. Adhesion Sci. Technol.* **16**, 1547 (2002)
84. Gindl M., Sinn G., Gindl W., Reiterer A., Tschegg S.: *Colloids and Surfaces A* **181**, 279 (2001)
85. de Meijer M., Haemers S., Cobben W., Militz H.: *Langmuir* **16**, 9352 (2000)
86. Wu S.: *J. Pol. Sci.* **C34** 19 (1971)
87. http://www.kruss.info/
88. Tomeček P., Horáková V., Kubice P., Lapčík L., Vojtěchovský K.: The effect of plasma modification on the surface tension of CMC and SiO_2 films, Proceedings of SILICON 2004 The Ninth Scientific and Business Conference, November 2^{th} – 5^{th} 2004, Volume 2, Tecon Scientific, s.r.o, Rožnov pod Radhoštěm, Czech Republic
89. Dalal E. N.: *Langmuir* **3**, 1009 (1987)
90. van Oss C. J., Giese R. J., Good R. J.: *Langmuir* **6**, 1711 (1990)
91. Della Volpe C., Siboni S.: *J. Adhesion Sci. Technol.* **14**, 235 (2000)

92. Radelczuk H., Hołysz L., Chibowski E.: *J. Adhesion Sci. Technol.* **16**, 1547 (2002)
93. van Oss C. J.: *J. Adhesion Sci. Technol.* **16**, 669 (2002)
94. van Oss C. J., Giese R. F., Li Z., Murphy K., Norris J., Chaudhury M. K., Good R. J.: *J. Adhesion Sci. Technol.* **6**, 413 (1992)
95. Kwok D. Y., Li D., Neumann A. W.: *Colloids and Surfaces A* **89** 181 (1994)
96. Kwok D. Y., Li D., Neumann A. W.: *Langmuir* **10**, 1323 (1994)
97. Della Volpe C., Siboni S.: *J. Colloid Interface Sci.* **195**, 121 (1997)
98. Della Volpe C., Siboni S.: *J. Adhesion Sci. Technol.* **14**, 235 (2000)
99. Li. D., Neumann A. W.: *Adv. Coll. Int. Sci.* **39,** 299 (1992)
100. Girifalco L. A., Good R. J.: *J. Phys. Chem.* **61**, 904 (1957)
101. Jańczuk B., Bruque J. M., González – Martín M. L., Moreno del Pozo J., Zdziennicka A., Quintana – Gragera F.: *J. Colloid Interface Sci.* **181**, 108 (1996)
102. Schneider R. P., Chadwick B. R., Jankowski J., Acworth I.: *Colloids and Surfaces A* **126**, 1 (1997)
103. Spelt J. K., Absolom D. R., Neumann A. W.: *Langmuir* **2**, 620 (1986)
104. Kwok D. Y., Gietzelt T., Grundke K., Jacobasch H.-J., Neumann A. W.: *Langmuir* **13**, 2880 (1997)
105. Seebergh J. E., Berg J. C.: *Chem. Eng. Sci.* **47**, 4468 (1992)
106. Sedev R., Fabretto M., Ralston J.: *Journal of Adhesion* **80**, 1 (2004)
107. Fabretto M., Ralston J., Sedev R.: *J. Adhesion Sci. Technol.* **18**, 29 (2004)
108. Spelt J. K., Neumann A. W.: *Langmuir* **3**, 588 (1987)
109. Chibowski E., Ontiveros-Ortega A., Perea-Carpio R.: *J. Adhesion Sci. Technol*. **16**, 1367 (2002)
110. E. Chibowski: *Adv. Coll. Int. Sci.* **103**, 149 (2003)
111. Chibowski E., Ontiveros – Ortega A., Perea – Carpio R.: *J. Adhesion Sci. Technol.* **16**, 1367 (2002)
112. Buckton G.: *J. Adhesion Sci. Technol.* **7**, 219 (1993)
113. Chawla A., Buckton G., Taylor K. M. G., Newton J. M., Johnson M. C. R.: *Eur. J. Pharm. Sci*. **2**, 253 (1994)
114. Bartell F. E., Whitney C. H.: *J. Phys. Chem.* **36**, 3115 (1932)
115. CAHN DCA 315, Instruction manual, Cahn Instruments, Inc., Madison, USA, 1996

Acta Univ. Palacki. Olomuc.
Fac. rer. nat. 2005
Chemica 44, 25-48

ACTA UNIVERSITATIS PALACKIANAE OLOMOUCENSIS
FACULTAS RERUM NATURALIUM (2005) CHEMICA 44

ANHYDROUS N-[3-[(4-AMINO-6,7-DIMETHOXY-2-QUINAZOLINYL)METHYLAMINO]PROPYL] TETRAHYDRO-2-FURANCARBOXAMIDE, ITS PREPARATION AND STABILISATION

Roman Gabriel[a], Pavel Hradil[a*] and Jan Walla[b].

[a]*Research and Development Farmak a.s., Na Vlčinci 3, 771 17 Olomouc, Czech Republic*
[b]*Laboratory of Growth Regulators, Institute of Experimental Botany AS CR & Palacký University, Šlechtitelů 11, 783 71 Olomouc, Czech Republic*

Received January 5, 2005
Accepted April 2, 2005

Abstract

Preparation and stabilisation of the anhydrous form of Alfuzosin hydrochloride is described. Alfuzosin is a hygroscopic compound. Anhydrous forms generally are not too stable and hydrates are formed quickly.

Key Words: *Stability, polymorph, crystallisation.*

Introduction

N-[3-[(4-amino-6,7-dimethoxy-2-quinazolinyl)methylamino]propyl]tetrahydro-2-furancarboxamide is known as an antagonist of α_1 adrenergic receptor and it is used as an antihypertensive agent and dysuria curing agent under the name of alfuzosin. No information concerning potential polymorphic or hydrate forms of alfuzosin hydrochloride has been found during literature search. One patent describes dihydrate and higher hydrate formation[1]. From the practical point of view, the dihydrate is the most useful modification[2] and its preparation is simple and stability is excellent. Unfortunately, application of this modification is restricted by a patent. When we studied this problem it was clear that we can use alfuzosin anhydrous as a patent non-infringing modification.

* Author for correspondence

Experimental

An identification of crystallographic modifications of alfuzosin was determined by powder diffraction X-ray analysis. Data were collected on a powder diffractometer XRD-7 from Seifert Co using CuK_α radiation (lambda = 1.54178 Å), with a step of 0.02°, integration time of 4s and 2Θ range 4 – 40°.

Synthesis of anhydrous alfuzosin hydrochloride

Alfuzosin base (10.0 g, 0.026 mol) was charged to a flask, and ethanol (220 ml) was added. The content of the reaction mixture was refluxed for 15 minutes, and the solid phase was dissolved. Activated charcoal was added; the suspension was stirred for 10 minutes and then filtered and washed by 10 ml of hot ethanol. The filtrate was cooled down to 20 to 25 °C and ethanol saturated by hydrogen chloride (3.0 ml) was added. Then diethyl ether (50 ml) and water (0.18 ml) were slowly added to the reaction mixture. Reaction mixture was stirred at laboratory temperature for 15-20 hours. Then the reaction mixture was cooled down to 0 – 5 °C and after one hour of stirring the product was filtered off and washed by 15 ml of diethyl ether. The crystalline product was dried at vacuum drier at 120 °C for minimum 8 hours. The yield of alfuzosin hydrochloride was 9.7 g; i.e. 88.7 % of theory.

Results and Discussion

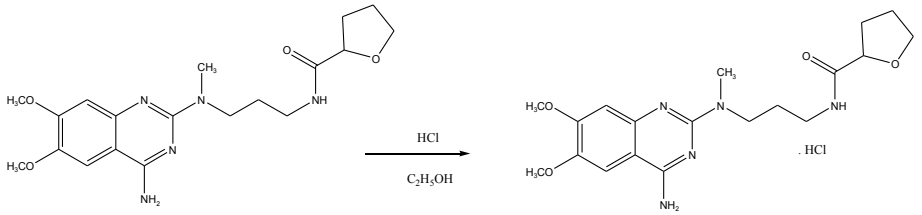

Scheme 1

Alfuzosin hydrochloride was prepared by four-step synthesis. The last step of this preparation is formation of alfuzosin hydrochloride from alfuzosin base and generation of right polymorph structure (Scheme 1).

We started with preparation of the product under anhydrous conditions. As a solvent, mixture of solvents was used. We used a solution of alfuzosin in ethanol and added ethanolic hydrochloric acid and diethyl ether as precipitation agents.

We were not able to reduce residual solvents as diethyl ether or ethanol to the demanded limit at temperature 110 °C.

This limit is defined by ICH guideline Q3C, which is 5000 ppm for ethanol and 1000 ppm for diethyl ether. We had to use temperature higher than 170 °C, but in this case colour of the product was out of the limit.

Then we found that addition of some amount of water solved this problem. If we used ethanol with probably 5% of water, we were able to isolate modification A (fig. 1). If the amount of water was higher, we isolated modification B (fig. 2). The average

crystallisation time was 4 hours, after that time we isolated 88 to 92% of alfuzosin from the solution. In this case, we have no problems with residual solvents. Ethanol and diethyl ether were not present at all.

Alfuzosin prepared in this way showed assay 2 % of water after drying. If this compound was kept in a bottle or in a plastic bag, the water assay grew and after several weeks it reached 6%. This is in accordance with amount of water in dihydrate. Crystal structure was also changed and instead of modification A (fig. 1), modification B was observed (fig. 2). Speed of transformation depends on the packing material, and how tight the container was. If we kept alfuzosin on the table, modification was changed during two weeks.

We had to solve this serious problem. The simplest solution for reprocessing of this material was drying. If we dried product with 6% of water, again we were able to receive the material with 0.5% of water. The isolated product was very hygroscopic, and phase B was formed quickly. We also tried to dry alfuzosin immediately after isolation at temperature 110 to 115 °C for less than 0.5 % of water. However, stability was not good and phase B was formed during several weeks. We found that to improve stability we have to use temperature 150 °C for drying and to prolong time for 6 to 8 hours. In this case the prepared product was of modification A and was more stable. Sometimes colour of the product reprocessed in this way was out of the limit. We believe that reason for this behaviour was a presence of a small amount of amorphous material in the crystalline material. This modification was isolated in the laboratory several times (fig. 3).

Surprisingly, we found that we could improve stability by prolonging time of stirring of the reaction mixture at the laboratory temperature. Based on general information about influence of time on polymorphism[3,4] we tried to prolong crystallisation time. Instead of 4 hours now we use probably 15 to 20 hours. We modify process and use probably 0.2 % weight of water in the reaction mixture. Since we use anhydrous solvents and material, we add calculated amount of water. In this case, we isolated product with modification A and amount of water lower than 0.5 %. For the time being, we have 3 year´s stability and modification A has been still stable.

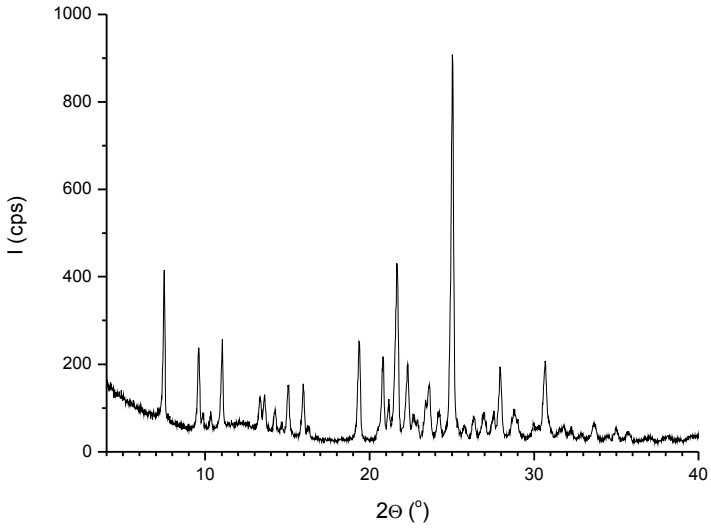

Figure 1. XRD spectrum of modification A

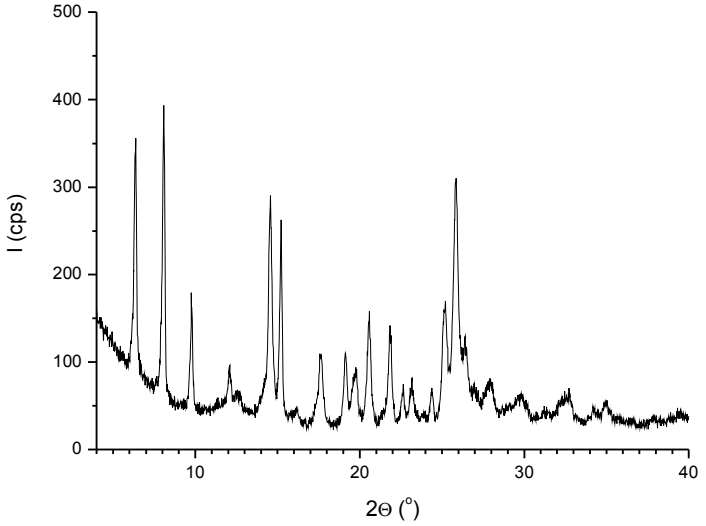

Figure 2. XRD spectrum of modification B

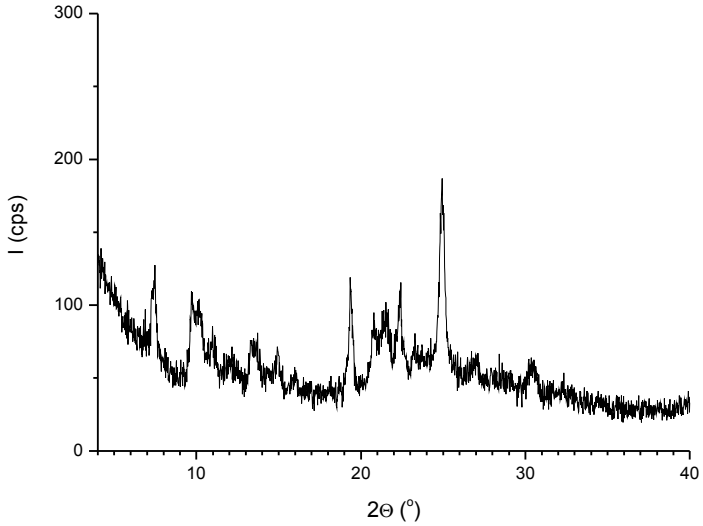

Figure 3. XRD spectrum of mixture of small particles modification A and amorphous phase

References

1. Borrega R. and Kitamura S., (Sanofi-Synthelabo), EP 0 663 398.
2. Borrega R. and Kitamura S., (Synthelabo) USP 5 545 738.
3. Mullin, J.W., Crystallization. 4th edn, Butterworth-Heinemann Ltd., Oxford (2001).
4. Brittain H.G., Polymorphism in Pharmaceutical Solids, Marcel Dekker New York (1999).

Acta Univ. Palacki. Olomuc.
Fac. rer. nat. 2005
Chemica 44, 49-53

ACTA UNIVERSITATIS PALACKIANAE OLOMOUCENSIS
FACULTAS RERUM NATURALIUM (2005) CHEMICA 44

THE USE OF α-KETOACIDS FOR SYNTHESES OF HETEROCYCLIC COMPOUNDS I. SYNTHESIS AND OXIDATIVE CYCLIZATION OF SOME SUBSTITUTED BENZIMIDAZOL-2-YL-FORMAZANES

Iveta Fryšová*, Vendula Růžičková, Jan Slouka and Tomáš Gucký

Department of Organic Chemistry, Palacký University, Tř. Svobody 8, 771 46 Olomouc, Czech Republic, E-mail: frysova@orgchem.upol.cz

Received May 31, 2005
Accepted September 23, 2005

Abstract

A series of 1,5-diaryl-3-formazylglyoxylic acids **1a-1d** was prepared by azocoupling of diazonium salts of o-toluidine, m-toluidine, 2-chloroaniline, 3-chloroaniline with sodium pyruvate. These compounds gave the corresponding 1,5-diaryl-3-(2-benzimidazol-2-yl)-formazanes **2a-2d** by condensation with o-phenylenediamine and corresponding dimethyl derivates **3a-3d** by condensation with 4,5-dimethyl-o-phenylenediamine. Oxidative cyclization of these compounds gave 2,3-diaryl-5-(benzimidazol-2-yl)-tetrazolium chlorides, which were transformed into the less hydroscopic picrates **4a-4d** and **5a-5d**.

Keywords: *1,5-diaryl-3-(2-benzimidazol-2-yl)-formazanes*

Introduction

α-Ketocarboxylic acids belong to the most important synthons for heterocyclic compounds. Some examples are syntheses of 6-azauracile and some other [1,2,4]triazine derivatives[1,2], quinoxaline[3] and pteridine derivatives[4]. Recently we have found that 1,5-diarylformazylglyoxylic acids react with 1,2-diaminobenzene in completely different course than the other α-ketocyrboxylic and benzimidazole derivatives were obtained[5-7]. A series of 1,5-diaryl-3-(benzimidazol-2-yl)-formazanes was prepared in this way.

* Author for correspondence

The matter of this communication is the synthesis and study of further transformations of some new 1,5-diaryl-3-(benzimidazol-2-yl)-formazanes substituted in benzimidazole cycle as well as on phenyl cycles.

Results and discussion

Using modified Bamberger and Műller method[8] we prepared a series of 1,5-diaryl-3-formazylglyoxylic acids **1a-1d** by azocoupling of diazonium salts with sodium pyruvate in alkaline medium. These compounds were condensed with o-phenylenediamine resp. 4,5-dimethyl-1,2-diaminobenzene ane we received a series of formazanes **2a-2d** and **3a-3d**. The oxidative cyclization of formazanes **2a-2d** and **3a-3d** was performed by the action of lead(IV)tetraacetate in chloroform and the series of 2,3-diaryl-5-(2-oxo-1,2-dihydro-quinoxaline-3-yl)-tetrazolium chlorides **4** and **5** was prepared. Compounds **4** and **5** form corresponding hydrates by the crystallization from water. The chlorides were also transformed to the corresponding picrates **4a-4d** and **5a-5d**[6, 7].

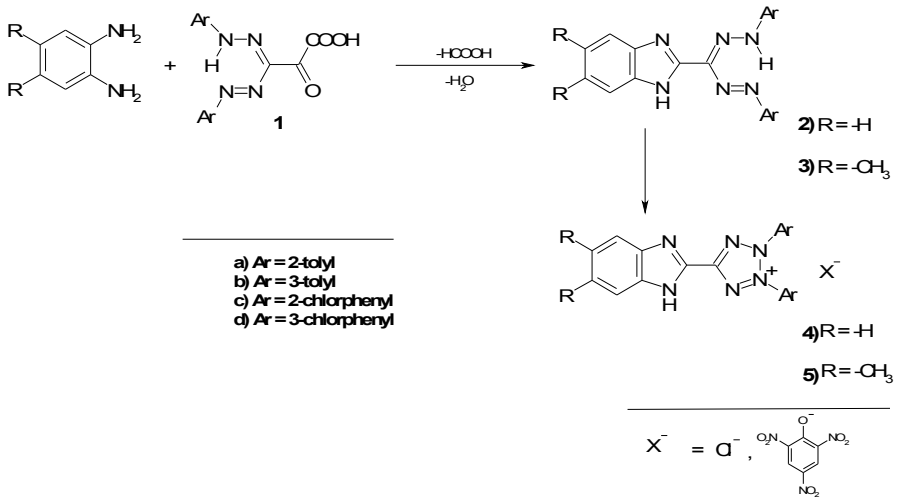

Materials and methods

Melting points (Boetius) are not corrected. Infrared spectra were measured as potassium bromide disks and scanned on an ATI Unicam Genesis FTIR instrument. The NMR spectra were measured in DMSO-d_6 solutions on a Bruker AMX-300 spectrometer (300MHz) with TMS as internal standard. Elemental analyses were performed using an EA Elemental Analyzer (Fison Instrument).

1,5-Diaryl-3-formazylglyoxylic acids (1a-1d)
General procedure:

A solution of $NaNO_2$ (1.38g, 20.0 mmol) in ice-cold water (5 ml) was added portionwise under stirring to the solution of corresponding aromatic amine (20.0 mmol) in a mixture of HCl (37 %, 10.0 ml) and water (10-20 ml), which was cooled in an ice-bath. The solution was left to stand for 20 min in an ice bath and then was added portionwise during 3 min under stirring to a pre-cooled solution of sodium pyruvate (4.0 g, 36.35 mmol) and KOH (30 g) in water (300 ml). Reaction mixture was left in an ice bath for 20 min with vigorous stirring. Small amount of separated precipitate of 1,5-diaryl-3-arylazoformazane was filtered off and washed with water. The combined filtrates were acidified under vigorous stirring with HCl (37 %) to pH=1. After several hours, the separated red compound was collected with suction, thoroughly washed with water. For further details see tables 1-3.

1,5-Diaryl-3-(benzimidazol-2-yl)formazanes (2a-2d)

General procedure:

The mixture of formazylglyoxylic acid (**1a-1d**) (1.00 mmol) and 1,2-diaminobenzene (108.14 mg; 1.00 mmol) refluxed for 5 min in ethanol (6.0 ml). After cooling to 20 °C, the red crystalline compound was filtered off, washed with water and dried. It was purified by recrystallization from ethanol. For further details see tables 1-3.

1,5-Diaryl-3-(4,5-dimethyl-benzimidazol-2-yl)formazanes (3a-3d)

General procedure:

The mixture of formazylglyoxylic acid (**1a-1d**) (1.00 mmol) and 4,5-dimethyl-1,2-diaminobenzene (136.2 mg; 1.00 mmol) refluxed for 5 min in ethanol (6.0 ml). After cooling to 20 °C, the red crystalline compound was filtered off, washed with water and dried. It was purified by recrystallization from ethanol. For further details see tables 1-3.

2,3-Diaryl-5-(benzimidazol-2-yl)tetrazolium picrates (4a-4d)

General procedure:

Lead(IV)tetraacetate (0.50 g; 1.12 mmol) was added with stirring to a solution of 1,5-diaryl-3-(benzimidazol-2-yl)formazan (**2a-2d**) (1.00 mmol) in $CHCl_3$ (50-150 ml). The solution was stirred for 3 h at room temperature and filtered. The filtrate was evaporated *in vacuo*, the residue dissolved in H_2O (10 ml) and acidified with conc. HCl to pH=2. The precipitate was filtered off and the filtrate was evaporated *in vacuo*. The residue was dissolved in methanol (7-10 ml), filtered and evaporated again. The residue was dried in vacuum dessicator over KOH. These compounds are hygroscopic and they were transformed into less hydroscopic picrates. General procedure: A solution of sodium picrate (251.0 mg; 1.00 mmol) in H_2O (5 ml) was added to the stirred solution of tetrazolium chloride (1 mmol) in H_2O (1-3 ml) and stirring continued for 5 minutes. The precipitated compound (**4a-4d**) was collected with suction and dried. For further details see tables 1-3.

2,3-Diaryl-5-(4,5-dimethyl-benzimidazol-2-yl)tetrazolium chlorides (5a-5d)

General procedure:

Lead(IV)tetraacetate (0.50 g; 1.12 mmol) was added with stirring to a solution of 1,5-diaryl-3-(4,5-dimethyl-benzimidazol-2-yl)formazan (**3a-3d**) (1.00 mmol) in $CHCl_3$ (50-150 ml). The solution was stirred for 3 h at room temperature and filtered. The filtrate was evaporated *in vacuo*, the residue dissolved in H_2O (10 ml) and acidified with conc. HCl to pH=2. The precipitate was filtered off and the filtrate was evaporated *in vacuo*. The residue was dissolved in methanol (7-10 ml), filtered and evaporated again. The residue was dried in vacuum dessicator over KOH. These compounds are hygroscopic and they were transformed into less hydroscopic picrates. General procedure: A solution of sodium picrate (251.0 mg; 1.00 mmol) in H_2O (5 ml) was added to the stirred solution of tetrazolium chloride (1 mmol) in H_2O (1-3 ml) and stirring continued for 5 minutes. The precipitated compound (**5a-5d**) was collected with suction and dried. For further details see tables 1-3.

Table 1. Characteristic data of compounds 1-5

Compound	M.p. (°C) Yield (%)	Formula M.w.	Elemental Analysis (Calcul./Found)		
			%C	%H	%N
1a	150-151 73.0	$C_{17}H_{16}N_4O_3$ 324.34	62.95 63.05	4.97 5.00	17.27 17.09
1b	141-142 72.1	$C_{17}H_{16}N_4O_3$ 324.34	62.95 62.86	4.97 4.90	17.27 17.11
1c	142-143 69.0	$C_{15}H_{10}N_4O_3Cl_2$ 365.27	49.32 49.20	2.76 2.80	15.34 15.30
1d	133-134 70.8	$C_{15}H_{10}N_4O_3Cl_2$ 365.27	49.32 49.39	2.76 2.72	15.34 15.28
2a	222-223 93.1	$C_{22}H_{20}N_6$ 368.44	71.72 71.80	5.47 5.49	22.81 22.71
2b	190-191 92.7	$C_{22}H_{20}N_6$ 368.44	71.72 71.83	5.47 5.40	22.81 22.77
2c	242-243 94.3	$C_{20}H_{14}N_6Cl_2$ 409.37	58.68 58.45	3.45 3.43	20.53 20.50
2d	240-241 96.6	$C_{20}H_{14}N_6Cl_2$ 409.37	58.68 58.51	3.45 3.50	20.53 20.47
3a	238-239 89.9	$C_{24}H_{24}N_6$ 396.49	72.70 72.62	6.10 6.02	21.20 21.36
3b	191-192 90.6	$C_{24}H_{24}N_6$ 396.49	72.70 72.72	6.10 6.15	21.20 21.13
3c	249-250 90.6	$C_{22}H_{18}N_6Cl_2$ 437.42	60.41 60.35	4.15 4.09	19.21 19.13
3d	238-239 92.4	$C_{22}H_{18}N_6Cl_2$ 437.42	60.41 60.32	4.15 4.21	19.21 19.16
4a	120-121 84.5	$C_{28}H_{21}N_9O_7$ 595.53	56.47 56.52	3.55 3.39	21.17 21.14
4b	118-119 89.7	$C_{28}H_{21}N_9O_7$ 595.53	56.47 56.60	3.55 3.42	21.17 21.07
4c	120-121 86.9	$C_{26}H_{15}N_9O_7Cl_2$ 636.46	49.07 48.99	2.38 2.29	19.81 19.77
4d	117-118 83.0	$C_{26}H_{15}N_9O_7Cl_2$ 636.46	49.07 49.16	2.38 2.45	19.81 19.70
5a	129-131 88.9	$C_{30}H_{25}N_9O_7$ 623.58	57.78 57.53	4.04 3.99	20.22 20.31
5b	126-127 89.1	$C_{30}H_{25}N_9O_7$ 623.58	57.78 57.66	4.04 4.12	20.22 20.42
5c	134-135 86.3	$C_{28}H_{19}N_9O_7Cl_2$ 664.51	50.61 50.59	2.88 3.01	18.97 19.00
5d	134-135 86.5	$C_{28}H_{19}N_9O_7Cl_2$ 664.51	50.61 50.64	2.88 3.00	18.97 18.72

Table 2. ^{1}H-NMR spectra of compounds 1-3

Compound	^{1}H-NMR spectrum
1a	2.41(s, 6H, CH_3); 7.35(m, 6H, ArH); 7.65(m, 2H, ArH); 14.28(s, 1H, NH)
1b	2.40(s, 6H, CH_3); 7.25(d, 2H, J=7.5, ArH); 7.43(t, 2H, J=7.5, ArH); 7.63(d, 4H, J=8.1, ArH); 14.55(s, 1H, NH)
1c	7.52(m, 4H, ArH); 7.67(m, 4H, ArH); 14.62(s, 1H, NH)
1d	7.48(d, 2H, J=7.8, ArH); 7.58(t, 2H, J=7.8, ArH); 7.80(d, 2H, J=8.1, ArH); 7.91(s, 2H, ArH); 13.91(s, 1H. NH)
2a	2.65(s, 6H, CH_3); 7.24(dt, 2H, J_1=1.2, J_2=7.5, ArH); 7.38(m, 6H, ArH); 7.74(d, 2H, J=7.5, ArH); 7.77(m, 2H, ArH); 13.77(s, 1H, NH)
2b	2.44(s, 6H, CH_3); 7.17(d, 2H, J=7.5, ArH); 7.38(q, 2H, J_1=3.0, J_2=6.0, ArH); 7.44(d, 2H, J=7.5, ArH); 7.64(m, 4H, ArH); 7.86(q, 2H, J_1=3.0, J_2=6.0, ArH); 13.88(s, 1H, NH)
2c	7.40(m, 4H, ArH); 7.59(m, 4H, ArH); 7.89(m, 4H, ArH); 13.94(s, 1H, NH)
2d	7.40(d, 4H, J=7.8, ArH); 7.57(t, 2H, J=7.8, ArH); 7.82(d, 4H, J=9.0, ArH); 7.97(s, 2H, ArH); 13.95(s, 1H, NH)
3a	2.38(s, 6H, CH_3); 2.64(s, 6H, CH_3); 7.23(t, 2H, J=7.5, ArH); 7.34(m, 4H, ArH); 7.55(s, 2H, ArH); 7.70(d, 2H, J=7.5, ArH); 13.67(s, 1H, NH)
3b	2.39(s, 6H, CH_3); 2.44(s, 6H, CH_3); 7.15(d, 2H, J=7.5, ArH); 7.42(t, 2H, J=7.5, ArH); 7.65(m, 6H, ArH); 13.81(s, 1H, NH)
3c	2.39(s, 6H, CH_3); 7.38(t, 2H, J=7.2, ArH); 7.53(t, 3H, J=7.2, ArH); 7.61(s, 4H, ArH); 7.71(d, 1H, J=8.1, ArH); 13.92(s, 1H, NH)
3d	2.38(s, 6H, CH_3); 7.39(d, 2H, J=9.0, ArH); 7.56(t, 2H, J=8.1, ArH); 7.61(s, 2H, ArH); 7.80(d, 2H, J=8.1, ArH); 7.94(s, 2H, ArH); 13.86(s, 1H, NH)

Table 3. IR spectra of compounds 1-3

Compound	IR spectrum
1a	2975, 1716, 1667, 1591, 1510, 1467, 1407, 1353, 1329, 1269, 1177, 1109, 969, 762, 743
1b	3062, 1738, 1718, 1670, 1524, 1519, 1405, 1358, 1304, 971, 786, 687
1c	3474, 3167, 1735, 1690, 1591, 1490, 1444, 1362, 1261, 1057, 755
1d	3333, 3117, 1729, 1681, 1600, 1477, 1429, 1366, 1273, 1078, 787
2a	3589, 3491, 3420, 3170, 1591, 1548, 1476, 1439, 1358, 1281, 1238, 1172, 744, 598, 452
2b	3471, 3167, 1549, 1467, 1403, 1347, 1287, 1228, 1209, 782, 685, 600, 426
2c	3398, 3168, 1547, 1497, 1288, 1215, 897, 788, 598
2d	3421, 3372, 1539, 1465, 1276, 1224, 888, 799, 602
3a	3497, 3379, 3099, 2947, 1549, 1477, 1225, 1012, 923, 895, 746, 598
3b	3589, 3251, 3167, 2918, 1549, 1492, 1357, 1281, 1228, 1156, 772, 687, 432
3c	3399, 3143, 2989, 1540, 1502, 1478, 1297, 1223, 902, 876, 777, 611
3d	3422, 3388, 3056, 2966, 1539, 1506, 1471, 1463, 1291, 1234, 893, 756, 593

Acknowledgements

We are grateful to the Ministry of Education, Youth and Sport of the Czech Republic, for the grant MSM6198959216.

References

1. Newnhoeffer H.: Chemistry of 1,2,3-triazines and 1,2,4-triazines, tetrazines and pentazines in The chemistry of heterocyclic compounds vol. **33**, p. 416-492, John Wiley a sous 1978.
2. Hadáček J., Slouka J.: Chemie der monocyclischen asymmetrischen Triazine Teil I. Die asymmetrischen Triazine mit den Funktions gruppen in der stellung 3 und 5 in Folia Fac. Sci. Natur. Univ. Purkyn. Brunensis VI, **3**, p.1-88 (1965).
3. Pratt Y.T.: The Quinoxalines in Heterocyclic Compounds, edit R. C. Elderfield, vol. **VI**, p. 464-472 (1957).
4. Bergman J., Damberg Ch., Vallberg H.: *Recl. Trav. Chim. Pays-Bas* **115**, 31 (1996).
5. Wiedermannová I., Slouka J.: *Heterocyclic Commun.* **7**, 55 (2001).
6. Wiedermannova I., Slouka J., Lemr K.: *Heterocyclic Commun.* **8**, 479 (2002).
7. Fryšová I., Slouka J., Gucký T.: *Arkivoc* **XV**, 1 (2005).
8. E. Bamberger, J. Műller: *J. Pract. Chem.* **64**, 199 (1901).

ACTA UNIVERSITATIS PALACKIANAE OLOMOUCENSIS
FACULTAS RERUM NATURALIUM (2005) CHEMICA 44

OXO DERIVATIVES OF QUINOXALINE IX[1]. THE STUDY OF REACTIVITY OF SUBSTITUTED 3-(2-AMINOPHENYL)-1,2-DIHYDRO-QUINOXALINE-2-ONES

Iveta Fryšová*, Pavlína Vorlická and Jan Slouka

Department of Organic Chemistry, Palacký University, Tř. Svobody 8, 771 46 Olomouc, Czech Republic. E-mail: frysova@orgchem.upol.cz

Received May 31, 2005
Accepted September 20, 2005

Abstract

This work deals with the study of reactivity of substituted 3-(2-aminophenyl)-1,2-dihydro-quinoxaline-2-ones **7a, 7b, 8a, 8b**. 3-(2-Amino-4,5-difluorophenyl)-1,2-dihydro-quinoxaline-2-one **7a**, 3-(2-amino-4,5-difluorophenyl)-6,7-dimethyl-1,2-dihydro-quinoxaline-2-one **7b**, 3-(2-amino-3,4-dichloro-phenyl)-1,2-dihydro-quinoxaline-2-one **8a**, resp. 3-(2-amino-4,5-dichlorophenyl)-6,7-dimethyl-1,2-dihydro-quinoxaline-2-one **8b** were prepared by the reaction of N-acetylisatine **3** resp. **4** with 1,2-diaminobenzene, resp. 4,5-dimethyl-1,2-diaminobenzene and further hydrolysis of acetyl group. Cyclization reaction of compounds **7a, 7b, 8a, 8b** in $POCl_3$ afforded indolo[2,3-b]quinoxalines **9a, 9b, 10a, 10b**.

Keywords: *3,6,7-trisubstituted 1,2-dihydro-quinoxaline-2-ones, indolo[2,3- b]quinoxaline*

Introduction

We have tried to prepared compounds with a potential biological activity and that´s why we devoted our attention to some dimethylderivatives of indolo-quinoxaline because of their certain structural similarity with a flavine system[2, 3].

The Korczynski and Marchlewski[4] described interesting reaction of substituted isatines (e.g. 5-bromoisatine, 5-fluoroisatine, 5,6-difluoroisatine and o-phenylenediamine). However, authors didn´t present any experimental details like proportion of reaction compounds, reaction time, yields, etc.

* Author for correspondence

Results and discussion

The 5,6-difluoro-N-acetylisatine **3** resp. 6,7-dichloro-N-acetylisatine **4** were prepared by heating of isatines **1**[5] resp. **2**[6] in acetic anhydride. The acetyl-derivatives **5a, 5b, 6a, 6b** were prepared by the reaction of o-phenylenediamine resp. 4,5-dimethyl-1,2-phenylenediamine with 5,6-difluoro-N-acetylisatine **3** resp. 6,7-dichloro-N-acetylisatine **4** and by the alkaline hydrolysis of compounds **5a, 5b, 6a, 6b** aminoderivatives **7a, 7b, 8a, 8b** were prepared. The aminoderivatives **7a, 7b, 8a, 8b** were cyclised to corresponding condensed heterocycles **9a, 9b, 10a, 10b** in $POCl_3$.

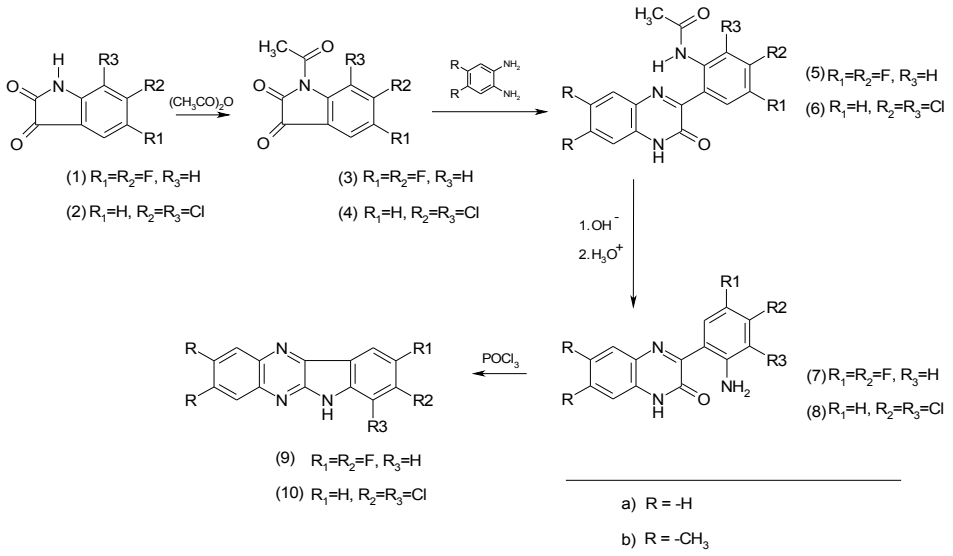

Experimental

The melting points were determined on a Boetius stage and are not corrected. The infrared spectra were measured in KBr disks and scanned on an ATI Unicam Genesis FTIR instrument. Elemental analyses were performed with an EA 1108 Elemental Analyses (Fison Instrument).

5,6-Difluoro-N-acetylisatine (3) resp. 6,7-dichloro-N-acetylisatine (4)

The mixture of corresponding isatine (0.02 mol) and acetanhydride (120 ml) was refluxed for 4 hours. The reaction mixture was left to stand until the next day at a room temperature. The crystalline compound was separated, washed with diethylether and dried. For further details see Tables 1-2.

3-(2-Acetyl-4,5-difluorophenyl)-1,2-dihydro-quinoxaline-2-one (5a), resp. dimethyl-derivative (5b), 3-(2-acetyl-5,6-dichlorophenyl)-1,2-dihydro-quinoxaline-2-one (6a) resp. dimethyl-derivative (6b)

To the solution of corresponding-N-acetylisatine **3-4** (11.94 mmol) in acetic acid (27 ml), which was heated up to 70-80 °C, a solution of o-phenylendiamine (1.37 g; 12.67 mmol) resp. 4,5-dimethyl-o-phenylenediamine (1.72 g, 12.67 mmol) in the mixture of water (3 ml) and acetic acid (3 ml) heated up to 70 °C was added with intensive stirring. After a few minutes of intensive stirring, a thick precipitate separed out from the solution. Reaction mixture was stirred for next 15 minutes and cooled down. On the next day, the crystalline compounds was collected with suction, washed with little acetic acid, mixture of acetic acid and water and finally with water. For further details see Tables 1-2.

3-(2-Amino-4,5-difluorophenyl)-1,2-dihydro-quinoxaline-2-one (7a) resp. dimethyl-derivative (7b), 3-(2-amino-5,6-chlorophenyl)-1,2-dihydro-quinoxaline-2-one (8a) resp. dimethyl-derivative (8b)

The mixture of corresponding acetylderivative **5a-5b, 6a-6b** (9.33 mmol) and the solution of KOH (4,78 g; 85,19 mmol) in solution of ethanole (7 ml) and water (7 ml) was heated to form a solution. The solution was then refluxed for 4 h by heating on a water bath, ethanol was evaporated from the reaction mixture and the solution was acidified with acetic acid to pH 5. The next day, a yellow crystalline compound was collected with suction, washed with water and dried. For further details see Tables 1-2.

5,6-Difluoroindolo[2,3-b]quinoxaline (9a) resp. dimethylderivative (9b), 6,7-dichloroindolo[2,3-b]quinoxaline (10a) resp. dimethylderivative (10b)

A mixture of corresponding amine **7a-7b, 8a-8b** (1.0 mmol) and $POCl_3$ (2 ml) was refluxed for 16 hours. After cooling to room temperature, the mixture was poured over crush ice. The next day, a crystalline compounds was collected with suction, washed with water and dried in air. Recrystallization from ethanol and water (1:1 v/v) afforded the white solid. For further details see Tables 1-2.

Table 1. Characteristic data of compounds 1-10

Compound	M.p. (°C) Yield (%)	Formula M.w.	Elemental Analysis (Calcul./Found)		
			%C	%H	%N
1	218-219 73.0	$C_8H_3NO_2F_2$ 183.12	52.47 52.35	1.65 1.49	7.65 7.69
2	195-196 72.1	$C_8H_3NO_2Cl_2$ 216.12	44.46 44.56	1.40 1.46	6.48 6.43
3	168-169 69.0	$C_{10}H_5NO_3F_2$ 225.15	53.35 53.29	2.24 2.12	6.22 6.16
4	160-161 70.8	$C_{10}H_5NO_3Cl_2$ 258.15	46.53 46.43	1.95 1.83	5.43 5.38
5a	310-311 93.1	$C_{16}H_{11}N_3O_2F_2$ 315.28	60.95 60.87	3.52 349	13.33 13.38
5b	320-321 92.7	$C_{18}H_{15}N_3O_2F_2$ 343.34	62.97 62.88	4.40 4.38	12.24 12.30
6a	317-318 94.3	$C_{16}H_{11}N_3O_2Cl_2$ 348.28	55.18 55.25	3.18 3.27	12.06 12.10
6b	333-334 96.6	$C_{18}H_{15}N_3O_2Cl_2$ 376.34	57.45 57.51	4.02 4.07	11.17 11.24
7a	288-289 89.9	$C_{14}H_9N_3OF_2$ 273.24	61.54 61.62	3.32 3.22	15.38 15.30
7b	290-291 90.6	$C_{16}H_{13}N_3OF_2$ 301.3	63.78 63.72	4.35 4.26	13.95 13.98
8a	262-263 90.6	$C_{14}H_9N_3OCl_2$ 306.2	54.91 54.95	2.96 3.02	13.72 13.70
8b	269-270 92.4	$C_{16}H_{13}N_3OCl_2$ 334.3	57.49 57.32	3.92 4.01	12.57 12.56
9a	300-301 84.5	$C_{14}H_7N_3F_2$ 255.23	65.88 65.82	2.76 2.79	16.46 16.40
9b	309-310 89.7	$C_{16}H_{11}N_3F_2$ 283.28	67.84 67.72	3.91 3.92	14.83 14.87
10a	302-303 86.9	$C_{14}H_7N_3Cl_2$ 288.23	58.34 58.39	2.45 2.39	14.58 14.57
10b	311-312 83.0	$C_{16}H_{11}N_3Cl_2$ 316.28	60.76 60.76	3.51 3.45	13.29 13.30

Table 2. IR spectra of compounds 1-10

Compound	IR spectrum
1	3110, 3056, 1761, 1730, 1619, 1497, 1472, 1349, 1213, 1150, 113, 876, 780, 746, 666
2	3242, 1754, 1742, 1610, 1435, 1316, 1154, 965, 835, 793, 581
3	3112, 1784, 1744, 1715, 1605, 1488, 1352, 1252, 1145, 1036, 968, 917, 819
4	3370, 1784, 1746, 1716, 1601, 1516, 1460, 1372, 1304, 1255, 1187, 1158, 983, 847
5a	3168, 3058, 2964, 1687, 1663, 1610, 1521, 1470, 1414, 1333, 1249, 1178, 876, 789, 590
5b	3178, 3049, 3000, 2954, 2940, 2899, 1690, 1653, 1611, 1533, 1489, 1413, 1332, 1233, 1189, 890, 793
6a	3264, 3169, 3028, 1667, 1642, 1574, 1535, 1452, 1400, 1311, 1250, 1032, 904, 811, 743
6b	3214, 3119, 3019, 2999, 2983, 1666, 1642, 1579, 1547, 1450, 1416, 1309, 1012, 989, 833, 741
7a	3451, 3105, 2936, 1662, 1585, 1518, 1425, 1298, 1148, 888, 834, 787, 600
7b	3449, 3115, 2976, 2917, 1665, 1660, 1581, 1506, 1463, 1277, 1138, 988, 901, 854, 789
8a	3333, 3005, 1662, 1572, 1543, 1488, 1410, 1304, 1254, 1212, 893, 607
8b	3345, 3111, 3000, 2983, 2978, 1670, 1600, 1579, 1540, 1479, 1408, 1300, 1234, 1210, 888
9a	3109, 1520, 1483, 1433, 1350, 1152, 1003, 875
9b	3113, 3009, 1538, 1499, 1475, 1446, 1361, 1112, 1068, 890
10a	3105, 1559, 1490, 1341, 1210, 996, 828
10b	3105, 2999, 2879, 1538, 1510, 1456, 1369, 1311, 1219, 1005, 899

Acknowledgements

We are grateful to the Ministry of Education, Youth and Sport of the Czech Republic, for the grant MSM6198959216.

References

1. Fryšová I., Otyepka M., Slouka J.: *Acta Univ. Palacki. Olomuc, Fac. Rerum Natur* **43**, 73 (2004).
2. Kim D.K.; Kim J.; Park H.J. *Bioorg. Med. Chem.* **2004**, *14(40)*, 2401.

3. Li H.Y.; Wang Y.; Yan L.; Campbell R.M.; Anderson B.D.; Wagner J.R. Yingling J.M. *Bioorg. Med. Chem.* **2004**, *14(13)*, 3585.
4. Korczynski M., Marchlewski L.: *Ber. Dtsch. Chem. Ges.* **35**, 4334 (1902).
5. Yen V. Q., Buu-Hoy N. P., Xuong N.D.: *J. Org. Chem.* **23**, 1858 (1958).
6. Sadler P. W., Warren R. L.: *J. Am. Chem. Soc*. **78**, 1251 (1956).

Acta Univ. Palacki. Olomuc.
Fac. rer. nat. 2005
Chemica 44, 63-68

ACTA UNIVERSITATIS PALACKIANAE OLOMOUCENSIS
FACULTAS RERUM NATURALIUM (2005) CHEMICA 44

SYNTHESIS, CHARACTERIZATION AND ANTIMICROBIAL STUDIES OF TRANSITION METAL COMPLEXES WITH TETRAAMINE SCHIFF BASE MACROCYCLIC LIGANDS

N. Nishat*, Rahis-ud-din and M. Mazharul Haq

Department of Chemistry, Jamia Millia Islamia (Central University), New Delhi-110025, India: E-mail: nishat_nchem03@yahoo.co.in

Received April 5, 2005
Accepted July 2, 2005

Abstract

The reaction of 1,1,1,2,2,3,3-heptafluoro-7,7-dimethyl-4,6-octanedione with ethylenediamine or 1,3-diaminopropane in ethanol give two novel macrocycles, 1,5,8,12-tetraaza-4,11-bis-(1′,1′-dimethylethyl)-2,9-bis(1″,1″,1″,2″,2″,3″,3″-heptafluoropropyl)-cyclotetradeca-1,4,8,11-tetraene (L^1), and 1,5,9,13-tetraaza-4,12-bis-(1′,1′-dimethylethyl)-2,10-bis(1″,1″,1″,2″,2″,3″,3″-heptafluoropropyl)-cyclohexadeca-1,4,9,12-tetraene (L^2). Their complexes with Cr(III), Mn(II), Fe(III), Co(II), Ni(II), Cu(II) and Zn(II) ions have also been synthesized in CH_3OH. They are characterized by elemental analyses, magnetic susceptibility measurements, molar conductance measurements, IR, EPR, ^1H NMR and UV-Visible spectra. The molar conductance values show that the complexes of Cr(III) and Fe(III) are 1:1 electrolytes, the Ni(II) and Cu(II) ions are 1:2 electrolytes while those of Mn(II), Co(II) and Zn(II) appear to be non ionic. An octahedral structure has been proposed for all of these metal ions except for those of Cu(II) and Ni(II), which appear to be square-planar. The β values indicate a considerable orbital overlap in the metal-ligand bond. Antimicrobial activities of the macrocyclic ligands and their complexes have been extensively studied on some strains (gram-positive bacteria) *Staphylococcus aureus* and (gram-negative bacteria) *Escherichia coli.* Most of the complexes show higher activity than the ligands. Therefore, results show that these compounds inhibit the growth of bacteria.

Keywords: *pendant macrocycles, Ni(II) and Cu(II) complexes, antimicrobial activity*

* Author for correspondence

Introduction

The synthesis and coordination chemistry of macrocycles and their transition and non transition metal complexes originated in 1960s and at that time Ni(II) ion was used as a templating agent[1]. Now a days a large number of macrocycles have been synthesized and many other template process have also been discovered[2,3]. The heterobinuclear cores are kinetically retarded towards metal dissociation and thermodynamically stable, so the heterobinuclear macrocycles are more important acyclic ligands. The pendant armed macrocycles are more important[4,5], as they can form complexes with amino acids and also the pendant units (as acetates) of their host can again interact with guest macrocycles stabilize the host-guest complexes[6], furthermore macrocycles have wide application in treatment of kidney stones, in cancer diagnosis[7,8] and in catalyst. Tetradentate Schiff base macrocyclic complexes are important for designing model complexes related to synthetic and natural oxygen carriers. They are also useful as magnetic resonance imaging (MRI) contrast agents[9]. Due to the different applications of macrocycles we have synthesized the new macrocycles, namely 1,5,8,12-tetraaza-4,11-bis-(1′,1′-dimethylethyl)-2,9-bis(1″,1″,1″,2″,2″,3″,3″-heptafluoropropyl)-cyclotetradeca-1,4,8,11-tetraene (L^1), and 1,5,9,13-tetraaza-4,12-bis-(1′,1′-dimethylethyl)-2,10-bis-(1″,1″,1″,2″,2″,3″,3″-hepta-fluoropropyl)-cyclohexadeca-1,4,9,12-tetraene, (L^2) by the interaction of 1,1,1,2,2,3,3-heptafluoro-7,7-dimethyl-4,6-octanedione with ethylenediamine or 1,3-diaminopropane in 2:2 ratios in ethanol. We describe here the synthesis and characterization of the macrocycles, (L^1 and L^2) and their transition metal complexes. In order to explore their nature and mode of bonding, we have synthesized their transition metal complexes with Cr(III) Mn(II), Fe(III), Co(II), Ni(II), Cu(II) and Zn(II) ions.

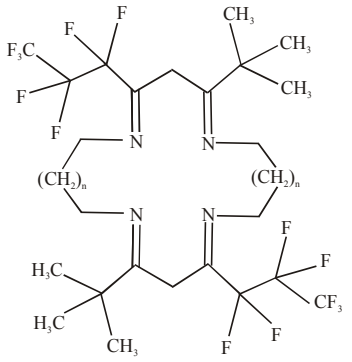

Figure 1. L^1 (n = 0) and L^2 (n = 1)

Materials and methods

Materials

1,1,1,2,2,3,3-heptafluoro-7,7-dimethyl-4,6-octanedione (SCM), ethylenediamine (CDH), 1,3-diaminopropane, (E. Merck), transition metal chlorides (s. d. fine-chem.) were used as received.

Preparation of Ligands (L^1 and L^2)

Synthesis of the ligand 1,5,8,12-Tetraaza-4,11-bis-(1′,1′-dimethylethyl)-2,9-bis-(1″, 1″,1″,2″,2″,3″,3″-heptafluoropropyl)-cyclotetradeca-1,4,8,11-tetraene, (L^1)
The ethylenediamine (40 mmol, 2.6 cm^3) was added dropwise to the solution of 1,1,1,2,2,3,3-heptafluoro-7,7-dimethyl-4,6-octanedione (40 mmol, 9.2 cm^3) in CH_3OH (75 cm^3), in 250 cm^3 round bottom flask. The resulting mixture was refluxed for 4 h, cooled at 0ºC and it was kept in refrigerator for 2 days. A light orange product was collected by filtration, washed with dry Et_2O and dried in vacuum desiccator. Yield: 54%.

The ligand L^2 (1,5,9,13-tetraaza-4,12-bis-(1′,1′-dimethylethyl)-2,10-bis(1″,1″,1″,2″,2″,3″,3″-heptafluoropropyl)-cyclohexadeca-1,4,9,12-tetraene) was also synthesized by the same procedure using 1,3-diaminopropane (40 mmol, 3.2 cm^3) and 1,1,1,2,2,3,3-heptafluoro-7,7-dimethyl-4,6-octanedione (40 mmol, 9.2 cm^3) in CH_3OH (75 cm^3). A red product was obtained by filtration, washed with dry Et_2O and dried in vacuum desiccator. Yield: 62%.

Synthesis of complexes of ligands (L^1 and L^2)

The L^1 solution (10 mmol, 6.5 g) in CH_3OH and conc. HCl mixture (40 cm^3 and 1 cm^3) was added slowly to the nickel(II) chloride (10 mmol, 2.4 g) in CH_3OH (25 cm^3) with constant stirring. The solution mixture was refluxed for about 4 h, in order to complete reaction. An orange precipitate that formed, was filtered, washed with hexane and dry Et_2O and dried in vacuum desiccator. Yield: 50%.

Nickel(II) complex of the ligand (L^2) was synthesized by the similar method. The brown product that formed was filtered, washed with hexane and dry Et_2O and dried in vacuum desiccator. Yield: 51%.

Similar procedure was employed for the synthesis of Mn(II), Co(II), Cu(II), Zn(II) complexes of L^1. The immediately precipitated complexes were collected, washed with, hexane and dry Et_2O and dried in vacuum desiccator. Yields: 52-60%.
The synthesis of Cr(III) complex of the ligand (L^1) was carried out by addition of CH_3OH and conc. HCl solution (40 cm^3 and 2 cm^3) of L^1 (10 mmol, 6.5 g) to the chromimum(III) chloride (10 mmol, 2.7 g) solution in CH_3OH (25 cm^3). The resulting mixture was refluxed with constant stirring for 9 h, yielding light green product. The precipitate was filtered, washed with acetone and dry Et_2O and dried in vacuum desiccator. Yield: 62%. The iron(III) complex of L^1 was synthesized by the similar above procedure. The light brown precipitate that formed was filtered, washed with dry Et_2O and dried in vacuum desiccator. Yield: 56%.

The complexes of ligand (L^2) were synthesized by the similar procedure as applied for the ligand (L^1) complexes. Yields: 41-59 %.

Antibacterial screening

Antibacterial activity of the ligands (L^1 and L^2) and their complexes were evaluated by filter paper disc method[10]. In the case of quantitative estimation, minimum inhibitory concentrations (MIC) in mm were determined. The sterile discs (5 mm diameter) of the filter paper (Whatman No. 4) were dipped into solution of test compounds of 0.5-1.0 mg/cm^3 concentration in DMSO, placed over seeded plates, left for diffusion and incubated at 37 ^{0}C for 24 h, where clear inhibition zones were detected around the disc. The compound diffuses into nutrient agar plate prevents the growth of bacterium. Control plates for the solvent DMSO and gentamicin as a standard antibacterial agent were compared with the test compound. Antibacterial activities can be calculated as a mean of three replicates.

Physical measurements

Elemental analyses (CHN) were performed on a Carlo Erba 1106 Thomas and Coleman analyzer. The IR spectra of the ligands and their complexes were recorded in KBr pellets with a Perkin Elmer 621 spectrophotometer in the 4000-200 cm^{-1} range. The UV-visible spectra were recorded on a Lambda EZ201 Perkin Elmer spectrometer in DMSO and magnetic susceptibility measurements were done with an Allied Research model 155 vibration sample magnetometer at room temperature. The conductivity measurements were carried out on a CM-82T Elico conductivity bridge in DMSO at room temperature (c=10^{-3} mol/dm^3). The EPR spectra were recorded on Bruker Scientific X-band spectrometer (ESP-300). The ^{1}H NMR spectra of macrocyclic ligands and their copper(II) complexes were run in DMSO-d_6 on a JOEL-FX-100 spectrometer, using TMS as an internal standard. Chlorine was estimated gravimetrically[11] and the metals were determined by using EDTA titration method[12]. The solvent were distilled and dried by conventional methods before use.

Results and discussion

The colour, melting point, yield percentage, molar conductance and analytical data of the ligands (L^1 and L^2) and their complexes are summarized in Table 1. The analytical data of the complexes correspond well with the general formulae $[MLCl_2]$, $[M'LCl_2]Cl$, where M = Mn(II), Co(II), Zn(II) and M' = Cr(III), Fe(III), and $[M''L]Cl_2$, where M'' = Cu(II), Ni(II) and L = L^1 and L^2. all of the compounds are stable at room temperature at air. The complexes are soluble in DMSO and CH_3CN. The molar conductance values of $[MLCl_2]$ complexes, M = Mn(II), Co(II), Zn(II) in DMSO (11-32 S cm^2 mole^{-1}) indicate their non-electrolytic nature. While for the complexes of Fe(III) and Cr(III) ions, the value is (55-68 S cm^2 mole^{-1}), show their 1:1 electrolytic behavior and for the Ni(II), Cu(II) complexes the molar conductance values (128-136 S cm^{2}mole^{-1}) suggest that they are 1:2 electrolytes[13].

The reactions for the formation of the ligands and their metal complexes are shown below:

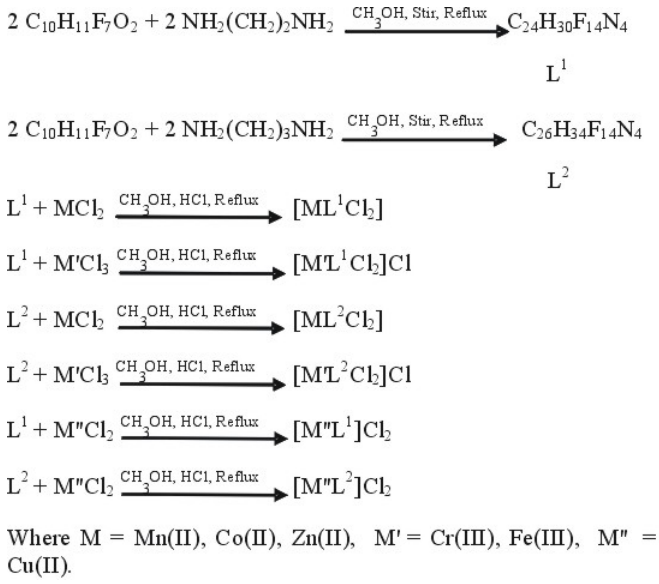

Where M = Mn(II), Co(II), Zn(II), M' = Cr(III), Fe(III), M'' = Ni(II), Cu(II).

IR spectra

The relative IR bands and their assignments are listed in Table 2. The pendant ligands and their complexes were studied by IR spectroscopy as KBr discs. As a consequences of the interaction of the 1,1,1,2,2,3,3-heptafluoro-7,7-dimethyl-4,6-octanedione with ethylenediamines or 1,3-diaminopropane, the carbonyl frequencies have been replaced by ν(C=N) bands. The uncoordinated ligands (L^1 and L^2) exhibit a medium absorption at 1608 cm^{-1} and 1615 cm^{-1}, respectively, which can be assigned to ν (C=N) stretching mode[14]. In order to study the binding mode of the schiff base to metal in the complexes, their spectra of free ligands were compared with the spectra of the metal complexes. The ν(C=N) bands in the complexes are shifted to lower wave number region (20-40 cm^{-1}) indicating the involvement of azomethine nitrogen atom on coordination to the metal ion[15]. It is further confirmed by decreasing ν(C-N) stretching frequencies in the complexes. The metal chelates show some new bands at 345-420 cm^{-1}, which are due to the formation of M-N bands. In addition to these bands, the two (M-Cl) have been found to appear at 260-290 cm^{-1}.

Electronic spectra and magnetic moments

The electronic spectra in DMSO and magnetic moments are given in Table 3. The chromium(III) complexes display three bands at 35220 cm^{-1}, 34780 cm^{-1}, 20240 cm^{-1}, 21290 cm^{-1} and 18240 cm^{-1}, 19380 cm^{-1} for L^1 and L^2 complexes respectively. Out of three spin allowed bands, the highest energy bands are assignable to the $^4T_{1g}(P) \leftarrow {}^4A_{2g}(F)$

transitions. The observed magnetic moment values (3.62-3.76 B.M.) are closer to the calculated value for three unpaired electrons. These studies indicate the octahedral geometry for chromium(III) ion.

The electronic spectra of Mn(II) complexes of L^1 and L^2 in DMSO show weak absorption bands at 24380 cm^{-1}, 24360 cm^{-1}, 21240 cm^{-1}, 21280 cm^{-1} and 17180 cm^{-1}, 17260 cm^{-1} respectively, characteristics of the octahedral geometry for these complexes. The observed μ_{eff} values (Table 3) confirm the geometry around the Mn(II) ion[16].

The majority of iron(III) complexes in high-spin state have μ_{eff} 5.9 B.M. The observed magnetic values 5.79 B.M. for L^1 and 5.82 B.M for L^2 complexes are very close to the calculated value. The complexes exhibit three main *d-d* bands that can be attributed to transitions $^4E_g(G) \leftarrow {}^6A_1$, $^4T_{2g}(G) \leftarrow {}^6A_{1g}$ and $^4T_{1g}(G) \leftarrow {}^6A_{1g}$, respectively. On the basis of magnetic moment values and electronic spectral studies, an octahedral geometry is proposed for Fe(III) ion.

For $[CoL^1Cl_2]$ and $[CoL^2Cl_2]$ complexes three transitions have been observed and assigned to their respective transitions (Table 3). The room temperature magnetic moment values lie in the range of 4.12-4.22 B.M. These studies are in consonance with the octahedral environment around the Co(II) ion[17,18].

The nickel(II) complexes of L^1 and L^2 show one charge transfer bands at 20280 cm^{-1}, 21240 cm^{-1}, in addition two more bands appear at 19280 cm^{-1}, 20202 cm^{-1}, 18680 cm^{-1}, 18660 cm^{-1} respectively and can be assigned to the transitions $^1B_{1g} \leftarrow {}^1A_{1g}$ and $^1B_{2g} \leftarrow {}^1A_{1g}$. These bands suggest the square planar[19] structure of Ni(II) ions.

The electronic spectra of copper(II) complexes show a charge transfer band at 26680 cm^{-1}, 26610 cm^{-1} and another bands at 18520 cm^{-1}, 18220 cm^{-1}, 14480 cm^{-1}, 15540 cm^{-1}. The observed magnetic moments are 1.82 B.M. for L^1 and 1.80 B.M. for L^2 complexes correspond to the square planar geometry for copper(II) ion.

The 10 Dq values for the complexes follow the order

Cr(III) > Mn(II) > Co(II) > Fe(III)

^1H NMR spectra

The ^1H NMR spectra of ligand L^1 and L^2 in DMSO-d_6 show peak at δ(1.72-1.79 ppm) due to the six terminal -CH_3 groups. The two singlets at δ(3.82 ppm) and a triplet at δ(3.42-3.56 ppm) adjacent to N-atom can be ascribed to the methylene groups (-CH_2-, 4H)[20]. The peaks for -CH_2- in the L^2 additional band appear at δ(3.75-3.81 ppm) as a triplet. The Ni(II) complexes of the ligands (L^1 and L^2) exhibit high δ values, due to the low electron density after complex formation.

EPR spectra

The g terms or values of the copper(II) complexes are used to derive the ground state. In the square planar geometry, the nonbonded electron lies in the d_{x2-y2} orbital and give $^2B_{1g}$ as ground state where $g_\pi > g_\perp > 2.00$ but when the unpaired electron goes in the d_{z2} orbital, and has $^2A_{1g}$ ground state in which $g_\perp > g_\pi > 2.00$. In the complexes, the values show that $g_\pi > g_\perp > 2.00$ which indicate the square planar[21] geometry around Cu(II) ion.

Antibacterial activity

The results of antibacterial screening are tabulated in Table 4. The free ligands and their metal complexes were tested against the bacteria species *Staphylococcus aureus* and *Escherichia coli*. An antibiotics gentamicin was evaluated for the antibacterial activities and its results compared with the free ligands and their metal complexes. The results showed that all the metal complexes have antibacterial activities towards tested bacteria than the ligands and the control. The results indicate that the compounds inhibit the growth of bacteria to a greater extent as concentration is increased due to the effect of the metal ion on the normal cell process.

On the basis of above studies the structures in Figure 2 have been proposed for the macrocyclic metal complexes. Unfortunately, all our attempts to prepare crystals appropriate for X-ray analysis were unsuccessful.

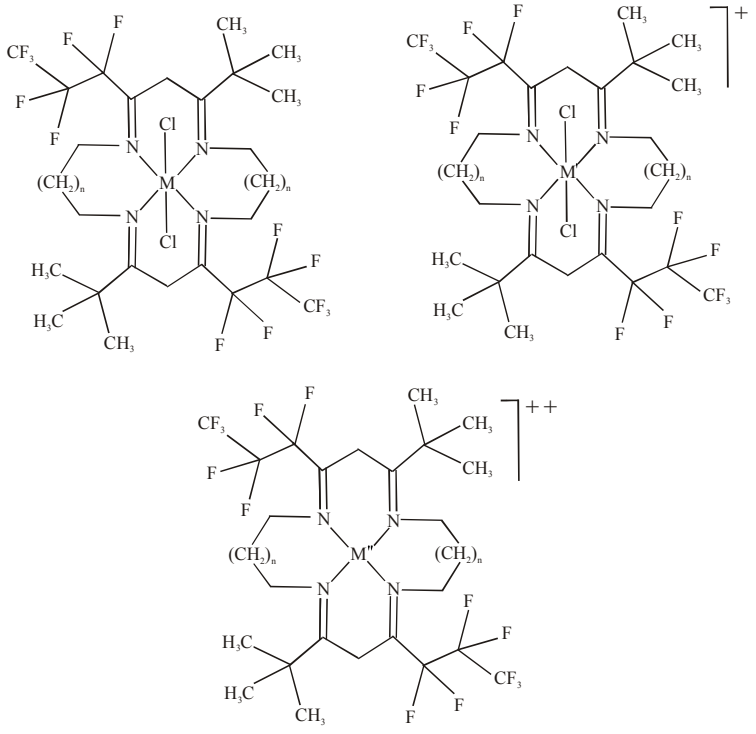

Figure 2. Suggested structures of the metal complexes of L^1 and L^2. *Key:* M = Mn(II), Co(II), Zn(II), M' = Cr(III), Fe(III), M'' = Ni(II), Cu(II), L^1; n = 0; L^2; n = 1

Table 1. Colours, m.p., yield percentage, molar conductances and analytical data of ligands and their complexes.

Compounds	Colour	M.p. (°C)	Yield (%)	Λ_M (S.cm^2 mole^{-1})	Found (Calcd.) %				
					C	H	N	M	Cl
$C_{24}H_{30}F_{14}N_4$, (L^1) (648.44)	Light orange	124	54	-	44.40 (44.45)	4.63 (4.66)	9.90 (9.86)	-	-
$[CrL^1Cl_2]Cl$ $[C_{24}H_{30}F_{14}N_4CrCl_2]Cl$ (806.78)	Light green	240 d	62	68	35.66 (35.72)	3.76 (3.74)	7.88 (7.92)	6.40 (6.44)	13.12 (13.18)
$[MnL^1Cl_2]$ $[C_{24}H_{30}F_{14}N_4MnCl_2]$ (774.28)	Light Pink	288 d	52	15	37.12 (37.22)	3.95 (3.90)	8.24 (8.26)	7.02 (7.09)	9.12 (9.15)
$[FeL^1Cl_2]Cl$ $[C_{24}H_{30}F_{14}N_4FeCl_2]Cl$ (810.64)	Light brown	202 d	56	55	35.52 (35.55)	3.72 (3.73)	7.85 (7.89)	6.92 (6.90)	13.05 (13.12)
$[CoL^1Cl_2]$ $[C_{24}H_{30}F_{14}N_4CoCl_2]$ (778.27)	Pink	230 d	56	32	37.08 (37.03)	3.90 (3.88)	8.15 (8.21)	7.50 (7.57)	9.08 (9.11)
$[NiL^1]Cl_2$ $[C_{24}H_{30}F_{14}N_4Ni]Cl_2$ (778.03)	Orange	220 d	50	136	37.02 (37.05)	3.85 (3.89)	8.16 (8.22)	7.48 (7.54)	9.04 (9.11)
$[CuL^1]Cl_2$ $[C_{24}H_{30}F_{14}N_4Cu]Cl_2$ (782.84)	Bluish green	268 d	58	128	36.76 (36.82)	3.82 (3.86)	8.12 (8.17)	8.05 (8.11)	9.00 (9.05)
$[ZnL^1Cl_2]$ $[C_{24}H_{30}F_{14}N_4ZnCl_2]$ (784.73)	Colour less	275 d	60	25	36.70 (36.73)	3.80 (3.85)	8.17 (8.15)	8.25 (8.33)	9.02 (9.03)

Table 1. Contd……

Compounds	Colour	M.p. (°C)	Yield (%)	Λ_M (S cm^2 $mole^{-1}$)	Found (Calcd.) %				
					C	H	N	M	Cl
$C_{26}H_{34}F_{14}N_4$, (L^2) (676.48)	Red	151	62	-	46.12 (46.16)	5.02 (5.06)	9.40 (9.45)	-	-
$[CrL^2Cl_2]Cl$ $[C_{26}H_{34}F_{14}N_4CrCl_2]Cl$ (834.82)	Greenish blue	280 d	59	60	37.36 (37.40)	4.15 (4.10)	7.60 (7.66)	6.18 (6.22)	12.70 (12.74)
$[MnL^2Cl_2]$ $[C_{26}H_{34}F_{14}N_4MnCl_2]$ (802.32)	Pink	220 d	41	11	38.88 (38.91)	4.22 (4.27)	7.92 (7.97)	6.82 (6.84)	8.79 (8.83)
$[FeL^2Cl_2]Cl$ $[C_{26}H_{34}F_{14}N_4FeCl_2]Cl$ (838.68)	Brown	195 d	48	66	37.20 (37.23)	4.10 (4.08)	7.66 (7.62)	6.60 (6.65)	12.65 (12.68)
$[CoL^2Cl_2]$ $[C_{26}H_{34}F_{14}N_4CoCl_2]$ (806.31)	Pink	224 d	52	22	38.74 (38.72)	4.18 (4.24)	7.88 (7.93)	7.27 (7.30)	8.75 (8.79)
$[NiL^2]Cl_2$ $[C_{26}H_{34}F_{14}N_4Ni]Cl_2$ (806.06)	Brown	210 d	51	136	38.70 (38.73)	4.20 (4.25)	7.86 (7.93)	7.32 (7.28)	8.74 (8.80)
$[CuL^2]Cl_2$ $[C_{26}H_{34}F_{14}N_4Cu]Cl_2$ (810.88)	Blue	284 d	58	138	38.47 (38.50)	4.18 (4.22)	7.92 (7.88)	7.77 (7.83)	8.72 (8.74)
$[ZnL^2Cl_2]$ $[C_{26}H_{34}F_{14}N_4ZnCl_2]$ (812.77)	Colourless	232 d	54	26	38.35 (38.41)	4.16 (4.21)	7.80 (7.86)	8.05 (8.04)	8.68 (8.72)

Table 2. IR spectral bands (cm^{-1}) of the ligands and their complexes.

Compound	ν(C=N)	ν(C–N)	ν(C–C)	ν(M–N)	ν(M–Cl)
Ligand [L^1]	1608 m	1415 s	1055 w	-	-
[CrL^1Cl_2]Cl	1570 m	1396 s	1058 w	410 s	290 m
[MnL^1Cl_2]	1568 m	1390 s	1060 w	370 s	260 m
[FeL^1Cl_2]Cl	1585 m	1382 s	1063 w	420 s	273 m
[CoL^1Cl_2]	1588 m	1388 s	1060 w	385 s	265 m
[NiL^1]Cl_2	1576 m	1398 s	1063 w	345 s	275 m
[CuL^1]Cl_2	1580 m	1381 s	1058 w	352 s	288 m
[ZnL^1Cl_2]	1575 m	1394 s	1056 w	375 s	280 m
Ligand [L^2]	1615 m	1400 s	1065 w	-	-
[CrL^2Cl_2]Cl	1587 m	1376 s	1058 w	385 s	285 m
[MnL^2Cl_2]	1580 m	1386 s	1048 w	358 s	265 m
[FeL^2Cl_2]Cl	1575 m	1372 s	1058 w	415 s	268 m
[CoL^2Cl_2]	1595 m	1378 s	1063 w	345 s	272 m
[NiL^2]Cl_2	1590 m	1382 s	1055 w	367 s	265 m
[CuL^2]Cl_2	1588 m	1381 s	1050 w	350 s	282 m
[ZnL^2Cl_2]	1578 m	1386 s	1045 w	365 s	276 m

Table 3. Electronic Spectral Bands, Magnetic Moments and Ligand Field Parameters of the Macrocyclic Complexes

Compounds	$\mu_{eff.}$ (B.M.)	Electronic Bands (cm^{-1})	ε^a	Possible Assignment	10 Dq (cm^{-1})	(B) (cm^{-1})	β
$[CrL^1Cl_2]Cl$	3.62	35220 20240 18240	16 10 12	$^4T_{1g}(P) \leftarrow {}^4A_{2g}(F)$ $^4T_{1g}(F) \leftarrow {}^4A_{2g}(F)$ $^4T_{2g}(P) \leftarrow {}^4A_{2g}(F)$	13226	778	0.755
$[MnL^1Cl_2]$	5.48	24380 21240 17180	18 11 15	$^4E_g\,(G) \leftarrow {}^6A_{1g}$ $^4T_{2g}\,(G) \leftarrow {}^6A_{1g}$ $^4T_{1g}\,(G) \leftarrow {}^6A_{1g}$	9102	740	0.77
$[FeL^1Cl_2]Cl$	5. 79	22150 20570 16780	13 15 12	$E_g\,(G) \leftarrow {}^6A_{1g}$ $^4T_{2g}\,(G) \leftarrow {}^6A_{1g}$ $^4T_{1g}\,(G) \leftarrow {}^6A_{1g}$	8129	655	0.60
$[CoL^1Cl_2]$	4.12	20280 19280 12390	19 12 16	$^4T_{1g}(P) \leftarrow {}^4T_{1g}(F)$ $^4A_{2g}(F) \leftarrow {}^4T_{1g}(F)$ $^4T_{2g}(F) \leftarrow {}^4T_{1g}(F)$	8570	553	0.57
$[NiL^1]Cl_2$	Diamag.	20280 19280 18680	12 10 17	Charge Transfer $^1B_{1g} \leftarrow {}^1A_{1g}$ $^1A_{2g} \leftarrow {}^1A_{1g}$	-	-	-
$[CuL^1]Cl_2$	1.82	26680 18520 14480	15 16 11	Charge Transfer $^2A_{1g} \leftarrow {}^2B_{1g}$ $^2E_g \leftarrow {}^2B_{1g}$	-	-	-
$[ZnL^1Cl_2]$	Diamag.	-		-	-	-	-

($^a\varepsilon = dm^3mol^{-1}cm^{-1}$)

Table 3. Contd…….

Compounds	$\mu_{eff.}$ (B.M.)	Electronic Bands (cm^{-1})	ε^a	Possible Assignment	10 Dq (cm^{-1})	(B) (cm^{-1})	β
$[CrL^2Cl_2]Cl$	3.76	34780 21290 19380	13 12 15	$^4T_{1g}(P) \leftarrow {}^4A_{2g}(F)$ $^4T_{1g}(F) \leftarrow {}^4A_{2g}(F)$ $^4T_{2g}(P) \leftarrow {}^4A_{2g}(F)$	13456	841	0.82
$[MnL^2Cl_2]$	5.60	24360 21280 17260	18 15 10	$^4E_g\,(G) \leftarrow {}^6A_{1g}$ $^4T_{2g}\,(G) \leftarrow {}^6A_{1g}$ $^4T_{1g}\,(G) \leftarrow {}^6A_{1g}$	9028	734	0.76
$[FeL^2Cl_2]Cl$	5. 82	21755 19880 16230	13 18 12	$^4E_g\,(G) \leftarrow {}^6A_{1g}$ $^4T_{2g}\,(G) \leftarrow {}^6A_{1g}$ $^4T_{1g}\,(G) \leftarrow {}^6A_{1g}$	7847	638	0.58
$[CoL^2Cl_2]$	4.22	18900 14830 11600	21 16 12	$^4T_{1g}(P) \leftarrow {}^4T_{1g}(F)$ $^4A_{2g}(F) \leftarrow {}^4T_{1g}(F)$ $^4T_{2g}(F) \leftarrow {}^4T_{1g}(F)$	9906	780	0.80
$[NiL^2]Cl_2$	Diamag.	21240 20202 18660	15 18 14	Charge Transfer $^1B_{1g} \leftarrow {}^1A_{1g}$ $^1A_{2g} \leftarrow {}^1A_{1g}$	-	-	-
$[CuL^2]Cl_2$	1.80	26610 18220 15540	18 12 11	Charge Transfer $^2A_{1g} \leftarrow {}^2B_{1g}$ $^2E_g \leftarrow {}^2B_{1g}$	-	-	-
$[ZnL^2Cl_2]$	Diamag.	-		-	-	-	-

($^a\varepsilon = dm^3mol^{-1}cm^{-1}$)

Table 4. Antibacterial activity of ligands and complexes (Zone formation in mm)

Compound	*S. aureus*		*E. coli*	
	0.5 mg/cm^3	1.0 mg/cm^3	0.5 mg/cm^3	1.0 mg/cm^3
*Gentamicin	8	10	7	9
Ligand L^1	10	11	10	13
Ligand L^2	11	13	11	14
CrL^1	14	19	13	25
MnL^1	16	24	17	20
FeL^1	15	19	16	27
CoL^1	15	18	17	24
NiL^1	18	20	15	21
CuL^1	15	22	16	25
ZnL^1	14	23	19	23
CrL^2	15	25	14	18
MnL^2	18	27	14	20
FeL^2	17	25	15	22
CoL^2	15	23	16	25
NiL^2	16	20	18	21
CuL^2	15	19	16	26
ZnL^2	13	23	15	27

*Bactericides

Acknowledgements

The authors are thankful to the Third World Academy of Sciences Italy for financial support through research grand scheme No.00-047 RG/CHE/AS. We are greatful to Dr. Syed Farooq for antibacterial activity in Microbiology Laboratory, Himalya Drugs Co. Najafgarh road, New Delhi, India.

References

1. Curtis N. F., *Coord. Chem. Rev.,* **3**, 3 (1968).
2. Comba P., Curtis N. F., Laurance G. A., Sargeson A. M., Skelton B. W. and White A. H., *Inorg. Chem.*, **25,** 426 (1986).
3. Comba P., Curtis N. F., Lawrence G. A., O'Leary M. A., Skelton B. W. and White A. H., *J. Chem. Soc. Dalton Trans.,* 497 (1988).
4. Bernhardt P. V. and Sharpe P. C., *Inorg. Chem.,* **39,** 2020 (2000).
5. Fenton R. R., Lindoy L. F., Luckay R. C., Turville F. R. and Wei G., *Aust. J. Chem.,* **54,** 59 (2001).
6. Fitzmaurice R. J. Kyne G. M., Douheret D. and Killburn J. D., *J. Chem. Soc. Perkin Trans*., **1,** 841 (2002).
7. Bernhardt P. V. and Sharpe P. C., *Inorg. Chem.,* **39,** 4123 (2000).
8. McAuley A., Subramanian S., Zaworatko M. J. and Biradha K., *Inorg. Chem.,* **38,** 5078 (1999).
9. Comblen V., Gilsoul D., Herman M., Jacques V., Masbhi M., Sauvge C. and Desteux J. F., *Coord. Chem. Rev.,* **185,** 451 (1999).
10. Verma R. S. and Imam S. A., *Indian J. Micobiol.,* **13,** 45 (1979).
11. Vogel A. I., Gravimetric Analysis. In *A Text book of Quantitative Inorganic Analysis,* 3rd Edn.; Longman: London, 460 (1968).
12. Reilley C. N., Schmid R. W. and Sadek F. S., *J. Chem. Educ.,* **36**, 555 (1959).
13. Geary W. J., *Coord. Chem. Rev.,* **7,** 81 (1971).

14. Herrera A. M., Kalayda G. V., Disch J. S., Wikstrom J. P., Korendovych I. V., Staples R. J., Campana C. F., Nazarenko A. Y., Hass T. E. and Rybak-Akimova E. V., *J. Chem. Soc. Dalton Trans.,* 4482 (2003).
15. Gibson V. C., Spitzemesser S. K., White A. J. P. and Williams D. J., *J. Chem. Soc. Dalton Trans.,* 2718 (2003).
16. Franceschi F., Hesschenbrouck J., Solari E., Floriani C., Re N., Rizzoli C. and Chiesi-Villa A., *J. Chem. Soc. Dalton Trans.,* 593 (2000).
17. Makowska-Grzyska M. M., Szajna E., Shipley C., Arif A. M., Mitchell M. H., Halfon J. A. and Berreau L. M., *Inorg. Chem.,* **42,** 7472 (2003).
18. Gonzalez S., Valencia L., Bastida R., Fenton D. E., Macias A. and Rodriguez A., *J. Chem. Soc. Dalton Trans.,* 3551 (2002).
19. McAuley A. and Subramanian S., *Inorg. Chem.,* **36,** 5376 (1997).
20. Branco L., Costa J., Delgado R., Drew M. G. B., Felix V. and Goodfellow B. J., *J. Chem. Soc. Dalton Trans.,* 3539 (2002).
21. Harrison A., Henderson D. K., Lovatt P. A., Parkin A., Tasker P. A. and Winpenny R. E. P., *J. Chem. Soc. Dalton Trans.,* 4271 (2003).

Acta Univ. Palacki. Olomuc.
Fac. rer. nat. 2005
Chemica 44, 69-82

ACTA UNIVERSITATIS PALACKIANAE OLOMOUCENSIS
FACULTAS RERUM NATURALIUM (2005) CHEMICA 44

PREPARATION, IDENTIFICATION AND STRUCTURAL CHARACTERISATION OF ONE-DIMENSIONAL COORDINATION POLYMER Cu(*aepn*)Ni(CN)$_4$·H$_2$O (*aepn* = *N*-(2-AMINOETHYL)-1,3-PROPANEDIAMINE)

Jana Paharová [a*], Juraj Černák [a] and Zdirad Žák [b]

[a] *Department of Inorganic Chemistry, Institute of Chemistry, P.J. Šafárik University, Moyzesova 11, 041 54 Košice, Slovakia. E-mail: paharova@upjs.sk*
[b] *Department of Inorganic Chemistry, Masaryk University, Kotlářská 2, 61 137 Brno, Czech Republic*

Received December 7, 2004
Accepted January 12, 2005

Abstrakt

Cu(*aepn*)Ni(CN)$_4$·H$_2$O (*aepn* = *N*-(2-aminoethyl)-1,3-propanediamine) was prepared and characterised by chemical analysis and infrared spectroscopy. The results of single-crystal structure analysis showed that the structure of the title compound consists of one-dimensional coordination polymer exhibiting composition [-Cu(*aepn*)-*cis*-μ-NC-Ni(CN)$_2$-μ-CN-Cu(*aepn*)-*trans*-μ-NC-Ni(CN)$_2$-μ-CN-]$_n$. Cu(II) atom is penta-coordinated by a tridentate *aepn* chelate bonded ligand and two bridging cyano ligands. There are two crystalografically independent Ni(II) atoms in the unit cell, both of them are square-planarly coordinated by four cyano groups and two bridging cyano groups are as in *cis* as *trans* positions, respectively. The water molecules is involved hydrogen bonds of the type O-H···N(≡C) and O···N-H types.

Keywords: *Copper(II), aepn, tetracyanonickellate, X-ray structure analysis, one-dimensional structure*

Introduction

Cyanocomplexes are intensively studied for their interesting magnetic properties at present [1, 2]. Magnetic studies often require preparation of new coordination oligomers and polymers based on cyano ligands with various

* Author for correspondence

dimensionalities. For this purpose the so called “brick and mortar” method can be used [3]. This method is based on linking suitable building blocks resulting in the desired structure. As the "brick" can be used complex cation which contains free coordination sites, and as "mortar" are used cyanocomplex anions, which via bridging cyano ligands link the complex cations. The dimensionality of the formed structure can be tuned by suitable choice of ligands coordinated to the central atom in the complex cation, e.g. chelating N-donor ligands (so called blocking ligands): if all co-ordination sites of central atoms are occupied by the blocking ligands, ionic structures are formed. On the other hand, if there remain some coordination sites unoccupied, these are used for the polymerisation process by the bridging cyano ligands. This approach was used in preparation of various coordination oligomers and polymers, e.g. [4, 5].

We are interested in 1D cyanocomplexes [6]. In this work our aim was to prepare 1D cyanocomplex based on Cu(II) as central atom and tetracyanonickellate anion ("mortar"). It is known that Cu(II) often exhibits penta-coordination [7], and at the same time, that *aepn* usually acts as a three N-donor chelating ligand [8]. In our synthetic procedure according to the "brick and mortar” method we have used *aepn* as blocking ligand. As a result we have obtained the compounds Cu(*aepn*)$Ni(CN)_4 \cdot H_2O$. Here we report its synthesis, identification and crystal structure.

Materials and methods

Materials

Copper nitrate trihydrate (p.a., Lachema Brno) and *aepn* (Alldrich, >97%) were used as received. $K_2[Ni(CN)_4] \cdot H_2O$ was prepared from nickel sulphate heptahydrate (p.a., Lachema Brno) and potassium cyanide (p.a., Lachema Brno) by the literature procedure [9].

Synthesis and identification

To 1 ml 1 M aqueous solution of $Cu(NO_3)_2$ (1 mmol) were successively added 0.13 ml of *aepn* (1 mmol) in 20 ml of water and 10 ml 0.1 M aqueous solution of $K_2[Ni(CN)_4]$ (1 mmol). The obtained blue-violet solution was filtered and kept for crystallisation at laboratory temperature. Dark blue needles appeared after few days. The crystal were separated by filtration, washed with small portion of cold water and dried on air. (Yield was 55.3 %). *Anal*. (Fisons Instrument) Found: C, 36.12; H, 4.92; N, 27.21. Calc. (M_r = 361.53): C, 29.9; H, 4.74; N, 27.12%. IR spectra were recorded on FT-IR Avatar 330 firm Thermo-Nicolet instrument using KBr pellets technique in the range of 4000–400 cm^{-1}. The observed absorption bands are: ν(OH): 3577vs, 3461s, ν(NH_2): 3350vs, 3305vs, 3279vs, 3227vs, ν(CH_2): 2964m, 2948m, 2890m, ν(CN): 2169s, 2161vs, 2143vs, 2122vs, δ(H_2O): 1635, δ(NH_2): 1585s, δ(CH_2): 1470w, 1450m, 1427m, ν(C-C): 1113w, ν(C-N): 1028vs, ρ(H_2O): 690w, ρ(NH_2): 647m, ν(Ni-C): 530m, δ (chel. ring): 518w, 494vw, δ(Ni-CN): 422vs.

X-ray experiment

Cell parameters and data for Cu(*aepn*)Ni(CN)$_4$·H$_2$O were collected on KUMA-KM4 diffractometer equipped with a CCD area detector and a graphite monochromator utilising MoK$_\alpha$ radiation (λ = 0.71073 Å) at 293 K on a single crystal with dimensions 0.20 x 0.20 x 0.10 mm. The relevant crystal data are: monoclinic, C2/c, a = 15.637(3), b = 25.428(5), c = 7.630(2) Å, β = 107.84(3)°, V = 2887.9(11) Å^3, Z = 8, μ = 3.268 mm^{-1}, ρ_c = 1.988 g.cm^{-3}. Totally 4377 reflections were collected, θ range was 3.63 – 27.49° and Miller indices limits were: $-10 \leq h \leq 20$, $-31 \leq k \leq 26$, $-8 \leq l \leq 10$. After data reduction 2865 independent reflections were obtained (R_{int} = 0.0560), of these 1986 were observed ($I > 2\sigma(I)$). The structure was solved by heavy atom method using the SHELXS86 program [10]. Refinement based on intensities was performed using the SHELXL93 program [11]. All atoms with exclusion of the hydrogen ones were refined anisotropically. Hydrogen atoms of the water molecule were found in the difference map and their positions were refined using common isotropic thermal parameter; the remaining hydrogen atoms from the *aepn* ligand were placed in the calculated positions and their common group isotropic thermal parameters were refined (totally 184 parameters). The final parameters were: R1 =0.0849, S = 1.106, wR2 = 0.2133 (all data), R1 = 0.0501, wR2 = 0.1557 (observed). The final atomic positions, selected geometric parameters and possible hydrogen bonds are gathered in Tables 1, 2 and 3, respectively. For geometric calculations (hydrogen bonds geometry) the program PARST95 was used. The figures were drawn with DIAMOND programme [12].

Results and Discussion

Preparation

Using the "brick and mortar" method [3], from the aqueous system containing [Cu(*aepn*)]$^{2+}$ cations and [Ni(CN)$_4$]$^{2-}$ anions as building blocks, we have isolated dark blue crystals suitable for X-ray work. The results of chemical analyses indicated composition Cu(*aepn*)Ni(CN)$_4$·H$_2$O. Our attempt to prepare complex containing [Cu(*aepn*)$_2$]$^{2+}$ from the same system with higher Cu : *aepn* ratio (1 : 2) were unsuccessful. It is interesting to note that CCDS [13] does not contain any crystal structure with such cation. Similar procedure with *dien* (*dien* = *N*-(2-aminoethyl)-1,2-ethane-diamine, diethylenetriamine) in presence of *mea* (*mea* = 2-aminoethanol) led to formation of Cu(*dien*)(*mea*)Ni(CN)$_4$·2H$_2$O [14]. Similarly, CSDS doesn't contain entry with [Cu(*dien*)$_2$]$^{2+}$ cation in the form of cyanocomplex; only bromide [15], saccharinate [16] and bis(N-2-(benzothiazole)naphthalenesulfonamidate) [17] were structurally characterized.

Crystal and Molecular Structure

The results of single-crystal structure analysis showed that the structure of the title compound is 1D and consists of chains exhibiting composition [-Cu(*aepn*)-*cis*-μ-NC-Ni(CN)$_2$-μ-CN-Cu(*aepn*)-*trans*-μ-NC-Ni(CN)$_2$-μ-CN-]$_n$ (Fig. 1).

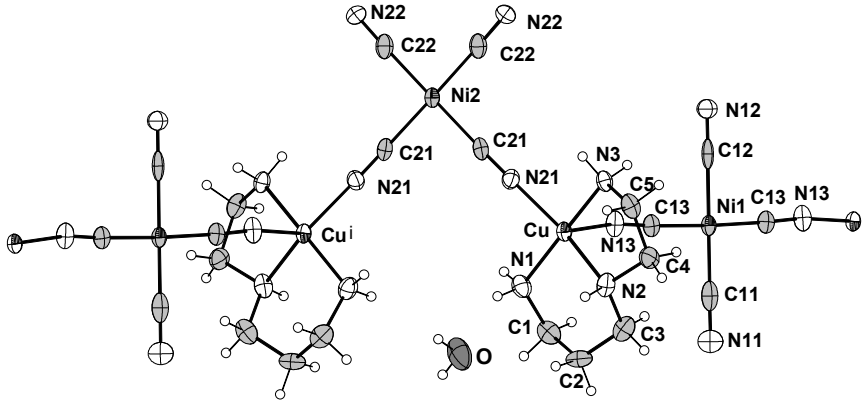

Figure 1. View of the chain structure of Cu(*aepn*)Ni(CN)$_4$·H$_2$O. Symmetry code for Cu^i: ½-x, ½-y, -z.

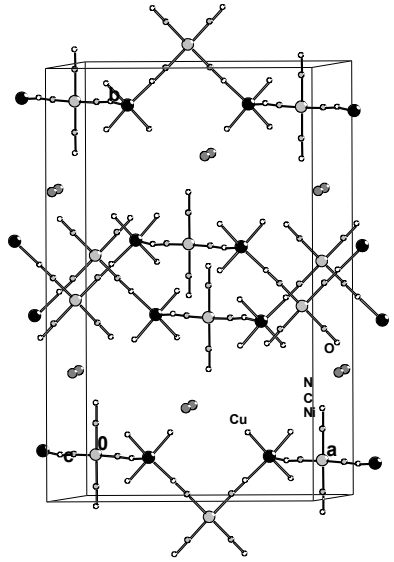

Figure 2. Packing diagram for the Cu(*aepn*)Ni(CN)$_4$·H$_2$O.

The water molecule of crystallization is located between the chains. Similar 1D chain of [-Cu(*en*)$_2$-trans-μ-NC-Ni(CN)$_2$-μ-CN-]$_n$ (*en* = ethylenediamine) composition was found in Cu(*en*)$_2$Ni(CN)$_4$ [18], but in this compound the Cu(II) is hexacoordinated. Pentacoordinated atom Cu(II) was found in 1D compound Cu(*dien*)(CN)Cu(CN)$_2$ [19], but with different chain type (1,3).

The Cu(II) atom is pentacoordinated. Its coordination sphere is formed by three nitrogen atoms from the *aepn* chelate bonded ligand and two nitrogen atoms from the

bridging cyano groups. The Cu-N coordination bonds are in range from 2.009(6) to 2.043(5) Å; these values are in good agreement with thus found in the similar compound $[Cu(\textit{dien})]_3[Fe(CN)_6]_2 \cdot 6H_2O$ [20]. The value of the τ parameter [21] is 19.1 % indicating distorted tetragonal pyramid as the coordination polyhedron (chromophore CuN_3N_2).

In the unit cell there are two crystallographically independent Ni(II) atoms placed on the symmetry centres. Both of them exhibit square-planar coordination by four cyano groups *via* carbon atoms. In the first $[Ni(CN)_4]^{2-}$ anion (Ni1) the two bridging cyano groups are in *trans* positions, while in the second $[Ni(CN)_4]^{2-}$ anion (Ni2) are in c*i*s positions. As a consequence, the formed chain is of the CCCT type. Previously, this chain type was found in compound $Ni(\textit{en})_2Ni(CN)_4 \cdot 2.16H_2O$ [22].

Table 1. Fractional atomic coordinates and equivalent thermal parameters for $Cu(\textit{aepn})Ni(CN)_4 \cdot H_2O$.

Atom	x	y	z	U_{eq}
Cu	0.21800(4)	0.41014(3)	-0.31148(10)	0.0193(3)
Ni	0.5000	0.41128(4)	0.2500	0.0192(3)
Ni	0.0000	0.54841(5)	-0.2500	0.0214(3)
N1	0.1494(4)	0.3537(2)	-0.2278(8)	0.0300(13)
N2	0.2800(3)	0.3557(2)	-0.4280(8)	0.0276(13)
N3	0.2800(3)	0.4624(2)	-0.4301(8)	0.0227(11)
C1	0.2006(5)	0.3054(3)	-0.1443(11)	0.035(2)
C2	0.2428(5)	0.2789(3)	-0.2728(10)	0.035(2)
C3	0.3171(5)	0.3095(3)	-0.3134(11)	0.034(2)
C4	0.3507(4)	0.3836(3)	-0.4862(10)	0.031(2)
C5	0.3154(4)	0.4375(3)	-0.5643(10)	0.029(2)
N11	0.5000	0.2919(4)	0.2500	0.045(2)
C11	0.5000	0.3390(5)	0.2500	0.033(2)
N12	0.5000	0.5306(3)	0.2500	0.029(2)
C12	0.5000	0.4849(5)	0.2500	0.029(2)
N13	0.3213(4)	0.4156(2)	-0.0471(8)	0.0262(12)
C13	0.3904(4)	0.4127(3)	0.0657(9)	0.0225(13)
N21	0.1299(3)	0.4645(2)	-0.2844(8)	0.0262(12)
C21	0.0800(4)	0.4956(3)	-0.2752(9)	0.0245(14)
N22	-0.1238(4)	0.6336(2)	-0.1952(9)	0.0338(14)
C22	-0.0775(4)	0.6010(3)	-0.2179(10)	0.029(2)
O	-0.0242(4)	0.2870(3)	0.0070(10)	0.061(2)

Both hydrogen atoms of the water molecule are involved in hydrogen bonds (HBs) of the O-H···N type with the terminal cyano groups; the O····N distances are from the range 2.914(12) - 3.072(9) Å. It is interesting to note that H2 atom is involved in two HBs with two acceptors (Table 3). Water molecules each other doesn't create HB; the shortest distance between oxygen atoms from water molecules is 3.550(23) Å. Water molecule is also an acceptor for the HB N1-H1B····O with a N1····O distance 2.946(9) Å. This HB links water molecule with the amine ligand. At the same weaker HB of the N-H····N(C) types links amine nitrogen atoms with the terminal cyano ligands. Similarly to H2 atoms also H3B hydrogen atom is involved in bifurcated HB.

Table 2. Selected geometric parameters [Å, °] for Cu(*aepn*)Ni(CN)$_4$·H$_2$O with e.s.d.'s in parentheses.

Cu-N1	2.009(6)	N1-Cu-N3	172.2(2)
Cu-N2	2.043(5)	N1-Cu-N2	91.4(2)
Cu-N3	2.016(5)	N2-Cu-N3	83.9(2)
Cu-N13	2.168(6)	N13-Cu-N21	101.5(2)
Cu-N21	2.007(6)	Cu-N13-C13	161.1(5)
Ni1-C11	1.838(13)	Cu-N21-C21	177.7(6)
Ni1-C12	1.871(12)	C11-Ni1-C13	91.1(2)
Ni1-C13	1.854(6)	C21-Ni2-C21^{i}	89.1(4)
Ni2-C21	1.885(7)	Ni1-C13-N13	177.2(6)
Ni2-C22	1.870(7)	Ni2-C21-N21	177.6(6)

Symmetry transformations used to generate equivalent atoms:
i: -x, y, -z-1/2

Table 3. Possible hydrogen bonds for Cu(*aepn*)Ni(CN)$_4$·H$_2$O [Å, º].

D-H...A	d (D-H)	d (D...A)	d (H...A)	D - H...A
O-H1....N22^{i}	.82(8)	3.072(9)	2.282(80)	161(8)
O-H2....N11^{ii}	.86(10)	2.914(12)	2.147(94)	148(8)
O-H2....N11^{iii}	.86(10)	2.914(12)	2.147(94)	148(8)
N1-H1A....N22^{i}	.900	3.387(11)	2.603	146
N1-H1B....O^{iv}	.900	2.946(9)	2.114	153
N2-H2....N22^{v}	.910	3.161(8)	2.362	146
N3-H3B....N12^{vi}	.900	3.296(5)	2.614	133
N3-H3B....N12^{vii}	.900	3.296(5)	2.614	133

Equivalent positions:
i -x, -y+1, -z
ii -x+1/2,-y+1/2,-z
iii x-1/2,-y+1/2,+z-1/2
iv -x,y,-z-1/2
v -x,-y+1,-z-1
vi x,-y+1,z-1/2
vii -x+1,-y+1,-z

Table 4. H atoms (for deposit)

Atom	x	y	z	Ueq
H1A	0.12596	0.36789	-0.14465	0.03601
H1B	0.10320	0.34375	-0.32520	0.03601
H2	0.23837	0.34380	-0.53192	0.03318
H3A	0.24079	0.48768	-0.48583	0.02725
H3B	0.32529	0.47780	-0.34253	0.02725
H1C	0.24718	0.31491	-0.03206	0.04217
H1D	0.16022	0.28092	-0.11212	0.04217
H2A	0.19629	0.27194	-0.38803	0.04221
H2B	0.26664	0.24521	-0.22023	0.04221
H3C	0.36021	0.32090	-0.19889	0.04122
H3D	0.34807	0.28717	-0.37736	0.04122
H4A	0.36649	0.36314	-0.57903	0.03756
H4B	0.40426	0.38788	-0.38147	0.03756
H5A	0.36355	0.45848	-0.58369	0.03447
H5B	0.26855	0.43360	-0.68109	0.03447
H1	0.01881	0.30137	0.08101	0.04148
H2	-0.00082	0.26288	-0.03075	0.02846

Table 5. Anisotropic coefficients for Cu(*aepn*)Ni(CN)$_4$·H$_2$O.

Atom	U11	U22	U33	U23	U13	U12
Cu	0.0164(4)	0.0262(5)	0.0160(5)	-0.0006(3)	0.0047(3)	-0.0010(3)
Cu	0.0165(4)	0.0253(5)	0.0160(4)	-0.0007(3)	0.0049(3)	-0.0010(3)
Ni1	0.0157(5)	0.0271(7)	0.0140(6)	0.000	0.0033(4)	0.000
Ni2	0.0158(5)	0.0272(7)	0.0218(7)	0.000	0.0066(4)	0.000
N1	0.029(3)	0.034(3)	0.029(3)	0.004(2)	0.011(2)	-0.003(2)
N2	0.024(2)	0.040(4)	0.019(3)	-0.009(2)	0.007(2)	0.002(2)
N3	0.021(2)	0.028(3)	0.021(3)	0.002(2)	0.008(2)	-0.002(2)
C1	0.039(4)	0.033(4)	0.031(4)	0.002(3)	0.008(3)	-0.006(3)
C2	0.051(4)	0.023(4)	0.029(4)	-0.002(3)	0.009(3)	-0.001(3)
C3	0.034(3)	0.041(4)	0.025(4)	0.000(3)	0.005(3)	0.010(3)
C4	0.031(3)	0.032(4)	0.037(4)	-0.003(3)	0.020(3)	0.001(3)
C5	0.028(3)	0.041(4)	0.020(3)	-0.002(3)	0.012(3)	-0.008(3)
N11	0.045(5)	0.032(6)	0.058(7)	0.000	0.014(5)	0.000
C11	0.019(4)	0.066(8)	0.015(5)	0.000	0.005(4)	0.000
N12	0.029(4)	0.017(4)	0.039(5)	0.000	0.006(4)	0.000
C12	0.011(3)	0.064(8)	0.011(4)	0.000	0.002(3)	0.000
N13	0.021(3)	0.041(4)	0.015(3)	-0.002(2)	0.003(2)	0.001(2)
C13	0.025(3)	0.030(4)	0.017(3)	-0.001(2)	0.013(3)	-0.001(2)
N21	0.021(2)	0.030(3)	0.027(3)	0.003(2)	0.006(2)	0.001(2)
C21	0.016(3)	0.039(4)	0.018(3)	0.003(3)	0.005(2)	-0.002(3)
N22	0.029(3)	0.028(3)	0.046(4)	-0.007(3)	0.014(3)	0.002(2)
C22	0.020(3)	0.043(4)	0.023(4)	0.001(3)	0.005(3)	0.000(3)
O	0.040(3)	0.065(5)	0.064(5)	-0.032(4)	-0.006(3)	0.013(3)

IR Spectra

The presence of the cyano ligands is evidenced by strong and sharp absorption bands due the ν(CN) stretching vibrations. In line with the literature data [23, 24] the bands at higher wavenumbers (2169, 2161 and 2143 cm^{-1}) were assigned to the bridging cyano groups and the band at lower wavenumber (2122 cm^{-1}) was assigned to the terminal cyano groups. The absorption band arising from the deformation vibration δ(Ni-CN) (422 cm^{-1}) shows the presence of the tetracyanonickellate anion.

The presence of the *N*–donor ligand *aepn* is disclosed by absorption bands due to stretching and deformation vibrations of the CH_2 and NH_2 groups. Absorption bands due to stretching vibrations ν(NH_2) of the *aepn* ligand are observed at 3350, 3305, 3279 and 3227 cm^{-1} , while those arising from ν(CH_2) vibrations are observed in the region between 2964, 2948 and 2890 cm^{-1} what is in line with the literature data. The absorption bands due to δ(NH_2) and δ(CH_2) deformation vibrations are situated in the range 1600 to 1400 cm^{-1} in accordance with the literature [25, 26].

The water molecule displays in the IR spectrum asymmetric and symmetric ν (OH) stretching vibrations at 3577 and 3461 cm^{-1}. These absorption bands disappeared in the spectrum of the sample heated to 180 ºC. Moreover, in the spectrum of the title compound the absorption band assigned to the δ(OH) deformation vibration was found at 1635 cm^{-1}.

Conclusion

Synthetic design using the "brick and mortar" method led to formation of 1D structure exhibiting composition Cu(*aepn*)$Ni(CN)_4 \cdot H_2O$.

Supplementary material

Crystallographic data (excluding structure factors) for the structures reported in this paper have been deposited with the Cambridge Crystallographic Data Centre as supplementary publication no. CCDC 256913. Copies of the data can be obtained free of charge on application to CCDC, 12 Union Road, Cambridge CB2 1EZ, UK [Fax: int. Code +44(1223)336-033; E-mail: deposit@ccdc.cam.ac.uk.

Acknowledgments

This work was supported by Slovak Grant Agency VEGA (project 1/0447/03).

References

1. Dunbar K. R., Heintz R. A., Prog. Inorg. Chem. 45 (1997) 283.
2. Verdaguer M., Bleuzen A., Marvaud V., Vaissermann J., Seuleiman M., Desplanches C., Scuiller A., Train C., Garde R., Gelly G., Lomenech C., Rosenman I., Veillet P., Cartier C., Villain F., *Coord. Chem. Rev.,* 192 (1999) 1023.
3. Willett R. D., Wang Z., Molnar S., Brewer K., Landee C. P., Turnbull M. M., Zhang W. Mol. Cryst. Liq. Cryst. 233 (1993) 277.
4. Paharová J., Černák J., Boča R., Žák Z.: Inorg. Chim. Acta 346 (2003) 25.
5. Maľarová M, Kuchár J, Černák J, Massa W.: Acta Crystallogr. C59 **7** (2003) 280.

6. Černák J, Orendáč M, Potočňák I, Chomič J, Orendáčová A, Skoršepa J, Feher A : Coord. Chem. Rev. 224 (2002) 51.
7. Cotton F.A., Wilkinson G., Murillo C.A., Bochmann M. : Advanced Inorganic Chemistry, 6th ed. , J. Wiley, 1999
8. Chun H, Bernal I.: Acta Crystallogr. C56, 11 (2000) 1326.
9. Fernelius W.C.: Inorganic Synthesis, vol. II. McGraw-Hill, New York 1946, 227.
10. Sheldrick G.M.: SHELXS-86. Program for the solution of crystal structures. Univ. Göttingen, FRG, 1986.
11. Sheldrick G.M.: SHELXL-93. Program for the refinement of crystal structures. Univ. Göttingen, FRG, 1993.
12. DIAMOND – Visual Crystal Structure Information System, Crystal Impact D-53002 Bonn, Germany (1999).
13. Allen F.H., Bellard S., Brice M.D., Cartwright B.A., Doubleday A., Higgs H., Hummelink T., Hummelink-Peters B.G., Kennard O., Motherwell W.D.S., Rodgers J.R. & Watson D.G.: Cambridge Structural Database System (CSDS), Cambridge, U.K., 1994.
14. Kurihara H., Nishikiori S., Iwamoto T.: Acta Crystallogr., C53, (1997) 1409.
15. Stephens F.S.: J. Chem. Soc. (1969) 2233.
16. Johns C.A., Malik K.M.A.: Polyhedron 21 (2002) 395.
17. Gonzalez-Alvarez M., Alzuet G., Borras J., Macias B., Montejo-Bernardo J.M., Garcia-Granda S.: Z.Anorg.Allg.Chem. 629 (2003) 239.
18. Seitz K, Peschel S, Babel D.: Zeitschrift für Anorg. und Allgemeine Chemie 627 5 (2001) 929.
19. Huang S.F., H.H. Wei and Y. Wang, Polyhedron, 16 (1997) 1747.
20. Kou H.Z., Liao D.Z., Cheng P., Jiang Z.H., Yan S.P., Wang G.L., Yao X.K., Wang H.G.: J. Chem. Soc., Dalton Trans. (1997) 1503.
21. Addison, A.W., Rao, T.N., Reedijk, J., van Rijn, J., Verschoor, G.C.: J. Chem. Soc., Dalton Trans., (1984) 1349.
22. Černák J., Chomič J., Domiano P., Ori O., Andreetti G.D.: Acta Crystallogr. C46 (1990) 2103.
23. Nakamoto K.: Infrared & Raman Spectra of Inorganic & Coordination Compounds 5th ed., J. Wiley & Sons, New York, 1997.
24. Sharpe A.G.: The Chemistry of Cyano Complexes of the Transition Metals, Academic Press 1976.
25. Gabelica Z.: Spectrochimica Acta, 32A (1975) 327.
26. Horák M., Papoušek D.: Infračervená spektra a struktura molekul, Praha Academia (1976).

Acta Univ. Palacki. Olomuc.
Fac. rer. nat. 2005
Chemica 44, 83-91

Instructions to authors for AUPO Chemica

The journal Acta Universitatis Palackianae Olomucensis is published by the Palacký University Olomouc, Czech Republic. The Chemica chapter appears yearly in the printed form and it is abstracted by the Chemical Abstracts. All accepted contributions in electronic form will be published continuously also on the www-pages: **http://chemie.upol.cz/acta**

Articles submitted must be written in English, comprehensively and clearly and should be of

- original full-papers in all basic or applied chemistry branches
- review articles covered current and rapidly developing chemical research fields
- preliminary communications reported significant results assumed for full publication later (max. 2 pages incl. Figures and Tables)
- invited articles, research reports and editorial board contributions

The manuscripts are reviewed by the editorial board and will be published without charge.

Contributions should be submitted in one hardcopy (A4 paper, single-sheet typed only) and also on a floppy-disc, sent to:

Prof. Jiří Kameníček, Department of Inorganic Chemistry, Palacký University, Křížkovského 10, 771 47 Olomouc, Czech Republic.

The word processor MICROSOFT WORD should be used (for details see the sample of a style sheet provided on www). For electronic transmission, the following e-mail address may be used: **kamen@prfnw.upol.cz**

Figures and graphs should be both clearly marked with arabic numerals on the back as well as being mentioned in the text. A list of figure captions should be given on the separate sheet. For the electronic form, all figures and graphs must be pasted to the end of the text. The use of the .hpg or .cdr format is recommended.
Tables should be typed on separate sheets and numbered consecutively with roman numerals. The position of each table in the text, as well as a list of tables with descriptive captions, should be given.
X-ray crystallographic data should be submitted according to IUCr-recommendations after deposition at the CCDC. Less common abbreviations and symbols must be explained when they first appear in the text. All nomenclature should be consistent and unambiguous; following the rules established by IUPAC.

Copyright

The Authors, by sending in the contribution, agree with transfer of the copyright that covers the exclusive rights to reproduce and distribute the complete article, including reprints and www pages distributions.

ACTA UNIVERSITATIS PALACKIANAE OLOMUCENSIS
FACULTAS RERUM NATURALIUM

CHEMICA 44

Published by the Faculty of Science, Palacký University Olomouc

Editor-in-Chief: prof. Jiří Kameníček, Palacký University, Olomouc, Czech Rep.
Professional Editor: prof. Juraj Ševčík, Palacký University, Olomouc, Czech Rep.
Technical Editor: Mgr. Marek Pavlíček, UP Olomouc

Advisory Board:
prof. G. Anderegg, ETHZ Zürich, Switzerland,
prof. J. Černák, UJPŠ Košice, Slovakia,
prof. N. Duffy, Wheeling Jesuit University, U.S.A.,
assoc. prof. P. Hradil, FARMAK Olomouc, Czech Republic,
prof. L. Lapčík, Univerzita T. Bati, Zlín,
prof. P. Raithby, University of Bath, UK,
asoc. prof. J. Vičar, LF UP Olomouc, Czech Republic,
prof. Z. Žák, UJEP Brno, Czech Republic

Printed by Palacký University Press
First edition

ISBN 80-244-1171-7
ISSN 0232-0061